

Sleep, Glucose Variability, CVD Risk & CV Stress in Young Adults with T1DM

BY

Sarah Farabi
BSN, Saint Louis University, 2009

THESIS

Submitted as partial fulfillment of the requirements
for the degree of Doctor of Philosophy in Nursing Sciences
in the Graduate College of the
University of Illinois at Chicago, 2016

Chicago, Illinois

Defense Committee:

Laurie Quinn, Chair and Advisor
David W. Carley, Advisor
Shane Phillips, Applied Health Sciences
Mary Kapella, Biobehavioral Health Science
Chang Gi Park, Health Systems Science

I would like to dedicate my thesis to my family who continually inspire and motivate me to be a better and stronger version of myself. Notably, to my parents, Tom and Sally Schwarz, who raised me to be an independent woman and to never be discouraged in the face of adversity. To my sister, Amy Schwarz, who is always there to listen and motivate me and who has taught me to never be afraid to be myself and always to believe in myself. To my sister from another mister, Annie Tomber, who is always there to listen and is a source of unending positivity and support. To my brother from another mother, John Nolan, who is also always there supporting and reminding me to take breaks and relax. And, most importantly, to the love of my life and husband, Corey Farabi, who supports me in every decision I make, always reminds me to laugh at least once a day and without whom this dissertation may never have been accomplished.

ACKNOWLEDGMENTS

I would like to thank my committee (Dr. Laurie Quinn, Dr. David Carley, Dr. Shane Phillips, Dr. Mary Kapella and Dr. Chang Gi Park) for dedication of so much of their time and expertise to help me carryout my dissertation research. My two advisors, Dr. Quinn and Dr. Carley, spent countless hours with me from the inception of my research design, to collection of data as well as data analysis and dissection of my findings. Their guidance, instruction and positive support through this entire process have helped me to gain a strong foundation from which I can fully develop into an independent scientist.

A number of other individuals were very helpful in the data collection and analysis. I would like to acknowledge the staff at the Sleep Science Center at the University of Illinois at Chicago, who helped with each sleep study. I would also like to acknowledge Dr. Giamilla Fantuzzi and Rand Akasheh, PhD Candidate, who graciously allowed me to use laboratory space and importantly helped to run the ELISA biomarker assays.

SSF

TABLE OF CONTENTS

<u>CHAPTER</u>		<u>PAGE</u>
I.	INTRODUCTION	
A.	Pathophysiology of Type 1 Diabetes Mellitus and its Complications	1
1.	Incidence and Prevalence of T1DM	1
2.	Pathophysiology and Development of T1DM	2
a.	Normal Physiology of the Immune System.....	2
b.	Pathophysiologic Changes in T1DM.....	3
c.	Time Course and Diagnosis of T1DM	3
3.	Pathophysiology of T1DM Complications	5
B.	Cardiovascular Disease, Inflammation and Hypothalamic-Pituitary-Adrenal Activation in T1DM	6
C.	Sleep, Metabolism, Inflammation and HPA Activation.....	7
D.	Sleep in T1DM.....	8
E.	Framework and Aims for Study	10
F.	Overview of Dissertation Study	11
G.	Overview of Chapters	13
II.	COUPLING BETWEEN GLUCOSE VARIATIONS AND ACTIVITY DURING SLEEP AND WAKE OVER A 60-HOUR PERIOD	
A.	Introduction.....	15
B.	Methods	15
1.	Protocol.....	15
2.	Wavelet Coherence.....	16
3.	Bivariate Correlation	18
4.	Circadian Analysis.....	18
C.	Results	18
1.	Demographics	18
2.	Coherence	18
3.	Bivariate Correlation	25
4.	Circadian Analysis.....	26
D.	Discussion	28
III.	COUPLING BETWEEN EEG POWER AND GLUCOSE CHANGES DURING SLEEP	
A.	Introduction.....	31
B.	Methods	32
1.	Subjects	32
2.	Study Protocol.....	32
3.	Glucose Data	33
4.	EEG Data.....	34
5.	Statistical Analysis	34
a.	Wavelet Coherence Analysis.....	34
b.	Bivariate Correlation.....	36
C.	Results	36
1.	Subjects	36
2.	Coherence	37

TABLE OF CONTENTS (continued)

<u>CHAPTER</u>	<u>PAGE</u>
3. Bivariate Correlation	43
D. Discussion	46
 IV. CAUSAL RELATIONSHIPS BETWEEN EEG POWER AND GLUCOSE DURING SLEEP	
A. Introduction	50
B. Methods	51
1. Subjects	51
2. Study Protocol	51
3. Glucose Data	52
4. EEG Data	53
5. Statistical Analyses	53
a. Granger Causality	53
b. Cross-Correlation Function	55
c. Bivariate Correlation	56
C. Results	56
1. Subjects	56
2. Granger Causality	57
3. Cross-Correlation Function	61
4. Bivariate Correlation	65
D. Discussion	65
 V. RELATIONSHIP BETWEEN SLEEP, INFLAMMATORY MARKERS AND CORTISOL	
A. Introduction	72
B. Methods	73
1. Subjects	73
2. Study Protocol	73
3. PSG-Derived Sleep Measures	74
4. Inflammatory Cytokine and Cortisol Assays	74
5. Statistical Analysis	75
C. Results	76
1. Subjects and Sleep Characteristics	76
2. Temporal Variations of IL-6, TNF- α and Cortisol	77
3. IL-6, TNF- α and Cortisol in Relation to Average Glycemic Control	78
4. Correlations of TNF- α , IL-6 and Cortisol with Sleep and Glycemic Control Measures	80
D. Discussion	81
 VI. DISCUSSION	
A. Overview	86
B. Glucose Variability as a Driver of Sleep Disruption	88
C. Sleep as a Driver of Glucose Variability	89
D. Inflammation is Altered by Sleep Processes and Glycemic Control	91
E. Sleep, Glucose Variability and Inflammation: A Vicious Cycle?	92
F. Conclusions and Implications	95

TABLE OF CONTENTS (continued)

<u>CHAPTER</u>	<u>PAGE</u>
CITED LITERATURE.....	99
APPENDICES	
Appendix A.....	115
Appendix B.....	143
Appendix C.....	156
Appendix D	161
VITA.....	165

LIST OF TABLES

<u>TABLE</u>	<u>PAGE</u>
1. SUMMARY OF NUMBER AND DURATION OF INTERVALS OF SIGNIFICANT COHERENCE	21
2. PARAMETERS OF CIRCADIAN COSINOR REGRESSION FOR COHERENCE	28
3. DEMOGRAPHIC, GLYCEMIC CONTROL AND SLEEP CHARACTERISTICS OF SUBJECTS	37
4. BIVARIATE CORRELATIONS OF EEG/GLUCOSE COHERENCE WITH STANDARD MEASURES OF SLEEP AND GLYCEMIC CONTROL	45
5. DEMOGRAPHIC, SLEEP AND GLYCEMIC CONTROL CHARACTERISTICS OF SUBJECTS	57
6. NUMBER OF SUBJECTS WITH SIGNIFICANT GRANGER COEFFICIENTS ACROSS EEG BANDS	58
7. FREQUENCY OF POSITIVE AND NEGATIVE COEFFICIENTS FOR SIGNIFICANT VAR MODELS	61
8. DEMOGRAPHIC, GLYCEMIC CONTROL AND SLEEP CHARACTERISTICS	76
9. VALUES OF TNF- α , IL-6 AND CORTISOL BEFORE AND AFTER SLEEP	77
10. CORRELATION TABLE OF PRE-SLEEP, AWAKENING AND 1-HOUR POST AWAKENING RECIPROCAL VALUES OF IL-6 AND TNF- α AND SQUARE ROOT VALUES OF CORTISOL WITH STANDARD MEASURES OF SLEEP AND GLYCEMIC CONTROL.....	81

LIST OF FIGURES

<u>FIGURE</u>	<u>PAGE</u>
I. CONCEPTUAL FRAMEWORK FOR DISSERTATION STUDY.....	11
II. EXAMPLE OF COHERENCE BETWEEN ACTIVITY AND GLUCOSE OVER 60 HOUR PERIOD	20
III. MEAN COHERENCE BETWEEN ACTIVITY AND GLUCOSE DURING SLEEP AND WAKE STATES AT DIFFERENT FLUCTUATION PERIODS	23
IV. MEAN PHASE DELAY BETWEEN ACTIVITY AND GLUCOSE DURING SLEEP AND WAKE STATES AT DIFFERENT FLUCTUATION PERIODS	25
V. EXAMPLE CIRCADIAN COSINE WAVE FIT OF COHERENCE IN 3 BANDS OVER 60 HOURS	27
VI. EXAMPLE OF COHERENCE BETWEEN THETA EEG POWER AND GLUCOSE DURING SLEEP	38
VII. AVERAGE NUMBER AND DURATION OF INTERVALS OF SIGNIFICANT COHERENCE ACROSS FREQUENCY RANGES FOR ALL EEG BANDS.....	40
VIII. MEAN SIGNIFICANT COHERENCE FOR FREQUENCY RANGES ACROSS EEG BANDS	41
IX. MEAN PHASE DELAY BETWEEN “SLEEP” AND “WAKE” EEG BANDS FOR FLUCTUATION RANGES	43
X. IMPULSE RESPONSE FUNCTION EXAMPLES FOR GLUCOSE DRIVING ALPHA AND THETA EEG CHANGES	60
XI. CROSS-CORRELATION FUNCTIONS FOR ONE SUBJECT ACROSS EEG BANDS.....	63
XII. MEAN CROSS-CORRELATION FUNCTIONS ACROSS EEG BANDS.....	64
XIII. PEAK CORRELATION COEFFICIENT FOR ALPHA AND THETA IN SUBJECTS WITH OPTIMAL LAG BETWEEN ± 10 MINUTES.....	65
XIV. PRE- AND POST-SLEEP IL-6 AND TNF- α IN SUBJECTS WITH GOOD VERSUS POOR GLYCEMIC CONTROL	79
XV. SCHWARZ FARABI FRAMEWORK	97

LIST OF ABBREVIATIONS

AASM	American Academy of Sleep Medicine
AGE	Advanced Glycation Endproducts
AHI	Apnea Hypopnea Index
AIC	Akaike Information Criterion
Akt	Protein Kinase B
ANOVA	Analysis of Variance
APC	Antigen Presenting Cell
ARI	Arousal index
BIC	Bayesian Information Criterion
BMI	Body Mass Index
CD4+	Cluster of Differentiation 4 Antigen Expressing
CD8+	Cluster of Differentiation 8 Antigen Expressing
CGMS	Continuous Glucose Monitoring System
CoV	Coefficient of Variation
CV	Cardiovascular
CVD	Cardiovascular Disease
CONGA-1	Continuous Net Glycemic Action over 1 Hour
DNA	Deoxyribonucleic Acid
EEG	Electroencephalogram
EEG→Glucose	Electroencephalogram Changes Cause Glucose Changes
ELISA	Enzyme-Linked Immunosorbent Assay
ESS	Epworth Sleepiness Scale
ETC	Electron Transport Chain
FFT	Fast Fourier Transform

LIST OF ABBREVIATIONS (continued)

GAPDH	Glyceraldehyde Phosphate Dehydrogenase
GH	Growth Hormone
Glucose→EEG	Glucose Changes Cause Electroencephalogram Changes
HbA1c	Hemoglobin A1c
HLA	Human Leukocyte Antigen
IL-6	Interleukin-6
IRF	Impulse Response Function
IS	Insulin Sensitivity
MHC	Major Histocompatibility Complex
MHC I	Major Histocompatibility Complex Class I
MHC II	Major Histocompatibility Complex Class II
MVGC	Multivariate Granger Causality
NADH	Nicotinamide Adenine Dinucleotide
NADPH	Nicotinamide Adenine Dinucleotide Phosphate
NF-kB	Nuclear Factor Kappa-Light Chain-Enhancer of Activated B cells
NO	Nitric Oxide
NREM	non-Rapid Eye Movement
PARP	Poly-ADP Ribose Polymerase
PHQ-9	Patient Health Questionnaire-9
PKC	Protein Kinase C
PSG	Polysomnography
PSQI	Pittsburgh Sleep Quality Index
PVT	Psychomotor Vigilance Task
qEEG	Quantitative Electroencephalogram

LIST OF ABBREVIATIONS (continued)

RAGE	Receptor for Advanced Glycation Endproducts
REM	Rapid Eye Movement
ROS	Reactive Oxygen Species
SD	Standard Deviation
SE	Sleep Efficiency
SLAT	Sleep Latency
SSS	Stanford Sleepiness Scale
SWS	Slow Wave Sleep
TCA	Tricarboxylic Acid Cycle
T1DM	Type 1 Diabetes Mellitus
TNF- α	Tumor Necrosis Factor Alpha
TST	Total Sleep Time
UDP-GlcNac	UDP-N-Acteylglucosamine
VAR	Vector AutoRegressive
WASO	Wake After Sleep Onset
WCA	Wavelet Coherence Analysis
WGC	Wiener-Granger Causality

SUMMARY

Poor glucose control is believed to contribute importantly to cardiovascular disease (CVD) – a leading complication and cause of death in people with Type I Diabetes Mellitus (T1DM). Good sleep also has been shown to play an important role in maintaining cardiovascular and metabolic health, and sleep quality is reduced in people with T1DM. Nonetheless, minimal research has been conducted to define the simultaneous relationships between glucose variations, sleep quality and CVD risk in individuals with T1DM. To test the hypotheses that glucose variations are causally related to sleep disruption and that sleep disruption mediates inflammation and CVD risk in individuals with T1DM, two aims were proposed: 1) to quantify sleep disturbances and to determine their relationship to glucose variability and 2) to define the relationship between sleep disruption and markers of CVD risk in young adults with T1DM.

Thirty young adults, age 18-30, were enrolled for participation in the research study. Subjects wore a continuous glucose monitoring system and a sleep/activity monitor (actigraph) in home for three days and two nights and underwent polysomnography (PSG) in the laboratory on the third night. While actigraphy provided information about sleep and wake behavior throughout the test period, PSG complemented this by providing direct information on brain activity during sleep on the third night. The amount of power in five electroencephalogram (EEG) Bands – Delta and Theta (characteristic of sleep); Alpha, Beta and Gamma (characteristic of wakefulness) – was tracked throughout the PSG study night. Wavelet coherence analysis revealed a strong but time-varying and frequency specific coupling between glucose and sleep measured by both actigraphy and PSG. Evidence for a bi-directional causal relationship between glucose and brain activity was provided by Granger causality analysis. In the Delta, Theta, Alpha and Beta Bands, 69% to 92% of subjects demonstrated significant causal interactions between EEG and glucose. In the Theta and Alpha Bands, instances of glucose variations causing changes

SUMMARY (continued)

in EEG and EEG changes driving glucose variations occurred with approximately equal frequency. Increasing glucose caused increasing Alpha Power and decreasing Theta and Delta power, suggesting that glucose changes disturb sleep by causing arousal or awakening. Increases in Beta and Delta power consistently caused increasing glucose levels while increasing Theta power caused decreasing glucose. These findings argue that there is a bi-directional relationship between glucose and brain activity during sleep in young adults with T1DM. This study also provides evidence that both sleep disruption and poor glycemic control mediate increased inflammatory processes in T1DM. For example, plasma concentration of Tumor Necrosis Factor- α (TNF- α) consistently increased during the sleep period. Further, more frequent arousal from sleep was significantly associated with higher levels of interleukin-6 (IL-6) upon awakening, even after controlling for glycemic control. Only subjects with good glycemic control exhibited a normal pattern of decreased IL-6 upon awakening.

Overall, findings from this study demonstrate a bi-directional relationship between sleep and glucose changes, and that both sleep disruption and glycemic control may play important roles in mediating levels of inflammation, which are associated with CVD development in T1DM. These findings lay a foundation for future interventional studies including healthy control groups to provide information about the mechanisms behind these relationships. Understanding the relationships between sleep, glucose control and inflammation in T1DM is essential as this knowledge may lead to better clinical management of diabetes and ultimately improved quality of life.

I. INTRODUCTION

A. Pathophysiology of Type 1 Diabetes Mellitus and its Complications

Type 1 Diabetes Mellitus (T1DM) is characterized by autoimmune-mediated destruction of pancreatic beta cells. The incidence and prevalence of T1DM are increasing in the United States and around the world. T1DM results in a life-long need for exogenous insulin and, despite vigilant management, wide glucose variations are a common occurrence in afflicted individuals. Cardiovascular Disease (CVD) is a leading cause of morbidity and mortality in individuals with T1DM, but the role of glucose variability in CVD onset and progression remains controversial. Increasingly, sleep is being recognized as a key factor contributing to cardiovascular (CV) health, but interactions between sleep, sleep-disturbance and CVD have not been systematically studied in T1DM. Sleep architecture is known to be disrupted in individuals with T1DM, but the potential contribution of glucose variations to this disruption has been minimally investigated. This dissertation study was aimed to determine the role of glucose variations in sleep disruption and the potential mediating effect of sleep disturbance on markers of inflammation and CV stress in young adults with T1DM.

1. Incidence and Prevalence of T1DM

Approximately 1.25 million Americans are diagnosed T1DM, with the incidence and prevalence of this disorder increasing in the United States and worldwide (1–3). Reports from the Philadelphia Diabetes registry and the SEARCH for Diabetes registry between 2000 and 2004 estimated the incidence of T1DM in 0-20 year olds to be between 17.2 and 24.3 per 100,000 (4,5). Based on these studies, the highest incidence occurs in 10-14 year olds and non-Hispanic white children (4,5). Another study reported that between 1978 and 2004 T1DM incidence increased from 14.8 to 23.9 per 100,000 among children 0-17 years old (6). Non-Hispanic white youth exhibited the most rapid increase at 2.7% per year; the rate in Hispanic youth increased at 1.6% per year (6). Most recently, the overall prevalence of T1DM was estimated to have increased 21.1% between 2001 and 2009 (7). Imperatore and colleagues

(2012) project that the prevalence of T1DM may increase several-fold by 2050, making T1DM an immense health threat facing the United States population.

2. Pathophysiology and Development of T1DM

a. Normal Physiology of the Immune System

Two of the major cell types in the immune system are B- and T-lymphocytes, which provide protection against disease. Cluster of differentiation 4 antigen expressing (CD4+) cells are known as helper T-lymphocytes and are activated by antigen presenting cells (APCs). APCs digest and present small pieces of foreign particles (known as antigens) on their cell surface, with a major histocompatibility complex (MHC) protein. MHC proteins (including class I [MHC I] and class II [MHC II]) bind to the foreign particle, allowing recognition by the T-cell. Macrophages are antigen presenting cells that use MHC class II proteins. Activated macrophages secrete a host of inflammatory cytokines, such as interleukin-6 (IL-6) and tumor necrosis factor alpha (TNF- α). Binding of a CD4+ cell to the antigen presented by the macrophage activates the CD4+ cell to start secreting cytokines, initiating an immune response. Cluster designation 8 antigen expressing (CD8+) cells, also known as cytotoxic T-lymphocytes, are responsible for elimination of target cells. Normally, CD8+ cells recognize antigens presented on MHC I proteins. Once activated, the CD8+ cells initiate destruction in the target cell. In a healthy immune system, APCs can distinguish self from non-self antigens and only present foreign antigens to T-lymphocytes (8). Helper T-lymphocytes also activate B-lymphocytes. Once activated by the T-lymphocytes, B-lymphocytes proliferate and produce immunoglobulins (antibodies) against the specific antigen. These antibodies share a similar structure characterized by four polypeptide chains: two heavy chains and two light chains. Each chain has variable and constant regions. The variable regions are the sites of antigen binding and are specific to the antigen. Once formed to the antigen, the antibody can elicit various responses. Some antibodies coat the surface of foreign bodies to enhance phagocytosis;

other antibodies bind to the foreign particle and promote elimination; while other antibodies activate inflammatory cytokine responses resulting in cytotoxicity to the foreign cell (9).

b. Pathophysiologic Changes in T1DM

T1DM results from autoimmune destruction of the pancreatic beta cells, which are responsible for the production and secretion of insulin. Activated T- and B-lymphocytes as well as macrophages infiltrate the pancreas resulting in eventual destruction of all beta cells. In pancreases removed from cadavers who were diagnosed with T1DM near death, an islet infiltrate (insulinitis) has been noted, comprising CD4+ and CD8+ cells, macrophages and B-lymphocytes (10). This immune response is triggered by self-antigens inappropriately presented on APCs. In most cases, B-lymphocytes are activated to produce autoantibodies against the beta cells, and this may contribute to the diagnosis of T1DM. The most common autoantibodies seen in T1DM are raised against the islet cell, insulin, protein tyrosine phosphatase, or glutamic acid decarboxylase, or those against a key zinc transporter (essential for insulin storage and secretion) in the pancreatic beta cell (11–14). Autoantibodies can be detected years before clinical signs of hyperglycemia develop (11,13). Although the specific auto-antibodies may vary slightly between geographical locations, the detection of antibodies can predict up to 80% of people who will go on to develop T1DM (15,16).

Development of T1DM is also associated with certain polymorphisms in the genes encoding MHC proteins located on the human leukocyte antigen (HLA) region of the short arm of chromosome 6. Results of genetic studies have most consistently supported that polymorphisms in class II genes on chromosome 6 which encode for HLA D region subunit R and HLA D region subunit Q are associated with development of T1DM (17).

c. Time Course and Diagnosis of T1DM

T1DM can develop at any time in a person's life, but even a person carrying high-risk genetic alleles associated with T1DM may not ever develop the disease. Further, T1DM is more

common in certain geographic regions than in others. Together, these observations suggest that environmental triggers may play an epigenetic role in accelerating or inducing auto-immunity and development of T1DM. There have been several proposed environmental triggers, including infectious agents and dietary exposures (18,19). Enteroviruses have received attention in recent research as a possible trigger for T1DM onset (20,21). Research into dietary triggers has provided mixed results (18,22). The prospective and ongoing Environmental Determinants of Diabetes in the Young study, is designed to identify environmental triggers of T1DM onset (23), but findings remain to be published.

A model of the natural course of T1DM, originally proposed by Eisenbarth in 1986 (24) and updated in 2014 by Atkinson (12), suggests that there is a genetic predisposition to T1DM, with one or multiple precipitating events (occurring as early as *in utero*) which cause gradual loss of beta cell mass and insulin release. The model also proposes that environmental triggers may influence the rate of progression of T1DM and that some individuals with T1DM may retain low levels of beta cell mass long after disease diagnosis (12).

Diagnosis of diabetes is made if an individual has one of the following: a fasting plasma glucose \geq 126 mg/dl, a 2-hour glucose tolerance test of \geq 200 mg/dl or a random plasma glucose of \geq 200 mg/dl with clinical signs of hyperglycemia or hemoglobin A1c (HbA1c) \geq 6.5% (25). Once diagnosed with T1DM, an individual is faced with life-long replacement of insulin and self-management of glucose levels. Insulin can be administered via multiple daily injections or via insulin pump. The continuous insulin infusion pump provides a basal rate of fast-acting insulin and the individual programs additional bolus insulin doses to account for food intake, activity and other factors. Studies have shown that insulin pumps can provide better glycemic control (26,27) and reduce episodes of hypoglycemia (26,28) in people with T1DM. Further, a recent observational study found that pump therapy was associated with decreased cardiovascular risk, a major complication of T1DM (29).

3. Pathophysiology of T1DM Complications

The inability to produce insulin in T1DM leads to hyperglycemia when insulin is not appropriately replaced. Chronic hyperglycemia in T1DM often leads to the development of complications, including cardiovascular disease, stroke, neuropathy, nephropathy, and retinopathy. Each of these major complications arises from dysfunction of specialized cells (e.g. endothelial cells, glomerular cells, neurons) resulting from exposure to high levels of glucose. An important molecular mechanism potentially underlying this cellular damage is production of high levels of reactive oxygen species (ROS) by the mitochondria (30) secondary to hyperglycemia.

ROS are created via increased glycolysis, which augments activity of the tricarboxylic acid cycle (TCA). Up-regulation of the TCA cycle yields increased nicotinamide adenine dinucleotide (NADH; the main carrier for electrons to the Electron Transport Chain [ETC]), increasing superoxide (O_2^-) production via coenzyme Q. ROS (such as superoxide) react with lipids, DNA proteins and other proteins via electron donation or proton abstraction, deranging their function (30). One such interaction is increased transcription and translation of the enzyme poly-ADP ribose polymerase (PARP). PARP decreases the expression of GAPDH (glyceraldehyde phosphate dehydrogenase), a necessary enzyme for efficient glycolysis (31). Impaired glycolysis produces elevated glucose, increased glycolytic intermediates and activation of pathways for their breakdown. Unfortunately, these pathways can further exacerbate ROS production, increasing damage to the cells.

There are four main pathways activated via increased glycolytic intermediates. The first is activation of the polyol pathway in which the enzyme aldose reductase uses nicotinamide adenine dinucleotide phosphate (NADPH) to reduce glucose to sorbitol, which decreases NADPH supply. NADPH is necessary to maintain reduced glutathione, a key antioxidant in red blood cells which helps to decrease levels of ROS (32,33). The second pathway is activation of protein kinase C (PKC), an enzyme responsible for phosphorylation reactions in cells. PKC activation has numerous deleterious

downstream effects. One main effect is an increase in NADPH oxidase synthesis. NADPH oxidase is an enzyme which produces superoxide via electron transfer from NADPH to molecular oxygen (34). PKC activation also increases Nuclear Factor Kappa-light chain-enhancer of activated B cells (NF- κ B) production, a promoter of DNA transcription, leading to production of inflammatory cytokines, such as IL-6 and TNF- α (35,36). The third pathway is the hexosamine biosynthesis pathway, which increases UDP-N-acetylglucosamine (UDP-GlcNac). UDP-GlcNac modifies Protein Kinase B (Akt) resulting in decreased endothelial nitric oxide synthase and nitric oxide (NO) production (37). The fourth pathway induced by hyperglycemia is production of advanced glycation end products (AGE). AGEs are formed via glycation of amino acids and also through the breakdown of fructose and triose phosphates. These AGEs alter the function enzymes as well as proteins in the extracellular matrix (leading to decreased elasticity) and can also bind to specific cell surface receptors (RAGEs). Such binding activates intracellular pathways yielding increased ROS, inflammatory cytokine and cellular adhesion molecule production (38–40).

Continuous activation of these 4 pathways by constant hyperglycemia may ultimately overwhelm cellular mechanisms to offset the deleterious effects of ROS, especially in the vasculature (41). These cellular changes may contribute to complications including cardiovascular disease, retinopathy, neuropathy, and nephropathy (30,42).

B. Cardiovascular Disease, Inflammation and Hypothalamic-Pituitary-Adrenal Activation in T1DM

Despite advances in management of T1DM, CVD remains one of the leading causes of death (43–45). Tight control of glucose decreases risk, but hyperglycemia alone does not completely explain development of CVD (46,47) and the mechanisms underlying CVD in T1DM remain incompletely understood (45).

Glucose variability is a universal feature of T1DM and has been hypothesized to play a role in the onset and progression of overt CVD (48). Because glucose variability induced elevated levels of oxidative

stress and inflammation in human cell cultures, some investigators have hypothesized there to be an association between increased glucose variability and development of CVD complications (49,50). Further, microvascular complications have been associated with increased glucose variability (51,52). However, other investigators have failed to find an association between glucose variability and CVD complication development (53,54). Inflammation has been identified as a key factor in development of CVD (55,56). Both hyperglycemia (57–59) and hypoglycemia (60) have been associated with increased inflammatory markers, and elevated TNF- α and IL-6 levels correlate with hemoglobin A1c (HbA1c), a marker of glycemic control, in people with T1DM (61–63).

Elevated plasma cortisol, which is secreted from the hypothalamic-pituitary-adrenal (HPA) axis, has been reported in people with T1DM as compared to controls (64,65) and poor glycemic control is associated with elevated cortisol in children (66). Increased activation of the HPA has been linked to accelerated development of CVD in T1DM (67,68).

C. Sleep, Metabolism, Inflammation and HPA Activation

Research has shown that sleep plays an important role in metabolism. Physiologically, normal sleep is associated with characteristic changes in metabolism. Slow Wave Sleep (SWS) is associated with increased growth hormone secretion (69), which in turn decreases insulin sensitivity (70), altering glucose control. Rapid Eye Movement (REM) sleep is associated with decreased interstitial glucose concentration, perhaps due to increased brain glucose utilization (71). Experimentally restricting (73,74) or fragmenting sleep by brief arousals (72) resulted in decreased insulin sensitivity in healthy individuals.

Sleep also influences immune function, including inflammatory responses. In healthy individuals, monocyte and lymphocyte production decreases during sleep (75), and one night of sleep restriction (4 hours compared to 8 hours sleep) increases secretion of TNF- α and IL-6 by monocytes (76). One night of total sleep deprivation in healthy men, increased evening levels of TNF- α (77) as well as IL-6 and TNF- α receptor expression (78).

Disrupted sleep patterns also have been reported to cause altered cortisol secretion in healthy adults. Leproult and colleagues found elevated evening cortisol secretion after partial and total sleep restriction (79). Mendoza and colleagues reported an association between elevated evening cortisol secretion and parent-reported sleep problems in children (80). Decreased morning salivary cortisol levels have been reported in people with self-reported sleep disruption (81). Further, decreased salivary cortisol levels have been reported in young adult women after a night of sleep restriction (3 hours total sleep) (82).

From the above evidence, it is clear that sleep plays a role in maintaining metabolic health, normal levels of inflammatory activity and HPA activation. The impacts of sleep and sleep disruption on IL-6, TNF- α and cortisol levels have not been systematically investigated in young adults with T1DM.

D. Sleep in T1DM

Self-reported sleep quality is reduced in both children and adults with T1DM (83–85). Perfect et al. reported that children with T1DM spent less time in deep SWS and more time in lighter sleep as compared to healthy controls (86) and Jauch-Chara et al. reported a trend toward less SWS and increased light sleep in young adults with T1DM when compared to healthy controls (87).

Several groups of investigators have reported a correlation between HbA1c and sleep disturbances. Self-reported sleep disturbances and trouble with initiating sleep have been positively correlated with HbA1c in children with T1DM (88,89). Perfect and colleagues reported a negative association between HbA1c and percent of time in SWS in children with T1DM (86) and Barone et al. recently reported that HbA1c was positively associated with the number of full awakenings from sleep in adults with T1DM (90). Further, adults with T1DM who had short sleep duration (less than 6.5 hours per night) had significantly higher HbA1c levels as compared to those with sleep durations longer than 6.5 hours (91). One possible mechanism for these findings is that sleep disturbances result in decreased insulin sensitivity thus resulting in impaired glycemic control. Indeed, insulin sensitivity was decreased

after a single night of partial sleep restriction as compared to a normal night of sleep (4 hours compared to 8.5 hours) in young adults with T1DM (92).

Conversely, variations in glucose level commonly occur during the sleep period and likely influence sleep architecture in people with T1DM. The impact of hypoglycemia on sleep has been the focus of most investigations into the relationship between glucose level and sleep in T1DM. This is important as hypoglycemia-related seizures and death are more common during the night and this likely reflects the decreased response to hypoglycemia observed during sleep (93–95). Non-severe nocturnal hypoglycemia is common in patients with T1DM (96–99) and patients report difficulty falling back to sleep after awakening from hypoglycemia during the night (100,101). In a small study, there was no difference in sleep architecture found between teenagers with T1DM who experienced spontaneous hypoglycemia (<2.5 mmol/L) and those who did not become hypoglycemic. However, only six of the total 20 subjects experienced hypoglycemia in this study in which blood glucose was obtained via IV catheter every 30 minutes (102). Matyka and colleagues reported that the number of full awakenings was significantly higher in children with T1DM, but this was not related to occurrences of hypoglycemia as measured by a continuous glucose monitoring system (CGMS) (103). In the same study, SWS was significantly more prevalent during episodes of hypoglycemia (103). Increased motor activity, measured by actigraphy, was associated with hypoglycemia during sleep in adolescents with T1DM (104). In children, episodes of profound hypoglycemia were associated with increased SWS, but rapid declines in glucose (> 25 mg/dl/hour) were associated with increased awakenings from sleep (105). These results suggest that rapid fluctuations in glucose may impact sleep continuity in T1DM. Indeed, increased glucose variability was associated with number of awakenings in adults with T1DM (90). The effect of hyperglycemia on sleep has been minimally investigated in T1DM. In one recent study, investigators found that adults with T1DM with mean glucose levels > 154 mg/dL had decreased overnight urinary melatonin excretion (106). Thus, hyperglycemia may alter normal circadian cycling.

These findings highlight that there are physiological interactions between sleep and glucose homeostasis and that these may become disrupted or exaggerated in individuals with T1DM – who lack an intact pancreatic control system to regulate glucose level – leading to wide fluctuations in glucose level during both wakefulness and sleep. However, the role of glucose variability in sleep disruption in young adults with T1DM has not been systematically investigated.

E. Framework and Aims for Study

Review of the literature argues that altered glucose homeostasis, which is characteristic of T1DM, leads to development of inflammation and, as a consequence, to development of CVD. Sleep has been shown to play an important role in maintenance of metabolic and CV health and sleep disruption consistently is reported in people with T1DM, but the mechanisms behind this disruption are unclear. I hypothesize that glucose variability associated with T1DM may play a causative role in sleep disruption and this sleep disruption may contribute to increased inflammation over time in people with T1DM. Figure I provides an overview of the conceptual schema for my dissertation study. Aim 1 was to quantify sleep disturbances and to determine the relationship between glucose variability and sleep architecture in young adults with T1DM. Hypothesis: Fluctuations in interstitial glucose level as measured by a CGMS consistently precede and are causally related to sleep disruption (e.g. arousal, awakening, decreased electroencephalogram [EEG] delta power, increased EEG alpha power). Aim 2 was to quantitatively define the relationships among sleep, inflammatory cytokines, and endocrine stress markers measured before and after sleep in young adults with T1DM. Hypothesis: Plasma levels of IL-6, TNF- α , and cortisol are significantly elevated following sleep as compared to pre-sleep.

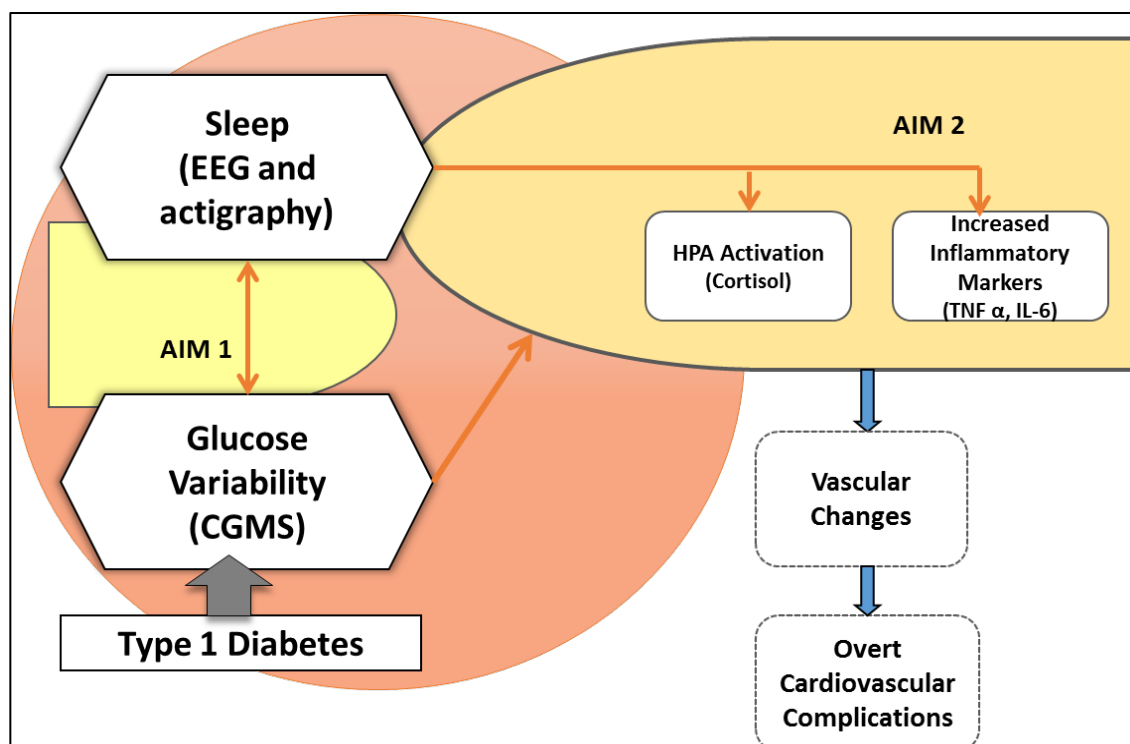


FIGURE I: CONCEPTUAL FRAMEWORK FOR DISSERTATION STUDY

I hypothesize that disturbed sleep plays a key role contributing to elevated CVD risk and CV stress markers in young adults with T1DM – both directly, and by mediating the impact of glucose variability. **Aim 1** is to quantify sleep disturbances and to determine the relationship between glucose variability and disturbed sleep in young adults with T1DM. **Aim 2** is to characterize the relationship between sleep and markers CV stress and CVD risk in young adults with T1DM measured before and after sleep.

F. Overview of Dissertation Study

Subjects who were 18-30 years old, with T1DM for at least five years and who used pumps for insulin delivery were recruited from the Chicago area. Subjects were excluded for any of the following reasons: worked night or rotating shifts; reported being pregnant; reported diagnosed CVD (with the exception of controlled hypertension); reported being diagnosed with diabetic complications (e.g. retinopathy, nephropathy or neuropathy); were diagnosed with psychiatric disease or were taking psychoactive medications; were diagnosed with a sleep disorder or reported use of medications to aid in

sleep; a score of 14 or greater on the Patient Health Questionnaire-9 (PHQ-9); reported active use of illicit drugs; reported use of corticosteroids; had uncontrolled thyroid disease; or reported severe metabolic instability (e.g. hospitalization for hypoglycemia; occurrence of hypoglycemic seizures or ketoacidosis) during the previous 2 months.

Subjects were contacted by telephone, screened to ensure eligibility and scheduled for their initial visit. Upon arrival to the second floor at the University of Illinois at Chicago College of Nursing, subjects were provided with informed consent documents. After completing initial informed consent, study procedures were begun. Subjects provided demographic information including age, race, ethnicity and gender. A brief health history was obtained including smoking status, alcohol and caffeine consumption and general health status. Subjects completed the PHQ-9, the Epworth Sleepiness Scale (ESS) and the Pittsburgh Sleep Quality Index (PSQI). The standardized sleep and food diaries used for this study were explained to the subjects and operational guidelines for use of the CGMS and actigraphy monitor were reviewed. Subjects were instructed to wear the actigraphy monitor on their non-dominant wrist and not to remove it. The sensor for the CGMS was inserted in the abdominal subcutaneous fat tissue, the transmitter was attached to the sensor and the system was covered with tegaderm to prevent the sensor from falling out. Subjects were instructed regarding procedures for calibrating the system every 12 hours with a capillary glucose measurement. A brief physical examination was performed to obtain height, weight, hip and waist circumferences and vital signs (blood pressure, heart rate, oxygen saturation, respiratory rate). The heart and lungs were auscultated and the thyroid was palpated to rule out major abnormalities. A capillary glucose measurement was taken and a blood sample was collected to measure HbA1c and to perform a complete blood count. If a subject reported using thyroid medication, an extra venous blood sample was obtained for a thyroid stimulating hormone assay to ensure euthyroid status. This completed the initial visit.

Each subject spent the next three days and two nights performing their usual routines. On the third night, subjects arrived at the Sleep Science Center at the University of Illinois at Chicago for overnight polysomnography (PSG). PSG monitoring was performed by a registered polysomnographic technologist. PSG comprised computer-based recording (Respironics, Alice5®) of: 2 central, 2 frontal and 2 occipital EEG leads, bilateral referential electrooculogram, chin and anterior tibialis electromyogram, lead I electrocardiogram, respiratory movement of thorax and abdomen by piezoelectric strain gauges, airflow via nasal pressure cannula and oronasal thermistors and arterial oxygen saturation of hemoglobin by pulse oximeter. Lights out for each subject was between 10 and 11 pm and lights on was 6 am to ensure at least 7 hours of time in bed. Just prior to lights out, a venous blood sample was taken to measure IL-6, TNF- α and cortisol levels. Additional samples were obtained just after lights on and one hour after lights on to measure the same three markers. After the end of the sleep study and between venipunctures, subjects completed the Stanford Sleepiness Scale (SSS; a measure of subjective sleepiness) and performed the psychomotor vigilance task (PVT; an objective measure of vigilance and motor reaction time). Subjects returned the CGMS and activity monitors and received a \$250 cash remuneration for participation in the study.

G. Overview of Chapters

The results of the study are provided as chapters and are formatted as manuscripts for submission to peer-reviewed journals. In view of this fact, several abbreviations are defined at their first instance in each chapter. The second, third and fourth chapters provide the results of Aim 1 and the fifth chapter provides the results of Aim 2. The last chapter is a discussion synthesizing the findings from all chapters. Appendix A presents the rationale and mathematical details of the methods used for data analysis in Chapters 2-4. Appendix B outlines the methods employed to validate the Matlab code developed to implement the methods of Appendix A. A detailed presentation and rationale for the

methods employed in assays of inflammatory cytokines is provided in Appendix C. Current Institutional Review Board approval is contained in Appendix D.

II. COUPLING BETWEEN GLUCOSE VARIATIONS AND ACTIVITY DURING SLEEP AND WAKE OVER A 60-HOUR PERIOD

A. Introduction

Glucose levels fluctuate widely throughout the day and night in individuals with Type 1 Diabetes Mellitus (T1DM). Factors impacting glucose level, such as insulin sensitivity, exhibit both a circadian rhythm (107,108) and differences between sleep and wakefulness (109,110). However, there has been limited investigation into circadian and sleep/wake influences on glucose control in individuals with T1DM.

Structured physical activity (exercise) also influences glucose level in both healthy individuals (111) and those with T1DM (112,113). Routine “free-living” daily activity also may contribute to glucose variations, but there are limited data regarding this relationship. It is possible that variations in routine daily activity between sleep and wake may contribute significantly to sleep/wake- or circadian-related changes in glucose; but, again, this possibility has not been systematically studied.

It is likely that the coupling between physical activity and glucose variation is bi-directional and that the nature and strength of this relationship changes over the course of a 24-hour period; but this has not been directly established in individuals with T1DM. Thus, the purposes of this investigation were to: 1) quantify the coupling between glucose variations and routine physical activity over a 60-hour period; 2) determine differences in this coupling between sleep and wakefulness; and 3) identify the strength and timing of circadian variations in glucose/activity coupling in young adults with T1DM.

B. Methods

1. Protocol

Twenty-seven subjects with T1DM for at least five years, who wore insulin pumps and did not work rotating or night shifts, participated in the study. Individuals using medication that might alter sleep or wakefulness, or with uncontrolled thyroid disease, or who reported diabetes

complications were excluded. The Institutional Review Board of the University of Illinois at Chicago approved all study procedures. Informed consent was obtained from all individual participants.

After subjects provided informed consent, a subcutaneous abdominal sensor was placed for the continuous glucose monitoring system (CGMS; Guardian-RT™, Medtronic) and an activity monitor (Actiwatch2™, Respironics) was applied to the non-dominant wrist. Subjects then went about their normal daily routine and on the third night came to the laboratory for an overnight sleep study. We analyzed glucose and activity data collected from 6 pm on the first day through 6 am on the fourth day of the study. Average interstitial glucose was recorded every 5 minutes by the CGMS. The Guardian CGMS included a disposable sensor, a wireless transmitter and a monitor. The sensor sampled glucose levels every 10 seconds and the average value of these samples was transmitted wirelessly and stored by the monitor every 5-minutes. The overall system required calibration with a capillary glucose level every 12 hours; a procedure performed by the subjects throughout the protocol. The CGMS reports interstitial glucose concentrations between 40 – 400 mg/dl. After each subject completed the protocol, their glucose values were downloaded from the monitor using CareLink® software provided by the manufacturer. Activity count totals were logged every 30 seconds, smoothed (5-minute moving average) and resampled every 5 minutes to allow alignment with glucose values. For missing data, the last non-missing value was carried forward until the next non-missing point (maximum cumulative missing data was 120 min [2 subjects]). Sleep periods were determined using Actiware software (Respironics), using the default settings provided by the software. The wake threshold 40 activity counts for 10 minutes, the sleep onset threshold was 10 minutes of immobility.

2. Wavelet Coherence

Wavelet coherence analysis (WCA) identifies time varying and frequency specific coupling between two processes (114) and wavelet theory has been reviewed elsewhere (115). Briefly, wavelets are time-limited mathematical functions useful to decompose recorded physical activity and

glucose waveforms into different frequency components and to then compute the time varying coherence (coupling) between them at each underlying frequency (114). We utilized the Morlet wavelet function, performing computations with the wavelet coherence toolbox (Matlab 2013a) provided by Grinsted et al. This yielded updated coherence values every 5 minutes for each of 84 underlying oscillations with periods ranging from 10 to 1248 minutes. For the present analyses, we excluded all coherence values potentially influenced by “end effects”, as described by Grinsted et al. (114). To facilitate interpretation of the 60-hour recordings, we collapsed the 84 wavelet “scales” into six Bands with differing fluctuation period ranges (Band 1: 10-30 min; Band 2: 30-60 min; Band 3: 60-120 min; Band 4: 120-240 min; Band 5: 240-480 min; Band 6: 480-960 min). Each recording also was segmented according to Sleep and Wake periods; with each Wake period being bisected into equal halves, yielding three approximate 8-hour segments for each circadian day. Due to their shorter length, each of these segments was assessed by WCA using only the first four Bands (periods of 10 to 240 minutes). Because ANOVA demonstrated no significant differences ($p > 0.05$ for each) among the 3 Sleep intervals or among the 4 Wake sub-intervals, these intervals were separately averaged to provide a single mean coherence and mean phase for Sleep and for Wake for each Band in each subject.

To identify which computed coherence values were statistically significant ($p < 0.05$), we utilized Monte Carlo simulations ($N = 500$) (114). The mean coherence, number of intervals of significant coherence and mean duration of these intervals were tabulated for each Band of each recording. To allow more intuitive interpretation, the phase relationship between glucose and activity was converted to an equivalent delay (in minutes) as a function of time in each Band. ANOVA was used to identify differences in coherence parameters among the Bands and between Sleep/Wake intervals using each of these factors as a repeated measure (STATA 14; StataCorp). Pairwise differences between Bands and Sleep/Wake intervals were determined by post-hoc tests controlled by Scheffe’s test.

3. Bivariate Correlation

Pearson correlation coefficients were determined for the mean coherence values in each Band in relation to Hemoglobin A1c (HbA1c), mean glucose, and the Epworth Sleepiness Scale (ESS) score, a subjective measure of daytime sleepiness. These correlations were computed for the 60-hour recordings, and also stratified according to Sleep/Wake state.

4. Circadian Analysis

To characterize circadian variations in coherence, we utilized cosinor analysis. For each Band of each recording, we fitted (least-squares regression) a cosine wave with a period of 1440 minutes (24 hours) to the coherence data:

$$\text{Coherence} = \text{amplitude} * \cos ((2\pi * \text{time}) / 1440 + \text{phase}) + \text{constant}$$

We report the average Pearson correlation coefficient (r^2), amplitude and acrophase (clock time of peak coherence) of the best-fit cosine wave for each Band.

C. Results

1. Demographics

Twenty-three (9 males) of 27 subjects completing the protocol were included in the present analysis (2 subjects with apnea/hypopnea index >5; 2 subjects with >2h missing data were excluded). Included subjects had a mean \pm SD age of 24 ± 4.0 years, diabetes duration of 12.2 ± 4.9 years, HbA1c of $7.6 \pm 1.0\%$ (60 ± 10.9 mmol/mol) and body mass index of 26.0 ± 3.6 kg/m². All subjects wore their own insulin pumps (various manufacturers) during the study, and no changes were made to their usual insulin regimens or diabetes care.

2. Coherence

Figure II depicts the characteristic patterns of physical activity and glucose associated with time of day and Sleep/Wake intervals for a single subject (top panel). The lower panel displays the time and frequency dependent coherence between these two processes as a heat map. Globally, the

group-mean coherence over the entire 60-hour recording interval and over all fluctuation periods (10-960 min) was 0.39 ± 0.14 (SD). Mean coherence by Band was: Band 1: 0.38 ± 0.02 ; Band 2: 0.35 ± 0.04 ; Band 3: 0.34 ± 0.06 ; Band 4: 0.38 ± 0.08 ; Band 5: 0.39 ± 0.10 ; Band 6: 0.46 ± 0.19 . Mean coherence in Bands 2 and 3 was significantly lower than that for Band 6 ($p \leq 0.01$ for each).

It is evident (Figure II) that even within each Band, the coupling (coherence) between glucose and activity was time-varying, with multiple discrete intervals of statistically significant coherence exhibited during the 60-hour recording. Table 1 summarizes the average number and duration of these statistically significant intervals. ANOVA revealed significant independent effects of Band ($p < 0.00005$) and Sleep/Wake state (more intervals during Wake than Sleep; $p < 0.04$) on the number of intervals, with no interaction. The number of intervals of significant coherence decreased progressively from Band 1 to Band 6 (Table 1). Post-hoc contrasts (Scheffe) revealed that the numbers of significant intervals in Bands 1-3 were significantly different from each other as well as from Bands 4-6 ($p \leq 0.0005$ for each comparison); Bands 4-6 did not differ from one another. For the Sleep and Wake intervals, Bands 3 and 4 were significantly different from Bands 1 and 2 for both Sleep ($p \leq 0.037$ for each comparison) and Wake ($p \leq 0.0005$ for each comparison), however Bands 3 and 4 were not different from each other during either Sleep or Wake.

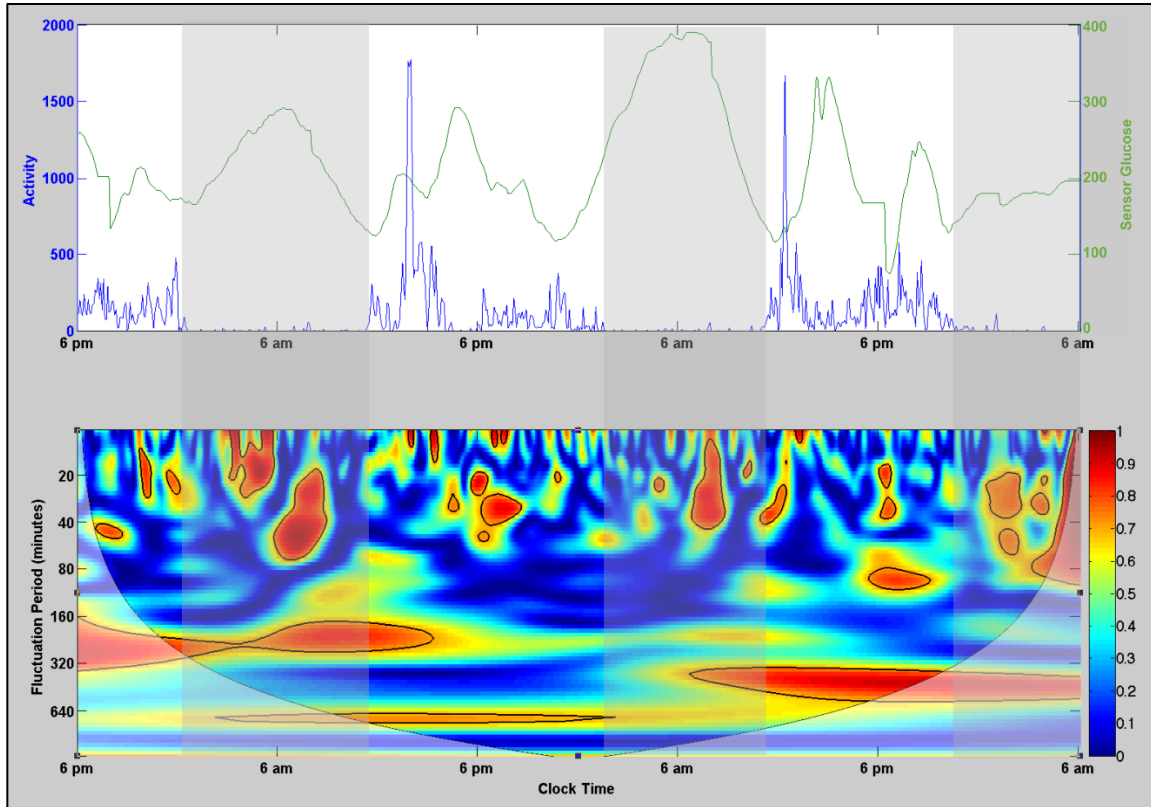


FIGURE II: EXAMPLE OF COHERENCE BETWEEN ACTIVITY AND GLUCOSE OVER 60 HOUR PERIOD

The top panel illustrates raw activity (total activity counts per 5-min; Blue) and glucose values (mg/dL; Green) over the 60-hour recording period, with clear daily (circadian) variations in both activity and glucose. Vertical shaded regions denote the recorded sleep periods for this subject. The bottom panel illustrates the time varying and frequency specific coherence between activity and glucose. The color bar at the right of this panel provides the scale for coherence (ranging from 0 – 1), with intervals of statistically significant coherence shaded red and enclosed by a black border.

		Band					
		1	2	3	4	5	6
60-Hour	N	23	23	23	22	20	14
	# Intervals	20.5 (2.5)	9.5 (2.5)	4.6 (1.3)	2.3 (0.9)	1.7 (0.6)	1.1 (0.3)
	Mean Duration	37.6 (8.0)	91.0 (22.3)	181.1 (82.7)	428.2 (214.2)	626.3 (301.2)	872.1 (477.7)
Wake	N	23	23	23	15	-	-
	# Intervals	9.3 (2.2)	4.5 (1.9)	2.3 (1.2)	1.5 (0.5)	-	-
	Mean Duration	35.5 (9.0)	79.5 (29.6)	139.0 (138.5)	311.1 (211.7)		
Sleep	N	23	23	23	18	-	-
	# Intervals	8.3 (2.3)	3.5 (1.3)	2.2 (1.1)	1.4 (0.6)	-	-
	Mean Duration	33.1 (11.7)	70.1 (32.3)	97.5 (66.9)	128.9 (84.9)	-	-

TABLE 1: SUMMARY OF NUMBER AND DURATION OF INTERVALS OF SIGNIFICANT COHERENCE

Mean Duration is reported in minutes. N indicates the number of subjects that had at least one discrete interval of significant coherence. Values in parentheses indicate standard deviation.

The mean duration of the intervals progressively increased from Band 1 to Band 6 for the 60-hour recordings. One-way ANOVA with post-hoc contrasts revealed that mean durations in Bands 1-3 were significantly shorter than in Bands 4-6 ($p < 0.02$ for each) and in Band 4 was significantly shorter than in Band 6 ($p \leq 0.0005$). Two-way ANOVA revealed significant effects of Band, Sleep/Wake state and their interaction on the mean duration of coherent intervals ($p \leq 0.0003$ for each). Stratified one-way ANOVA demonstrated (Table 1) that the mean duration of intervals of significant coherence in Band 4 was significantly shorter during Sleep than during Wake intervals ($F = 9.76$, $p = 0.004$). During Sleep and Wake, the mean duration of intervals in Band 1 was less than those in Bands 3 and 4 ($p \leq 0.001$ for

each [Sleep]; $p \leq 0.04$ for each [Wake]). During Sleep, Band 2 mean duration was significantly less than in Band 4 ($p = 0.02$) and during Wake, Bands 2 and 3 were significantly less than in Band 4 ($p < 0.0005$ for each).

Considering the temporal variations in coherence observed (Figure II; Table 1), we hypothesized that coupling would differ during Sleep versus Wake. Figure III illustrates the mean coherence within each Band for Sleep and Wake intervals. ANOVA using Band and Sleep/Wake state as within-subject repeated factors revealed a significant effect of Band ($F = 17.7$, $p < 0.00005$) on mean coherence, but the effects of Sleep/Wake state and its interaction with Band were not significant. One-way ANOVA with post-hoc comparisons revealed that mean coherence was highest in Band 4 (2 to 4 hour fluctuation periods) during both Sleep and Wake intervals ($F = 6.7$, $p = 0.0004$ and $F = 7.17$, $p = 0.0002$, respectively). The mean coherence in Band 4 differed significantly from coherence in Bands 1 and 2 during wake intervals ($p \leq 0.01$ for each) and from Bands 2 and 3 during Sleep intervals ($p \leq 0.013$ for each). In addition, in Band 1 (10–30 minute fluctuations) the mean coherence was significantly higher during Sleep (0.37 ± 0.04) than during Wake (0.34 ± 0.04) intervals ($F = 4.34$, $p = 0.04$).

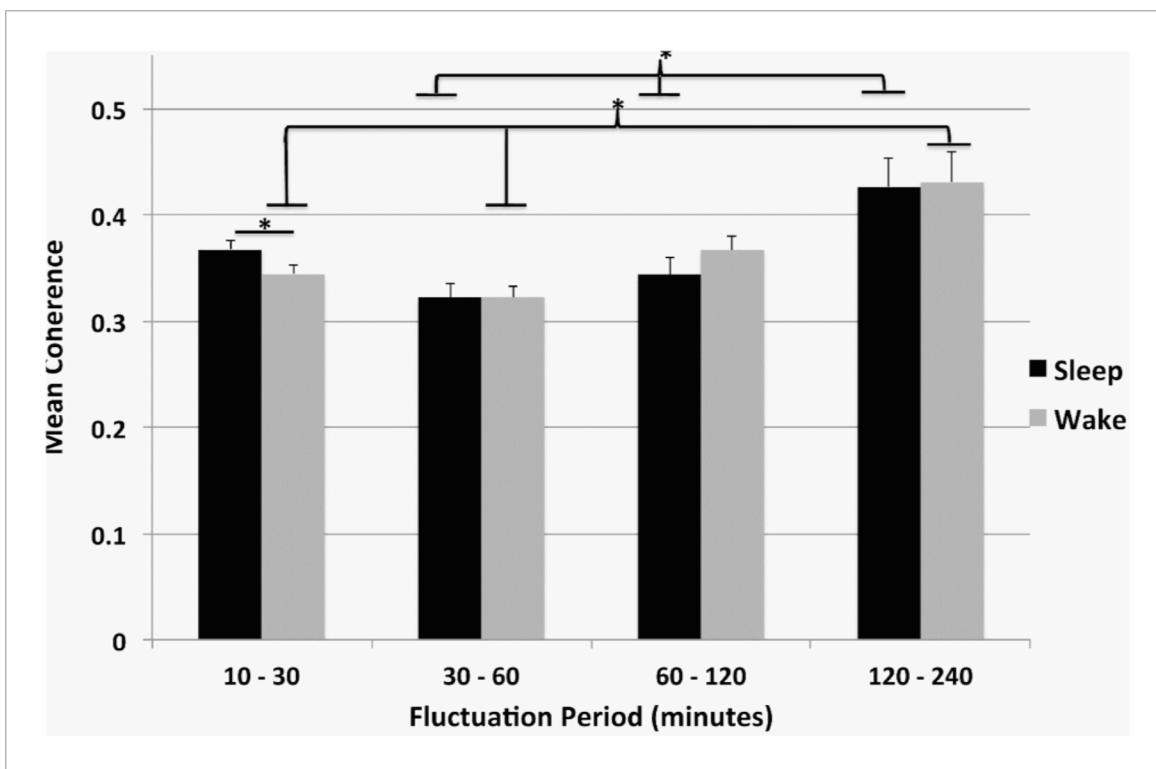


FIGURE III: MEAN COHERENCE BETWEEN ACTIVITY AND GLUCOSE DURING SLEEP AND WAKE STATES AT DIFFERENT FLUCTUATION PERIODS

* indicates $p < 0.05$.

Mean coherence was high (>0.30) for all Bands during both Sleep and Wake; with Band 4 exhibiting the highest mean coherence. Band 4 coherence was significantly higher than Bands 1 and 2 during Wake ($p < 0.05$ for each); and higher than Bands 2 and 3 during Sleep ($p \leq 0.05$ for each). Mean coherence in Band 1 (10-30 min fluctuations) was significantly higher during Sleep than during Wake

The temporal alignment between coherent fluctuations in glucose and activity is indicated by the phase calculation, which we converted to an equivalent delay, in minutes. Mean phase delay in Band 2 was significantly negative (changes in glucose leading changes in activity) for the 60-hour recordings (-1.5 ± 1.9 min, $p = 0.0014$); delays for all other Bands were not significantly different from zero. Figure IV presents the mean phase delay for each Band (1–4) during Sleep and Wake intervals. During Sleep intervals, the mean phase delay was negative in all Bands, indicating that changes in

glucose were consistently leading changes in activity. This negative delay was significantly different from zero only for fluctuation periods of 30 to 120 minutes (Bands 2 and 3; $p < 0.02$ for each; Figure IV). During wakefulness, the phase delay was significantly negative in Bands 1 and 2 ($p < 0.05$ for each) but was much more variable and, on average, positive (changes in activity leading changes in glucose) in Bands 3 and 4. One-way ANOVA revealed that mean phase in Band 3 was significantly more negative during Sleep versus Wake (-4.4 ± 7.1 min [Sleep] vs. 1.6 ± 4.9 min [Wake]; $F = 11.13$, $p = 0.0017$). The same Sleep/Wake trend was seen among Bands 2-4 (Figure IV).

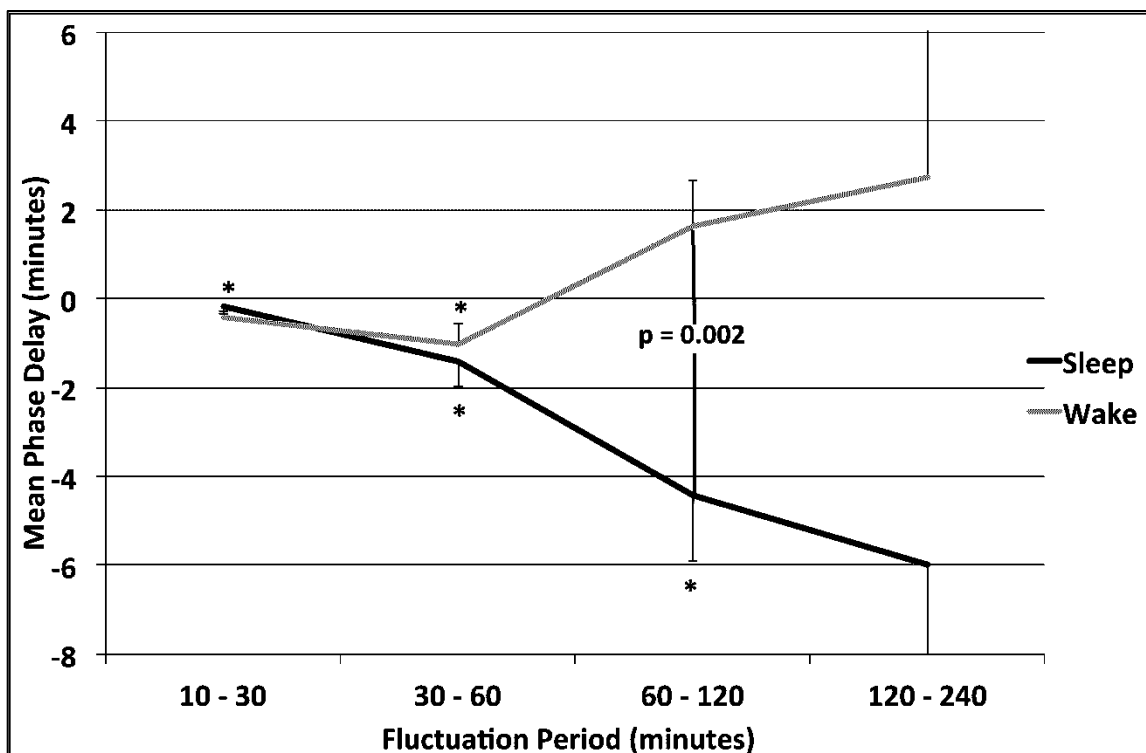


FIGURE IV: MEAN PHASE DELAY BETWEEN ACTIVITY AND GLUCOSE DURING SLEEP AND WAKE STATES AT DIFFERENT FLUCTUATION PERIODS

* indicates significantly different from zero ($p < 0.05$)

Data are mean \pm SD (reported in minutes); on average, changes in glucose occurred prior to (led) changes in activity during Sleep periods across all of the Bands; but no consistent pattern was observed across Bands during Wake periods. During Wake, the mean phase delay was significantly negative in Bands 1 and 2, whereas during Sleep, the mean phase was significantly negative in Bands 2 and 3 ($p < 0.05$ for each). In Band 3 the mean phase delay was significantly negative during Sleep with respect to Wake ($p = 0.007$).

3. Bivariate Correlation

Bivariate correlation applied to the 60-hour recordings revealed a significant negative relationship of mean coherence in Band 1 to mean glucose ($r = -0.60$, $p = 0.003$) and a trend for the relationship of mean coherence in Band 1 to HbA1c ($r = -0.32$, $p = 0.13$). Similar relationships were observed during Sleep intervals: mean coherence in Band 1 versus mean glucose ($r = -.55$, $p = 0.007$) and HbA1c ($r = -0.38$, $p = 0.07$). Mean coherence in Bands 1 and 2 during Sleep also demonstrated

significant correlations with the ESS score ($r = -0.44$, $p = 0.04$ for Band 1 and $r = -0.48$, $p = 0.02$ for Band 2); with higher coherence associated with less daytime sleepiness. Similarly, during Wake intervals there were significant negative correlations of mean coherence in Bands 1 and 2 with HbA1c ($r = -0.65$, $p < 0.001$ for Band 1; $r = -0.43$, $p = 0.04$ for Band 2)); and a trend for mean glucose ($p \leq 0.11$ for Bands 1 and 2). In contrast to Sleep, increasing coherence in Band 2 during Wakefulness was associated with increased daytime sleepiness measured by ESS ($r = 0.41$, $p = 0.05$). There was no relationship between ESS and mean coherence in any other Band during the Wake intervals ($p > 0.3$ for each).

4. Circadian Analysis

Figure V illustrates the best-fit circadian cosine waves overlaid on the time-varying coherence data for one 60-hour recording. For clarity, only Bands 2, 4 and 6 are presented; overall characteristics and fit for Bands 1, 3 and 5 were similar. The fit (r^2) tended to improve from Bands 1-4 and then decreased for Band 6. Table 2 provides the mean r^2 , amplitude and acrophase of the best-fit cosine waves for each Band. ANOVA ($F = 6.69$, $p \leq 0.0001$) with pairwise contrasts (Scheffe) revealed that the mean r^2 values for Bands 4 and 5 were significantly greater than those for Bands 1-3 ($p \leq 0.02$ for each) and 6 ($p < 0.0001$). ANOVA also demonstrated ($F = 4.43$, $p = 0.002$) that the amplitudes of circadian variations in coherence for Bands 1-3 and 5 were significantly lower than the amplitude for Band 4 ($p \leq 0.03$ for each comparison); and the amplitudes for Bands 2-5 were significantly higher than Band 6 ($p \leq 0.01$ for each comparison). The acrophase (time associated with peak coherence) ranged from 5 to 7 pm and was equivalent across all Bands.

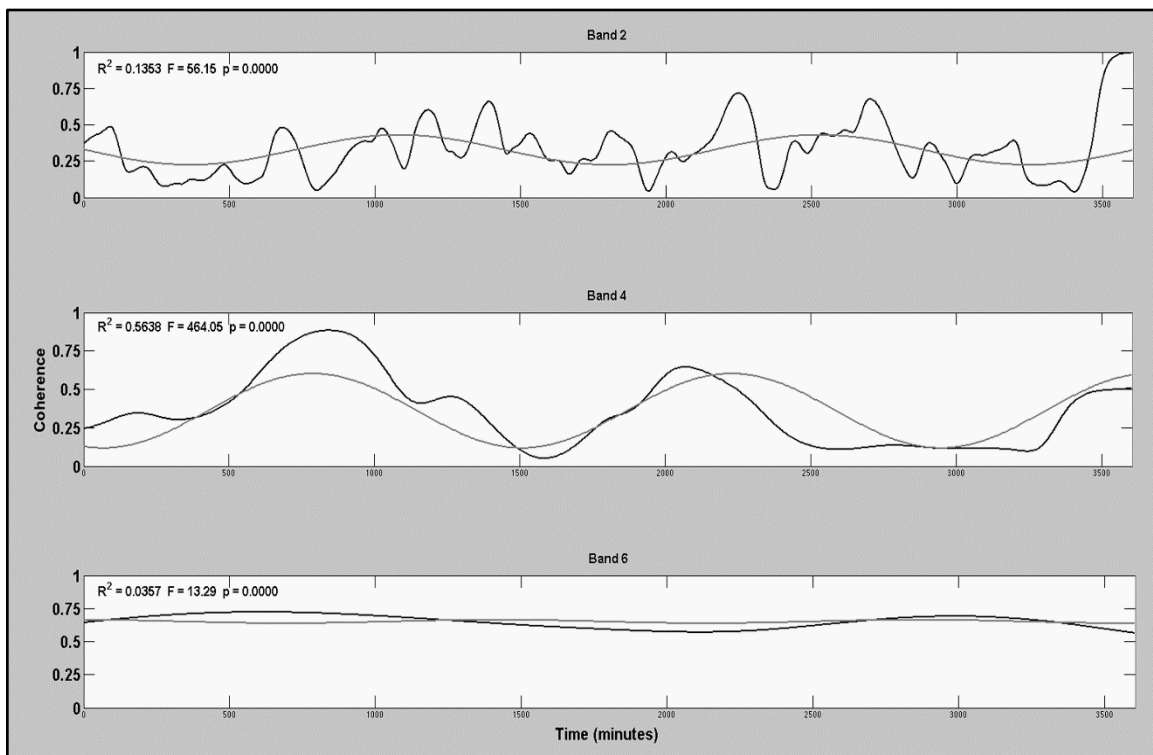


FIGURE V: EXAMPLE CIRCADIAN COSINE WAVE FIT OF COHERENCE IN 3 BANDS OVER 60 HOURS

Data are from one subject. In each subpanel, black line represents the actual time varying coherence data for one Band and the gray line depicts the best-fit cosine wave for that Band. For clarity only Bands 2, 4 and 6 are depicted.

Band	Mean r^2	Mean Amplitude	Acrophase (SD in min)
1	0.04 (0.03)	0.05 (0.02)	5:16 pm (210.6)
2	0.09 (0.05)	0.07 (0.03)	5:36 pm (172.7)
3	0.09 (0.08)	0.07 (0.04)	5:50 pm (185.7)
4	0.23 (0.17)	0.11 (0.06)	6:38 pm (201.5)
5	0.21 (0.18)	0.09 (0.04)	6:14 pm (203.4)
6	0.05 (0.05)	0.03 (0.02)	6:25 pm (199.5)

TABLE 2: PARAMETERS OF CIRCADIAN COSINOR REGRESSION FOR COHERENCE

*signifies statistical significance

Mean r^2 was significantly higher for Bands 4 and 5 than for other Bands ($p \leq 0.01$ for each comparison).

Mean Amplitude was significantly higher for Band 4 than Bands 1-3 and 6 ($p \leq 0.03$ for each). Acrophase did not vary significantly between Bands.

D. Discussion

The present study represents a systematic evaluation of the relationship between routine physical activity and glucose variations across Wake and Sleep periods for multiple days in young adults with T1DM. Coherence analysis demonstrated substantial coupling between physical activity and glucose variations, with one-third to one-half of their variance being shared during both wakefulness and sleep. Moreover, our findings suggest multiple modes of activity/glucose coupling with differing characteristic time scales and potentially different physiological mechanisms of control. For example, although mean coherence was broadly equivalent during both sleep and wakefulness, coherence nonetheless demonstrated significant circadian variations over a 60-hour time span, and this circadian rhythm in coupling was distinctly strongest for activity/glucose fluctuations with periods between 2 and 4 hours. Conversely, only the most rapid fluctuations (periods of 10 to 30 minutes) demonstrated significant differences between wake and sleep states; with mean activity/glucose coherence being higher during sleep than wakefulness. It is also noteworthy that for rapid fluctuations with periods from

10 to 60 minutes, changes in glucose consistently preceded coherent changes in activity. For slower fluctuations, this timing relationship was much more variable; with glucose changes tending to lead activity changes during Sleep periods and vice versa during wakefulness.

We observed a consistent pattern of time-varying and frequency specific glucose/activity coupling: 1) mean coherence was highest for the slowest fluctuations examined and a small number of extended intervals of significant coherence typically was observed in these Bands; 2) rapid fluctuations (10–30 minutes) were characterized by somewhat lower mean coherence but a larger number of brief intervals of significant coherence. This latter mode of coupling may be of particular importance during sleep, as the mean coherence of rapid fluctuations was higher during sleep than wakefulness (Figure III). Further, phase calculations demonstrated that rapid glucose variations consistently led activity changes (Figure IV), suggesting the possibility that rapid changes of glucose during sleep led to awakenings, and attendant physical movements (activity), as has been reported in children with T1DM (105). Matyka and colleagues also found that children with T1DM had more disrupted sleep than healthy children. These awakenings were not associated with hypoglycemia, but the relationship between glucose variability and awakenings was not reported (103). Radan et al. showed that motor activity, assessed by actigraphy, was increased during periods of nocturnal hypoglycemia documented by serial blood samples in teenagers with hypoglycemia (104). Perhaps paradoxically, strong coupling between rapid fluctuations in glucose and activity during sleep also may impart clinical benefits, as we found that higher coherence in this Band was positively correlated with better short and long term glucose control (lower mean glucose and lower HbA1c, respectively), as well as reduced daytime Sleepiness (ESS score).

During wakefulness, mean coherence for rapid fluctuations was lower than during sleep, with glucose fluctuations consistently leading changes in physical activity. However, for slower fluctuations the delay differed significantly between Sleep and Wake intervals, with activity changes tending to lead glucose changes during wakefulness, by the opposite during sleep. These findings suggest that the

relationship between glucose and physical activity is likely both bidirectional and operating on multiple time-scales, especially during wakefulness. This would not be surprising, as during the daytime many factors including at least: calorie intake (116); aerobic and resistance exercise (117–120); and work, school and family demands, impact daytime glucose control in people with T1DM. Future, larger scale trials should be aimed to determine the mechanistic basis and full physiological roles for coherence between rapid fluctuations of glucose and activity, especially during sleep.

Circadian influences also impact the coupling between glucose variations and physical activity, with coherence of 2–4 hour activity/glucose fluctuations demonstrating the greatest circadian modulation (Figure V and Table 2); and with peak coupling during the early evening hours (Table 2). Multiple biological processes exhibit circadian patterns, including insulin sensitivity in individuals with T1DM (121,122), with the lowest values during the early morning hours (109). These factors may contribute to the circadian pattern of coherence reported here. Further, we allowed our subjects to engage in their normal exercise routines. Moderate physical exercise during the day increases the likelihood of nocturnal hypoglycemia (118,119). In adolescents with T1DM, glucose needs remained elevated for as long as 7-11 hours after completion of moderate daytime exercise (118,119). To the extent that glucose utilization rate impacts glucose/activity coherence, the above findings suggest that exercise may have contributed to a circadian variation in coherence in our subjects.

In summary, we report strong time- and frequency-dependent coupling between routine unstructured physical activity and glucose variations in young adults with T1DM. The strength and nature of coupling differed between sleep and wake and demonstrated circadian periodicity, with the peak coherence characteristically observed during the early evening hours. The associations of coherence with HbA1c and daytime sleepiness indicate potential clinical relevance of coupling between routine activity and glucose variations. Larger-scale, interventional studies will be needed to establish the mechanisms underlying these interactions and their full clinical implications.

III. COUPLING BETWEEN EEG POWER AND GLUCOSE CHANGES DURING SLEEP

A. Introduction

Accumulating evidence suggests a physiological relationship between sleep and glucose control that is both bi-directional and time varying. This relationship may be of clinical importance for individuals with Type 1 Diabetes Mellitus (T1DM), who rely on administration of exogenous insulin for management of their disease. Despite improvements in insulin delivery systems and even with close management, serum glucose levels fluctuate widely in people with T1DM (96,97). Such glucose variations may contribute to both the impaired sleep quality (84) and difficulty returning to sleep after non-severe hypoglycemia (101) reported by individuals with T1DM. Further, an association between rapid glucose fluctuations and awakenings from sleep has been reported in children with T1DM (105).

Conversely, sleep also plays a role in glucose homeostasis (123). A single night of experimental sleep fragmentation (increased arousals during sleep) or sleep restriction (to 4 hours) resulted in decreased insulin sensitivity in healthy adults (72) and those with T1DM (92). Moreover, even during a single night, normal variations in sleep depth are associated with alterations in glucose metabolism; and deep sleep is associated with increased growth hormone secretion and decreased insulin sensitivity (69). Despite this evidence, minimal research has been conducted to characterize the likely bidirectional and time varying interactions between sleep level and glucose in individuals with T1DM.

Using continuous measures of glucose and brain activity measured by electroencephalogram (EEG), it is possible to characterize the relationship between sleep and glucose in T1DM. Quantitative Electroencephalogram (qEEG) analysis provides a continuous measure of EEG power and its distribution over frequencies during the sleep period. Thus qEEG is a useful tool for tracking temporal fluctuations in sleep depth and sleep fragmentation during the night (124,125). Continuous glucose monitoring systems (CGMS) provide a continuous measure of glucose throughout the night and are commonly employed to monitor glucose levels in people with T1DM (96,126). Wavelet coherence analysis (WCA) is

a method that permits the assessment of both time varying and frequency specific coupling between two time series (114,127). This method has been widely employed in both econometric and neuroscience studies, but has not been applied to studies of glucose homeostasis. The purpose of this investigation was to characterize the coupling between glucose variations and qEEG sleep measures using WCA in young adults with T1DM. We hypothesized that this coupling would exhibit both time-varying and frequency specific characteristics through the night and the relationships identified would vary between high and low EEG frequencies.

B. Methods

1. Subjects

Thirty young adults, aged 18-30 years, who had been diagnosed with T1DM for at least five years and who used pumps for insulin delivery were recruited for the study. Exclusion criteria included self-report of: pregnancy; shift-work (night or rotating shifts); use of corticosteroids; diagnosis of primary cardiovascular disease, retinopathy, nephropathy or peripheral neuropathy; diagnosed a primary sleep disorder or chronic use of oral sleep medications; use of psychoactive medications (e.g. antidepressants) or illicit drugs (e.g. marijuana or cocaine); or recent history (last 2 months) of severe metabolic instability (e.g. hospitalization for hypoglycemia; occurrence of hypoglycemic seizures or ketoacidosis). Individuals with well-controlled hypertension (systolic pressure < 130 mmHg) or thyroid disorder (thyroid stimulating hormone level within normal range) were eligible to participate.

2. Study Protocol

Subjects came to the College of Nursing at the University of Illinois at Chicago for their first visit. After informed consent was provided and inclusion/exclusion criteria were verified, a continuous glucose monitoring sensor (Guardian® REAL-Time System, Medtronic MiniMed) was placed in the abdominal subcutaneous tissue, an actigraphy monitor (Actiwatch2, Respironics) was placed on the non-dominant wrist and subjects were instructed in their use. Subjects completed demographic

questionnaires as well as the Pittsburgh Sleep Quality Index (PSQI) (128) and Epworth Sleepiness Scale (ESS) (129). A venous blood sample was collected to measure hemoglobin A1c (HbA1c). Subjects left the laboratory and spent three days and two nights carrying out normal routine activity. On the third night, subjects returned for overnight polysomnography (PSG) at the Sleep Science Center of the University of Illinois at Chicago. A registered polysomnographic technologist applied the sensors and conducted the PSG study for each subject. PSG testing comprised computer-based recording (Respironics, Alice5®) of: 2 central, 2 frontal and 2 occipital EEG leads, bilateral referential electrooculogram, chin and anterior tibialis electromyogram, lead I electrocardiogram, respiratory movement of thorax and abdomen by piezoelectric strain gauge, airflow via oronasal thermistor and nasal pressure cannula and arterial oxygen saturation of hemoglobin by pulse oximeter. Lights out for each subject was between 10 and 11 pm and lights on was 6 am, ensuring at least 7 hours of time in bed. After the end of the sleep study, subjects filled out the Stanford Sleepiness Scale (SSS), a measure of subjective sleepiness, which completed their participation in the study.

3. Glucose Data

The Guardian CGMS included a disposable sensor, a wireless transmitter and a monitor. The sensor, which was inserted into abdominal subcutaneous tissue, sampled glucose levels every 10 seconds and the average value of these samples was transmitted wirelessly and stored by the monitor every 5-minutes. The overall system required calibration with a capillary glucose level every 12 hours; a procedure performed by the subjects throughout the protocol. The CGMS reports interstitial glucose concentrations between 40 – 400 mg/dl. After each subject completed the protocol, their glucose values were downloaded from the monitor using CareLink® software provided by the manufacturer. Mean overnight glucose and two measures of glucose variability (standard deviation [SD] and continuous net glycemic action for one hour periods [CONGA-1]) were determined from the CGMS.

4. EEG Data

Six EEG derivations were recorded: two frontal (F3/A2 and F4/A1), two central (C3/A2 and C4/A1) and two occipital (O1/A2 and O2/A1). All EEG signals were bandpass filtered (0 to 200 Hz) and digitized 500 times per second. For analysis purposes, EEG data collected during the PSG were imported into Matlab utilizing the EEGLab plugin (130,131). For each EEG derivation, we determined power in the Delta (0.5 - 4.0 Hz), Theta (4.03 - 8.0 Hz), Alpha (8.03 - 15.0 Hz), Beta (15.03 - 30.0 Hz) and Gamma (30.03 - 80.0 Hz) Bands as follows. For each 30-second EEG epoch the Fast Fourier Transform (FFT) periodogram was calculated and both the absolute and normalized (% total) power were calculated for each Band. For each Band, these values were averaged over 10 consecutive 30-second epochs to provide a statistically consistent estimate of absolute and normalized EEG power for each Band every 5-minutes; allowing for temporal alignment with the simultaneous interstitial glucose measurements provided by the CGMS. Temporal alignment between EEG and glucose signals was performed using high-resolution time stamps provided by both the Alice5 and CGMS devices.

5. Statistical Analysis

a. Wavelet Coherence Analysis

WCA was used to determine the coupling between glucose variations and EEG power in each Band for each EEG channel. WCA is useful to identify time varying and frequency specific coupling between two signals, and such applications have been reviewed in detail elsewhere (114,115,132). WCA relies on wavelet transformation of signals from the time domain into a joint time-frequency domain. This approach is particularly advantageous over traditional Fourier transformation when the underlying time series is not stationary. Briefly, wavelet transformation decomposes a signal into a family of components, each having the same sampling rate as the original signal but with each component representing a different time scale. This wavelet decomposition process is thus analogous to applying a “filter bank” to the underlying signal. Wavelet coherence involves computing the time-

varying coupling, or coherence, between two signals that have undergone wavelet decomposition. The result is a matrix providing the coherence coefficient – which is analogous to the squared correlation coefficient – as a function of time and time scale (or equivalently, frequency) (114,127).

As recommended by Grinsted et al., we utilized the Morlet wavelet function for the present analysis (114), as this function provides a balance between time resolution and frequency resolution. We utilized the wavelet coherence toolbox provided by Grinsted and colleagues in Matlab 2014b. This yielded updated coherence values every 5 minutes for each of 48 underlying oscillation scales with periods ranging from 10 minutes to 160 minutes. However, as described by Grinsted et al., coherence values computed at the end and beginning of a recording may be influenced by “end effects” and thus should be considered not valid (114). The Wavelet Coherence toolbox identifies the “cone of influence” for each period, indicating the values at the beginning and end of the recording period which are influenced by end effects. We only consider, and report in this paper, on the coherence values outside of the cone of influence (not influenced by end effects). The coherence values (in relation to glucose variations) of each EEG power Band were averaged across all channels to provide an average coherence for each Band. Finally, to facilitate interpretation of results, for each EEG Band we determined average coherence during periods of statistically significant coupling within each of three Ranges of fluctuation periods: Rapid (10-30 min fluctuation period), Moderate (30-90 min fluctuation period) and Slow (90-160 min fluctuation period].

To identify statistically significant coherence values ($p < 0.05$), we utilized Monte Carlo simulations ($N = 500$) as described by Grinsted and colleagues (114). The mean coherence, the number of intervals of significant coherence and the mean duration of the intervals of significant coherence were tabulated for each of the fluctuation period Ranges for each EEG power Band of each recording. Coherence analysis also provided the phase relationship between variations in interstitial glucose and each EEG power Band at each time point in each Range. To allow more intuitive interpretation of this

information, phase was converted to an equivalent delay (in minutes) for each fluctuation period Range. To identify potential coherence differences (with respect to glucose variations) for Sleep-related and Wake-related EEG power, we separately averaged coherence, number of intervals of significant coherence, duration of these intervals and equivalent phase delay for the Delta and Theta Bands (Sleep-related EEG activity) and again for the Alpha, Beta and Gamma Bands (Wake-related activity).

ANOVA was used to identify differences in coherence parameters among the fluctuation period Ranges and EEG Bands using each of these factors as a repeated measure and with post-hoc contrasts controlled by Scheffe's test (STATA 14; StataCorp). Paired t-tests were used to compare differences between coherence parameters for the Sleep versus Wake EEG groups. P-values of ≤ 0.05 are reported as significant.

b. Bivariate Correlation

Pearson product-moment correlation coefficients were determined for the mean coherence values in each Band in relation to Hemoglobin A1c (HbA1c) (a measure of average glycemic control), mean glucose and glucose variability (SD and CONGA-1) during the PSG study, standard clinical measures reported from visual scoring of the sleep study (% of each stage of sleep, number of awakenings and number of arousals), PSQI and ESS scores.

C. Results

1. Subjects

A total of 29 subjects completed the protocol. Two of the subjects had mild sleep apnea (Apnea Hypopnea Index ≥ 5), and were excluded from the analysis. Subject characteristics are provided in Table 3.

N = 27	
Age (years)	23.8 (4.1)
Gender (M/F)	11 / 16
BMI (kg/m ²)	26.0 (3.3)
Duration of Diabetes (years)	12.1 (4.6)
HbA1c (%)	7.9 (1.4)
Mean Overnight Glucose (mg/dL)	137.6 (55.8)
CONGA-1 Glucose (mg/dL)	17.9 (9.3)
Std. Deviation Glucose (mg/dL)	22.7 (13.7)
ESS (0-24 range)	4.7 (2.6)
PSQI (0-21 range)	4.7 (2.3)
SSS (0-7 range)	2.4 (0.63)
Total Sleep Time (minutes)	372.8 (42.0)
Stage 1 (% Total Sleep Time)	6.4 (4.3)
Stage 2 (% Total Sleep Time)	51.1 (8.6)
Stage 3 (Deep Sleep) (% Total Sleep Time)	21.1 (5.0)
REM (% Total Sleep Time)	21.4 (6.2)
Sleep Efficiency (%)	81.4 (8.8)
Sleep Onset Latency (minutes)	36.2 (18.4)
# Arousals	30.7 (19.7)
# Awakenings	24.9 (9.4)
Wake After Sleep Onset (minutes)	52.7 (34.9)

TABLE 3: DEMOGRAPHIC, GLYCEMIC CONTROL AND SLEEP CHARACTERISTICS OF SUBJECTS

Mean (SD) is reported for all continuous variables, gender is reported as Male/Female breakdown. ESS: Epworth Sleepiness Scale (higher numbers indicate higher sleepiness, scores greater than 10 indicate clinically significant sleepiness); PSQI: Pittsburgh Sleep Quality Index (higher numbers indicate poorer sleep quality; scores > 5 indicates poor sleep); SSS: Stanford Sleepiness Scale (higher numbers indicate increased sleepiness, measured after PSG).

2. Coherence

The top panel in Figure VI plots glucose and power for the Theta EEG Band as a function of time throughout the PSG study for one EEG channel (O1/A2) of one subject. The bottom panel plots the coherence of glucose with Theta power. Intervals of statistically significant coherence are red in

color and surrounded by a black line. As illustrated, there were intervals of high coherence between the signals within all period Ranges at varying times through the PSG recording.

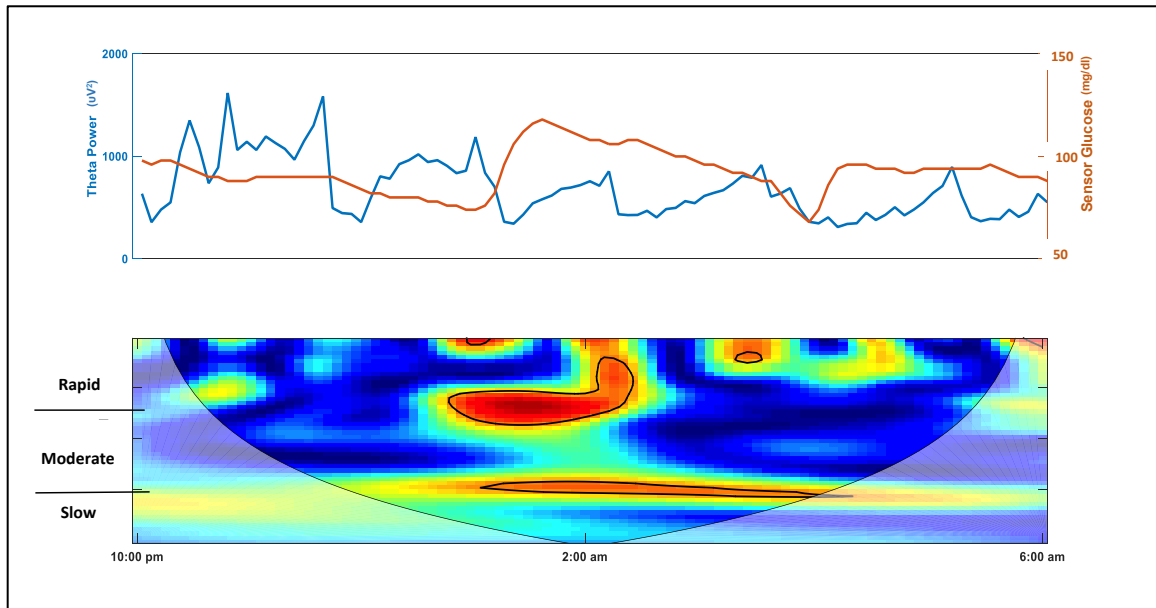


FIGURE VI: EXAMPLE OF COHERENCE BETWEEN THETA EEG POWER AND GLUCOSE DURING SLEEP

Top Panel: EEG power in Theta Band (blue) and glucose (red) sampled every 5 minutes for entire PSG study. **Bottom Panel:** Heat map depicting frequency specific and time varying coherence between EEG power in Theta Band and glucose over PSG study. Red areas bounded by a black line indicate statistically significant coherence ($p < 0.05$), based on Monte Carlo simulation. Ranges on the y-axis indicate the cut-points for the 3 fluctuation period Ranges (Rapid: 10-30 minutes; Moderate: 30-90 minutes; Slow: 90-160 minutes). The lighter shaded area indicates the cone of influence (COI) or areas where the results of coherence cannot be trusted. Only the values outside the COI (not shaded) were included in the analysis. More frequent but shorter intervals of significant coherence are present for the Rapid Range of fluctuations in comparison to Moderate or Slow fluctuations.

Figure VII illustrates the average number of intervals of statistically significant coherence, as well as the average duration of these intervals by Range for each EEG Band. Average number of intervals was highest for the Rapid Range of fluctuations in all Bands, and was never more than 1 for Slow Range

fluctuations. Repeated measures ANOVA revealed a significant effect of Range and subject ($p < 0.0001$ for each), but EEG Band did not have a significant effect ($p = 0.10$) on the number of intervals (Overall Model $F = 13.76$, $p < 0.0001$). Further, the duration of statistically significant intervals was shortest for Rapid and longest for Slow fluctuations ($F = 55.94$, $p < 0.0001$ for main effect of Range; $p \leq 0.0001$ for contrast between Rapid and Slow fluctuations), and was similar among all EEG Bands for Moderate and Slow fluctuations. For Rapid fluctuations, the aggregated mean duration of intervals in the Wake Bands (Alpha, Beta and Gamma; 28.3 ± 1.9 minutes [mean \pm standard error]) was significantly longer ($t = -2.15$, $p = 0.04$) than the aggregated mean duration of intervals for the Sleep (Delta and Theta; 22.2 ± 1.7 minutes) Bands.

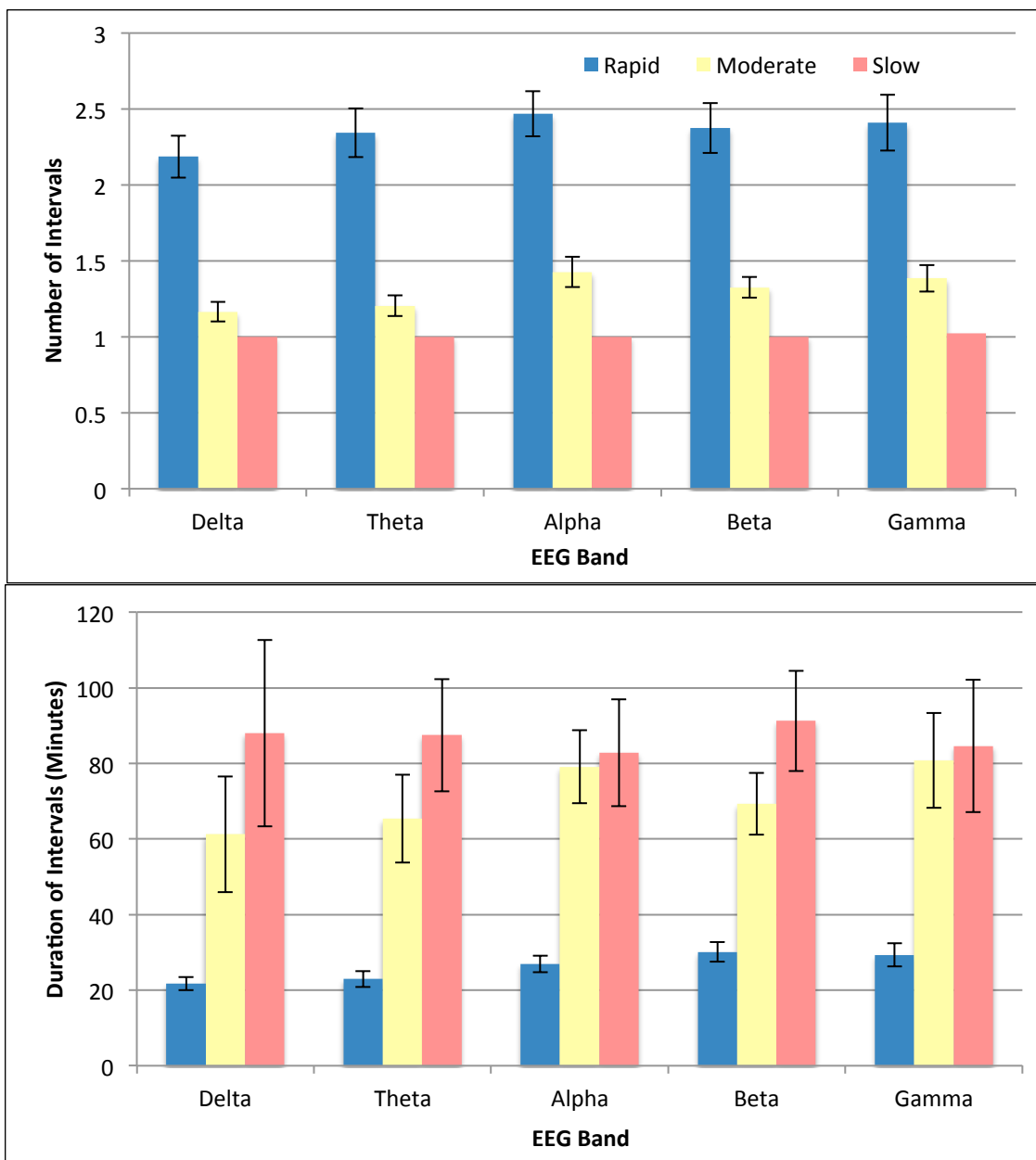


FIGURE VII: AVERAGE NUMBER AND DURATION OF INTERVALS OF SIGNIFICANT COHERENCE ACROSS FREQUENCY RANGES FOR ALL EEG BANDS

Top Panel Shows Number of Intervals and bottom Panel shows duration of Intervals. Slow Range fluctuations demonstrated significantly longer duration with fewer intervals of significant coherence as compared to the Rapid Range fluctuations across all EEG Bands.

Figure VIII illustrates the mean coherence values during intervals of significant coherence for each fluctuation period Range across the five EEG Bands. Mean coherence was significantly higher ($F = 5.27$, $p < 0.001$ for overall ANOVA) for Rapid fluctuations than for Moderate fluctuations ($p < 0.03$ for each Band). Slow fluctuations exhibited intermediate coherence (Figure VIII). These findings did not differ among the EEG Bands ($p = 0.40$).

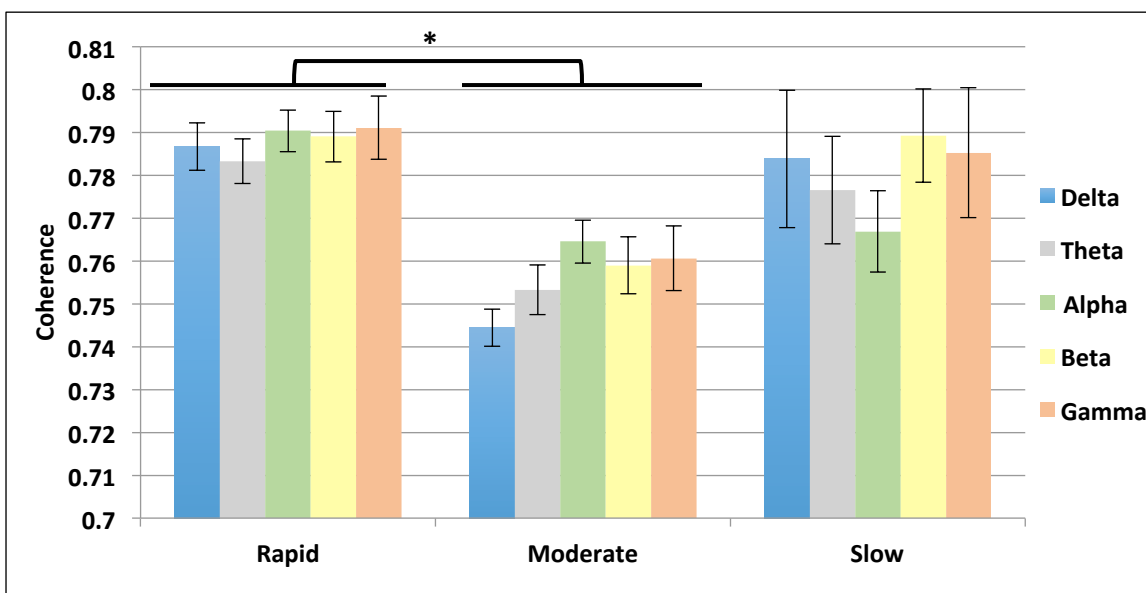


FIGURE VIII: MEAN SIGNIFICANT COHERENCE FOR FREQUENCY RANGES ACROSS EEG BANDS

* indicates significantly different

Mean Coherence for the Rapid Range (10-30 minutes) was significantly higher than the Moderate Range for all Bands ($p \leq 0.03$ for all comparisons). No differences were noted between EEG Bands.

Mean phase delay for Rapid and Moderate Range fluctuations was positive (EEG power leading glucose) in the Delta and Theta Bands and negative (glucose leading EEG power changes) in Alpha, Beta and Gamma Bands. For the Slow Range fluctuations this was largely inverted; phase delay for Delta, Theta and Beta was positive and for Alpha and Gamma was negative. However, these effects did not reach statistical significance using repeated measures ANOVA. As illustrated in Figure IX, a significant pattern did emerge, however, when pooling mean phase data for Delta and Theta (Sleep activity) versus Alpha, Beta and Gamma (Wake activity). Mean phase delay was significantly different from zero for the “Waking” EEG Bands in the Moderate Range (-3.81 ± 1.5 minutes, $t = -2.6$, $p = 0.02$), and this differed ($p = 0.06$) from the phase delay for the “Sleep” EEG Bands (1.7 ± 2.5 minutes) in this Range.

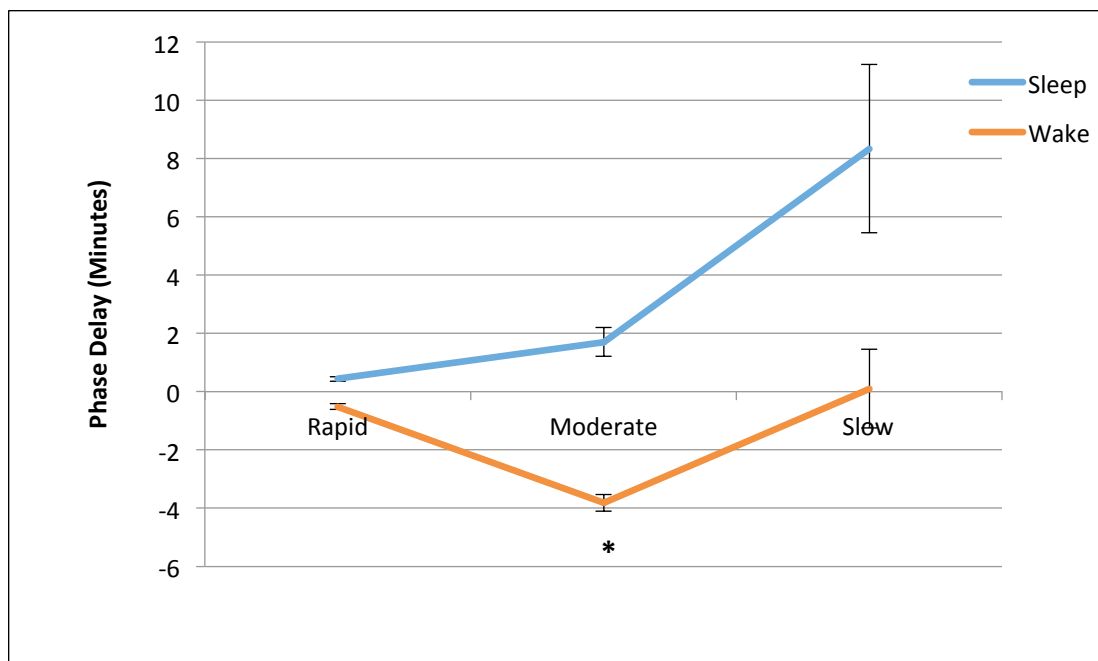


FIGURE IX: MEAN PHASE DELAY BETWEEN "SLEEP" AND "WAKE" EEG BANDS FOR FLUCTUATION RANGES

* Signifies significantly different from zero

On average, "Wake" EEG Bands (Alpha, Beta and Gamma) had negative phase delays and "Sleep" EEG Bands (Delta and Theta) had positive phase delays. Phase delay for Wake and Sleep EEG Bands were not different from each other for all the frequency Ranges, but Moderate Range fluctuations were significantly different from zero in the Wake EEG bands (-3.81 ± 1.5 minutes, $t = -2.6$, $p = 0.02$).

3. Bivariate Correlation

Table 4 provides a matrix of correlation coefficients assessed for coherence in each EEG Band and Range against measures of sleep, sleep quality, sleepiness and glycemic control. For Rapid fluctuations (10-30 minutes), significant negative correlations were found for Delta EEG Band coherence with SD of glucose ($r = -0.38$, $p < 0.05$) and sleep efficiency ($r = -0.41$, $p = 0.03$). There was a significant positive correlation between CONGA-1 and Gamma EEG Band coherence ($r = 0.48$, $p = 0.01$) in the Rapid Range. In the Moderate Range (fluctuations of 30-90 minutes), % of Rapid Eye Movement (REM) sleep was negatively associated with Theta EEG Band coherence ($r = -0.40$, $p = 0.04$) and CONGA-1 was

positively associated with Beta and Gamma EEG Band coherence ($r = 0.49$, $p = 0.01$ and $r = 0.41$, $p = 0.03$, respectively). Further, PSQI scores were positively associated with Beta and Gamma EEG Band coherence for fluctuations in the Moderate Range of periods ($r = 0.44$ and $r = 0.48$, $p < 0.02$, respectively). For Slow fluctuations, Theta EEG Band Coherence was significantly positively correlated with HbA1c ($r = 0.49$, $p = 0.02$) and Sleep Onset Latency ($r = 0.59$, $p = 0.004$).

N	Delta			Theta			Alpha			Beta			Gamma		
	Rapid 27	Mod 27	Slow 19	Rapid 27	Mod 27	Slow 21	Rapid 27	Mod 27	Slow 20	Rapid 27	Mod 27	Slow 21	Rapid 27	Mod 27	Slow 22
Mean Glucose	-0.36	-0.26	-0.04	-0.28	-0.01	0.27	0.12	0.21	-0.33	-0.09	-0.08	-0.15	-0.09	-0.01	-0.04
SD Glucose	-0.38*	-0.34	-0.07	-0.22	0.06	0.31	-0.15	0.22	-0.23	-0.02	0.23	-0.22	0.05	0.13	-0.11
CONGA-1	-0.17	-0.04	-0.03	-0.02	0.07	0.23	0.01	0.33	-0.10	0.34	0.49*	-0.16	0.48*	0.41*	0.05
HbA1c	-0.02	-0.23	0.18	-0.13	0.23	0.49*	-0.07	0.10	-0.39	-0.02	-0.15	0.08	-0.16	-0.18	-0.16
ESS	-0.29	0.01	-0.08	-0.10	-0.19	-0.08	-0.08	0.20	0.02	0.01	-0.11	0.09	-0.02	-0.18	-0.01
PSQI	-0.05	0.04	-0.25	0.07	0.21	0.00	0.37	0.16	0.03	0.16	0.44*	0.30	0.01	0.48*	0.06
# Arousals	0.01	-0.23	0.14	-0.14	0.09	0.27	-0.19	-0.03	-0.13	-0.17	-0.16	0.09	-0.31	-0.37	-0.11
# Awakenings	-0.09	0.06	-0.42	-0.15	0.17	-0.32	-0.04	0.01	-0.6*	0.09	0.10	-0.36	-0.12	-0.10	-0.41
% Stage 3	0.00	0.28	-0.03	0.01	0.12	0.05	0.20	0.13	0.27	0.08	0.18	0.01	0.14	0.15	0.30
% Stage 2	0.26	-0.26	0.03	-0.01	0.13	0.07	-0.19	-0.04	-0.24	-0.10	-0.09	-0.35	0.10	-0.04	-0.14
% Stage 1	-0.18	0.03	-0.17	0.01	0.16	-0.05	0.09	-0.05	-0.09	-0.02	0.05	-0.01	-0.16	0.03	-0.23
% REM	-0.23	0.11	0.10	0.00	-0.4*	-0.11	0.04	-0.02	0.21	0.08	-0.05	0.48*	-0.14	-0.09	0.08
WASO	0.29	0.10	-0.25	0.26	0.04	0.03	0.19	0.15	-0.02	0.03	0.31	-0.09	0.07	0.15	0.06
TST	-0.37	-0.06	0.15	-0.24	-0.16	-0.35	-0.21	-0.11	0.03	0.03	-0.15	0.05	-0.05	-0.03	-0.17
SE	-0.41*	-0.16	0.21	-0.28	-0.18	-0.29	-0.25	-0.19	0.05	-0.13	-0.25	0.17	-0.17	-0.21	-0.09
SLAT	0.32	0.12	0.19	0.20	0.23	0.59*	0.27	0.31	-0.01	0.22	0.03	0.03	0.21	0.10	0.26

Table 4: BIVARIATE CORRELATIONS OF EEG/GLUCOSE COHERENCE WITH STANDARD MEASURES OF SLEEP AND GLYCEMIC CONTROL

* indicates $p < 0.05$

Number under Frequency Range (Rapid; Mod; Slow) indicates number of subjects for each correlation.

D. Discussion

The present study demonstrates for the first time, to our knowledge, a high degree of time varying and frequency specific coupling between glucose variations and EEG power during sleep in young adults with T1DM. Statistically significant coherence, or coupling, was observed during a substantial portion of the night in all fluctuation period Ranges, but the temporal pattern of coupling differed among these Ranges. The strength of coherence during intervals of significance was highest for Rapid Range fluctuations (periods of 10-30 minutes) for all EEG power Bands (Figure VIII). Further, the average number of intervals of significant coherence was higher for Rapid fluctuation periods in all EEG power Bands. Our data also suggest differences in the nature of the coupling between glucose variations and EEG in sleep-related (Delta and Theta) versus wake-related (Alpha, Beta, Gamma) Bands during the sleep period. Specifically, both the average duration of intervals of significant coherence and the mean phase delay differed between wake-related and sleep-related Bands (Figures 7 and 9). Understanding the time-varying mutual relationship between glucose changes and brain activity during sleep may have future implications for disease management in people with T1DM.

Periods of strong coherence between variations in glucose and EEG power were seen in all three Ranges of fluctuation period and for all EEG power Bands. A relationship between glucose level and EEG power has been reported previously in people with T1DM. The neurons of the brain are dependent on glucose for fuel (133,134), thus a degree of coherence is expected between glucose variations and EEG power. Hypoglycemia, achieved using a hypoglycemic insulin clamp, has been shown to increase low frequency EEG power during wakefulness (135–137) as well as during sleep (138,139) in people with T1DM. A recent study in patients with T1DM revealed that spontaneous hyperglycemia during sleep was associated with increased power in both high and low EEG frequency Bands (140). Our findings extend the work of these investigators, as we found that fluctuations in glucose, irrespective of hyper or

hypoglycemia, are coupled to EEG power during sleep and that there is a time varying characteristic to this relationship, with the strength of coupling varying throughout the night.

We showed that intervals of significant coupling occurred most frequently and were of shorter duration for Rapid (10 to 30 minute) fluctuations (Figure VII). This suggests the possibility that rapid glucose fluctuations cause short-term awakening or arousals from sleep. Consistent with this view, it has been previously reported that children with T1DM had more awakenings than healthy controls (103) and that rapid changes (>25 mg/dL/hr) in glucose during sleep were associated with increased awakenings from sleep in these children (105). Adolescents (86) and young adults (141) with T1DM also exhibit reduced deep sleep and increased light sleep as compared to controls.

Significant coherence between glucose and EEG power also was observed for slower (periods from 30 to 160 minutes) fluctuations during discrete time intervals through the night (Figure VI). This observation supports the biological plausibility of slow changes in sleep depth driving, or causing, changes in glucose. Deep sleep exhibits a characteristic ultradian pattern of cycling through the night, with periodic increases of Delta power every 60 to 120 minutes (142). During deep sleep growth hormone secretion increases, which decreases insulin sensitivity and increases glucose (69,70,143). Thus, independent of the many other factors that may influence glucose level, after a period of delta sleep increased glucose would be expected. Although the present data do not directly address causality, intervals of significant coherence between glucose and EEG Delta power are consistent with the above mechanism. Likely due to the high rate of brain glucose utilization, REM sleep (manifested as reduced Delta and increased Theta power) is associated with decreased interstitial glucose levels (71). Thus, the normal cycling between deep and REM sleep may be expected to drive fluctuations in glucose with a period of 60 to 120 minutes. Again, the observed intervals of Delta and Theta power coherence with glucose on this time scale are at least consistent with this possible mechanism.

In the present study, glucose variability, measured by CONGA-1, was significantly associated with coherence between rapid (Rapid Range) fluctuations of glucose and EEG power in the Gamma Band. Further, CONGA-1 and PSQI score, a subjective measure of sleep quality, were significantly correlated with coherence in the Moderate Range fluctuations of glucose and EEG power for the Beta and Gamma Bands. The mechanisms underlying this association cannot be determined from the present study. But, to speculate, it is possible that changes in Beta and Gamma – EEG power associated with arousal/awakening – produced changes in glucose levels, possibly driven by sympathetic nervous system activation resulting in increased glucose variability and resulting in reduced subjective sleep quality.

Phase information derived from wavelet coherence analysis can identify the timing relationship between coherent oscillations of two signals. We converted the calculated phase information (in radians) to an equivalent phase delay (in minutes) to allow a more intuitive interpretation. This approach revealed that for 30 to 90 minute fluctuations, glucose changes were leading (and therefore potentially contributing to) wake-related EEG power changes, whereas sleep-related EEG power changes were leading (and therefore potentially contributing to) glucose fluctuations (Figure IX). Again, these relationships are consistent with the possible impact of slow-wave versus REM sleep on subsequent glucose levels described above. However, it should be noted that inter-subject variability for phase was high. Future studies with larger samples and healthy control subjects will be needed to identify consistent patterns of phase for coupled oscillations of glucose and EEG power in people with T1DM.

In summary, the present study shows, for the first time, a strong time and frequency specific coupling between EEG power and glucose variations in young adults with T1DM. Our findings are consistent with a bidirectional relationship between glucose and EEG power during sleep. Rapid fluctuations in glucose and EEG power exhibit periods of strong coupling, which suggests that rapid fluctuations in glucose may drive rapid changes in sleep EEG power. Strong coupling between slower

fluctuations of glucose and EEG also occur and may reflect characteristic changes of brain activity during sleep that alter glucose levels. Future studies with controlled interventions and healthy control subjects are needed to fully elucidate the causal mechanisms underlying the observed coupling between glucose and brain activity during sleep. Understanding this relationship in people with T1DM is clinically relevant, as both sleep and glycemic control are potentially modifiable. From this understanding, interventions may be developed to ultimately improve outcomes in people T1DM.

IV. CAUSAL RELATIONSHIPS BETWEEN EEG POWER AND GLUCOSE DURING SLEEP

A. Introduction

Recent research identifies sleep as an important process for maintenance of both cardiovascular (144) and metabolic (123) health. Children (85) and adults (84) with Type 1 Diabetes Mellitus (T1DM) report reduced sleep quality as compared to healthy age and gender matched individuals; and these reports are confirmed by objective laboratory polysomnography (PSG) (86,141). However, the mechanisms underlying disturbed sleep in people with T1DM remain poorly defined. Impaired glucose homeostasis has been hypothesized as a contributing factor to reduced sleep time and sleep continuity among individuals with T1DM. T1DM is characterized by inability of the Beta cells to produce insulin and a resulting reliance on exogenous insulin administration. Wide fluctuations in plasma and tissue glucose levels can occur anytime throughout the day or night, even with vigilant self-management.

Nocturnal hypoglycemia (96,97) and hyperglycemia (86) are common occurrences in T1DM. Moreover, rapid changes in glucose have been associated with arousals from sleep in children with T1DM (105). Beyond traditional visually assigned sleep stages and events, changes in electroencephalogram (EEG) power spectra may provide more sensitive information about sleep continuity and depth during a PSG study. Associations have been reported between quantitative EEG (qEEG) power and experimentally induced changes in glucose during wakefulness (136,137) as well as during sleep (138,139). However, little is known about the relationship between spontaneous glucose fluctuations and qEEG activity during sleep, and virtually nothing is known about potential cause and effect relationships between these processes in people with T1DM.

Granger causality analysis is a well-established methodology for identifying causal connectivity (145). The approach employs statistical estimation of the predictability of one time series based on knowledge of one or more others. Originally developed for econometric analysis, Granger causality has been extensively applied in neuroscience, but has not been used to examine interactions between

glucose and brain activity. Cross-correlation functions also have been used to support causal inferences by determining the “time shift” necessary to optimize the cross-correlation between two time series.

The notion here is that a cause must precede its effect, such that if a change in one signal consistently precedes (predicts) a subsequent change in a second signal, the former is a potential cause of the latter.

The aim of this study was to employ Granger causality and cross correlation function analysis to determine the relationship between spontaneous glucose fluctuations and qEEG measures of brain activity during sleep in young adults with T1DM. We hypothesized that: 1) sleep EEG and glucose exert bidirectional causal influences and 2) these causal interactions are EEG frequency specific.

B. Methods

1. Subjects

Young adults, 18-30 years old, diagnosed with T1DM for at least five years and treated with continuous subcutaneous insulin infusion were recruited for the study. Individuals were excluded if they: were pregnant; worked night or rotating shifts; reported use of corticosteroids; were diagnosed with primary cardiovascular disease, retinopathy, nephropathy or peripheral neuropathy; had uncontrolled hypertension or thyroid disease; were diagnosed with a primary sleep disorder or reported chronic use of oral sleep medications; reported use of psychoactive medications (e.g. antidepressants) or illicit drugs (e.g. marijuana or cocaine); or reported severe metabolic instability (e.g. hospitalization for hypoglycemia, hypoglycemic seizures or ketoacidosis) during the preceding 2 months.

2. Study Protocol

All procedures were approved by the institutional review board of the University of Illinois at Chicago. Informed consent was provided by all subjects prior to any study procedures. After verifying that all inclusion and exclusion criteria were met, a sensor (Guardian® REAL-Time System, Medtronic MiniMed) for the continuous glucose monitoring system (CGMS) was placed in the abdominal subcutaneous tissue and the CGMS was initialized for recording. An actigraphy monitor (Actiwatch2,

Respironics) was placed on the non-dominant wrist and subjects were instructed in the use of both devices. Subjects next completed the Pittsburgh Sleep Quality Index (PSQI) (128) and the Epworth sleepiness scale (ESS) (129), answered demographic questions and provided a venous blood sample for determination of hemoglobin A1c (HbA1c). Subjects then left the laboratory and spent three days and two nights carrying out their normal routine activity. On the third night, subjects underwent laboratory polysomnography (PSG) at the Sleep Science Center of the University of Illinois at Chicago. A registered polysomnographic technologist conducted all PSG procedures for each subject. Each PSG comprised computer-based recording (Alice5, Respironics) of: multiple EEG leads, bilateral referential electrooculogram, chin and anterior tibialis electromyogram, lead I electrocardiogram, respiratory movement of thorax and abdomen by piezoelectric strain gauges, airflow via nasal pressure cannula and oronasal thermistors and arterial oxygen saturation of hemoglobin by pulse oximeter. Lights out for each subject was between 10 and 11 pm and lights on was at 6 am, ensuring a minimum time in bed of 7 hours. After the PSG, subjects completed the Stanford Sleepiness Scale (SSS; a subjective measure of immediate sleepiness) to complete the protocol.

3. Glucose Data

The Guardian CGMS included a disposable sensor, a wireless transmitter and a monitor. The sensor, which was inserted into subcutaneous tissue, sampled glucose levels every 10 seconds and the average value of these samples was transmitted wirelessly and stored by the monitor every 5-minutes. The overall system required calibration with a capillary glucose level every 12 hours; a procedure performed by the subjects throughout the protocol. The CGMS reported interstitial glucose concentrations between 40 – 400 mg/dl. After each subject completed the protocol, their glucose values were downloaded from the monitor using CareLink[®] software provided by the manufacturer.

4. EEG Data

Six EEG derivations were recorded: two frontal (F3/A2 and F4/A1), two central (C3/A2 and C4/A1) and two occipital (O1/A2 and O2/A1). All EEG signals were bandpass filtered (0 to 200 Hz) and digitized 500 times per second. For analysis purposes, EEG data collected during the PSG were imported to Matlab utilizing the EEGLab plugin (130,131). For each EEG derivation, we determined power in the Delta (0.5 - 4.0 Hz), Theta (4.03 - 8.0 Hz), Alpha (8.03 - 15.0 Hz), Beta (15.03 - 30.0 Hz) and Gamma (30.03 - 80.0 Hz) Bands as follows. For each 30-second EEG epoch the Fast Fourier Transform (FFT) periodogram was calculated and both the absolute and normalized (% total) power were calculated for each Band. For each Band, these values were averaged over 10 consecutive 30-second epochs to provide a statistically consistent estimate of absolute and normalized EEG power for each Band every 5-minutes; allowing for temporal alignment with the simultaneous interstitial glucose measurements provided by the CGMS. Temporal alignment between EEG and glucose signals was performed using high-resolution time stamps provided by both the Alice5 and CGMS devices.

5. Statistical Analyses

a. Granger Causality

The statistical approach of Granger causality (146) was utilized to determine the relationship between changes in glucose and changes in EEG power in all 5 Bands. Briefly, Granger causality is a statistical test which identifies the predictability of one time series by one (or more) other time series. The Granger coefficient was determined through a series of vector autoregressive (VAR) linear models and was tested for significance. The non-negative Granger coefficient provides information about the rate of information transfer from one signal to the other (146). A significant Granger coefficient can be interpreted to mean that variable x Granger causes variable y because past values of x and y can better predict the present value of y than the past values of y alone (146,147). For each recording, we analyzed the possibility that EEG changes cause glucose changes (EEG→Glucose) and

the possibility that glucose changes cause EEG changes (Glucose→EEG). The Multivariate Granger Causality (MVGC) toolbox (148) for Matlab was used to perform the analysis (147). Stationarity (mean, variance and autocorrelation do not change with time) is an assumption of Granger causality and must be tested in order to ensure correct interpretation (146). The MVGC toolbox provides error checking which includes stationarity testing (147). Out of 780 total Granger tests, 39 did not meet the stationarity criteria (5%). Data from one subject violated stationarity for all EEG channels and this subject was not included in further analyses.

Whenever significant ($p < 0.05$) Granger causality was identified, the sense of the relationship between EEG power and glucose was examined in two ways: 1) the net sign of the significant VAR model coefficients was determined and 2) the direction and magnitude of the initial impulse response was measured. VAR modeling represented the impact of EEG on glucose as follows:

$$X_t = \sum_{k=1}^p A_{xx,k} * X_{t-k} + \sum_{k=1}^p A_{xy,k} * Y_{t-k} + \varepsilon_{x,t} + C$$

where:

X_t is glucose at time step t

Y_t is EEG power at time step t

$\varepsilon_{x,t}$ is the error term for x at time step t

p is the model order (determined using Akaike Information Criteria)

$A_{xx,k}$ is the kth order coefficient for x on x

$A_{xy,k}$ is the kth order coefficient for y on x

C is the constant for the regression equation

For each VAR model demonstrating significant causality, the regression process identified which of the $A_{xy,k}$ coefficients were statistically significant. The error term, $\varepsilon_{x,t}$, has a normal distribution with a mean of zero. To assess the directionality of the Granger causal influence of y on x, we determined the sign of the averaged significant coefficients. For example if the sign of averaged

significant coefficients was negative, we inferred that an increase in y caused a decrease in x . For any VAR model, the associated impulse response function (IRF) characterizes the impact of a one standard deviation increase in the input (y) for a single time step on the output (x). Although the IRF reflects the integrated effects of both y and x on future values of x , the initial response (time step 1) is determined solely by the influence of y on x . To explore the independent effect of y on x , we examined the IRF response of y on x exclusively at time step 1 (initial impulse response).

Across the 5 EEG Bands, the occurrence of significant Granger coefficients for EEG→Glucose and Glucose→EEG causality and the associated signs of the mean significant VAR coefficients and initial impulse response were tabulated using frequency tables and assessed using Pearson χ^2 . The median magnitude of the initial impulse response was compared between Bands using the Mann-Whitney U test. For each EEG Band, standard clinical measures of sleep architecture (149) (e.g. number of arousals, number of awakenings, wake after sleep onset [WASO], sleep efficiency [SE]) as well as glucose homeostasis (e.g. HbA1c, overnight mean glucose, standard deviation of glucose) were compared using t-tests between subjects who had significant Granger coefficients and those who did not.

b. Cross-Correlation Function

Cross-correlation function analysis determines the relationship between two time-series by applying a lag to one of the signals. The cross-correlation function extends simple correlation computation by identifying the best-fit lag. Extending the findings from the Granger causality analysis, the cross-correlation function can be useful to identify an optimal lag between two signals. Further, the correlation coefficient has a sign that provides information about the nature of the relationship between the two signals. The cross-correlation function between glucose and EEG power for each Band over the entire PSG recording was calculated, applying lags of -100 minutes to 100 minutes to glucose values. The maximum correlation-coefficient and the number of positive and negative extreme values (“peaks” and “troughs” with absolute values at least 50% of the maximum)

were calculated for each subject for all five EEG Bands for all 6 channels and then the coefficients and number of extreme values were averaged by Band across the channels. The correlation coefficients were z-transformed by calculating the inverse hyperbolic tangent of each coefficient to be able to compare average values to each other and to assess differences from zero (150). Reported values are untransformed values.

c. Bivariate Correlation

The Pearson product-moment correlation coefficient was determined for the normalized average power (% total) for all EEG Bands in relation to standard clinical measures of sleep and glycemic control.

C. Results

1. Subjects

A total of 30 subjects enrolled in the study and 29 completed the PSG. Of the 29, two had mild sleep apnea with an apnea hypopnea index (AHI) ≥ 5 , and were excluded from analysis. Table 5 presents the biometric characteristics, glucose control (HbA1c) and self-reported sleep quality and sleepiness of the 27 subjects included in the final analysis.

Descriptive Statistics (N = 27)	
Age (years)	23.8 (4.0)
Duration (years)	12.1 (4.6)
HbA1c (%)	7.8 (1.4)
BMI (kg/m ²)	26.0 (3.3)
Male (% total)	11 (39.3)
Caucasian (% total)	24 (88.9)
Current Smoker (% total)	1 (3.7)
PSQI (possible range 0-21)	4.7 (2.3)
ESS (possible range 0-24)	4.7 (2.6)
SSS (possible range 1-7)	2.3 (0.63)
Mean Overnight Glucose (mg/dL)	137.5 (55.8)
AHI (Apneas and hypopneas per hour)	0.83 (0.88)
TST (minutes)	372.8 (42.0)
Latency (minutes)	36.2 (18.4)
Efficiency (%)	81.4 (8.8)
Stage 1 Sleep (%)	6.5 (4.2)
Stage 2 Sleep (%)	51.1 (8.6)
Stage 3 Sleep (%)	21.1 (5.0)
REM Sleep (%)	21.3 (6.2)
WASO (minutes)	52.7 (34.9)
Number of Arousals	30.7 (19.7)
Number of Awakenings	24.9 (9.4)

TABLE 5: DEMOGRAPHIC, SLEEP AND GLYCEMIC CONTROL CHARACTERISTICS OF SUBJECTS

Data provided are Mean (SD) for all variables except Male and Caucasian which are reported as number (% total).

2. Granger Causality

Twenty-six out of the 27 subjects were included in the analysis because data from one subject violated tests for stationarity. Averaged across Bands, 51.6% of all subjects showed significant EEG→Glucose Granger causality and 27.0% of all subjects demonstrated significant Glucose→EEG Granger causality in at least one channel. There were 15 instances (2.0%) of mutual causality

(simultaneous EEG→Glucose and Glucose→EEG causality), 7 out of the 15 occurred in the Alpha Band.

As highlighted in Table 6, for both EEG→Glucose and Glucose→EEG causality, the proportion of tests exhibiting significant Granger coefficients varied among the EEG Bands. Statistically significant EEG→Glucose causality was more frequently observed in all EEG Bands. Statistically significant Glucose→EEG causality was observed most frequently for the Theta and Alpha (42.3%) Bands.

	Delta	Theta	Alpha	Beta	Gamma
EEG→Glucose	12 (46.2)	15(57.7)	12 (46.2)	15 (57.7)	13 (50.0)
Glucose→EEG	6 (23.0)	11 (42.3)	11 (42.3)	4 (15.4)	3 (12.0)

TABLE 6: NUMBER OF SUBJECTS WITH SIGNIFICANT GRANGER COEFFICIENTS ACROSS EEG BANDS

Number of Subjects with Significant Granger in at least one channel (%total), across all bands.

Figure X shows typical IRF graphs for Alpha and Theta Glucose→EEG causality for a single subject. As evidenced by the figure, the average initial impulse response was negative for Theta and positive for Alpha; Theta = $-8.57 \pm 28.9 \mu V^2$ (SD) and Alpha = $5.93 \pm 20.5 \mu V^2$, $p = 0.03$ for Median Test of equality. Table 7 provides the frequency of positive and negative values for significant VAR coefficients in subjects with significant Granger coefficients. In cases of significant Glucose→EEG causality, average VAR coefficients for the Theta EEG Band were most often negative and for the Alpha EEG Band were most often positive. Moreover, the proportion of negative versus positive VAR coefficients differed significantly between the Theta and Alpha EEG Bands ($\text{Chi}^2 = 6.7$, $p = 0.01$). Regarding significant Glucose→EEG causality in the Delta EEG Band, all subjects exhibited negative VAR coefficients ($p = 0.03$ versus equal likelihood of positive and negative coefficients) and the average initial impulse response

also was negative ($-542.7 \pm 1281 \mu V^2$). For significant EEG→Glucose causality in the Theta EEG Band, the VAR coefficients were more commonly negative and the average initial impulse response also was negative ($-0.33 \pm 0.7 \text{ mg/dL}$). The proportions of positive coefficients were significantly higher than negative coefficients for the Beta and Delta EEG Bands ($p = 0.01$ for each). The average impulse response was positive for Beta ($0.10 \pm 0.2 \text{ mg/dL}$) and nearly zero for Delta ($-0.04 \pm 0.15 \text{ mg/dL}$).



FIGURE X: IMPULSE RESPONSE FUNCTION EXAMPLES FOR GLUCOSE DRIVING ALPHA AND THETA EEG CHANGES

Impulse responses provide a measure of the impact of a one standard deviation change in the predictor variable (in this case glucose) on the dependent variable (EEG of Alpha and Theta) over time. After the initial step, the IRF is also influenced by the autoregressive effects of EEG changes on itself.

	Delta		Theta		Alpha		Beta		Gamma	
	Neg	Pos	Neg	Pos	Neg	Pos	Neg	Pos	Neg	Pos
EEG → Glucose	4	8	10	5	6	5	4	10	7	5
Glucose → EEG	5	0	7	3	2	6	2	0	2	1

TABLE 7: FREQUENCY OF POSITIVE AND NEGATIVE COEFFICIENTS FOR SIGNIFICANT VAR MODELS

Average net sign of significant coefficients for VAR models in Subjects with significant Granger coefficients, across EEG bands for each direction of causality. “Neg” indicates negative Sign and “Pos” indicates positive sign.

Subjects exhibiting significant Glucose→EEG causality in the Alpha or Theta EEG Bands experienced more arousals from sleep than did those without significant causality (39.42 ± 22.7 vs. 20.8 ± 10.0 , $p = 0.02$, respectively). The number of awakenings was significantly higher for subjects with significant Glucose→EEG causality in the Delta EEG Band as compared to those without significant causality (31.3 ± 9.3 vs. 22.2 ± 8.2 , $p = 0.02$). Subjects with significant Alpha Band EEG→Glucose causality had higher mean overnight glucose than did subjects without significant causality (163.2 ± 62.2 mg/dL vs 118.8 ± 42.5 mg/dL, respectively, $p=0.04$). Subjects with significant Theta Band EEG→Glucose causality had significantly less REM sleep and significantly more deep (Stage 3) sleep than did subjects without significant causality (REM: $19.0 \pm 6.2\%$ vs. $24.3 \pm 5.2\%$, $p = 0.03$; Stage 3: $23.1 \pm 5.4\%$ vs. $18.4 \pm 5.4\%$, $p = 0.02$).

3. Cross-Correlation Function

Figure XI shows the cross-correlation coefficients for one subject across all lags assessed for each of the five EEG Bands. A similar pattern was observed in most subjects: with the cross-correlation function characterized by multiple positive and negative extreme values for each Band, and with a prominent extreme value occurring at a lag near zero for all Bands. Out of 26 subjects, 24

(92.31%) subjects exhibited at least one negative and one positive peak in every EEG Band tested. Further, of the 26 subjects, 10 (38.5%), 13 (50%), 11 (42.3%), 12 (46.2%), and 16 (61.5%) exhibited extreme values at 0 ± 2 lags for the Delta, Theta, Alpha, Beta and Gamma Bands, respectively. Figure XII provides the average correlation coefficients across all lags for all subjects. There was a high degree of variability among subjects for the cross-correlation function at all lags assessed. On average, the peak correlation between glucose and EEG was provided by a lag near zero for all EEG Bands. The signs of the correlation coefficients for Delta and Theta Bands tended to be negative at a zero lag and tended to be positive for Alpha, Beta and Gamma.

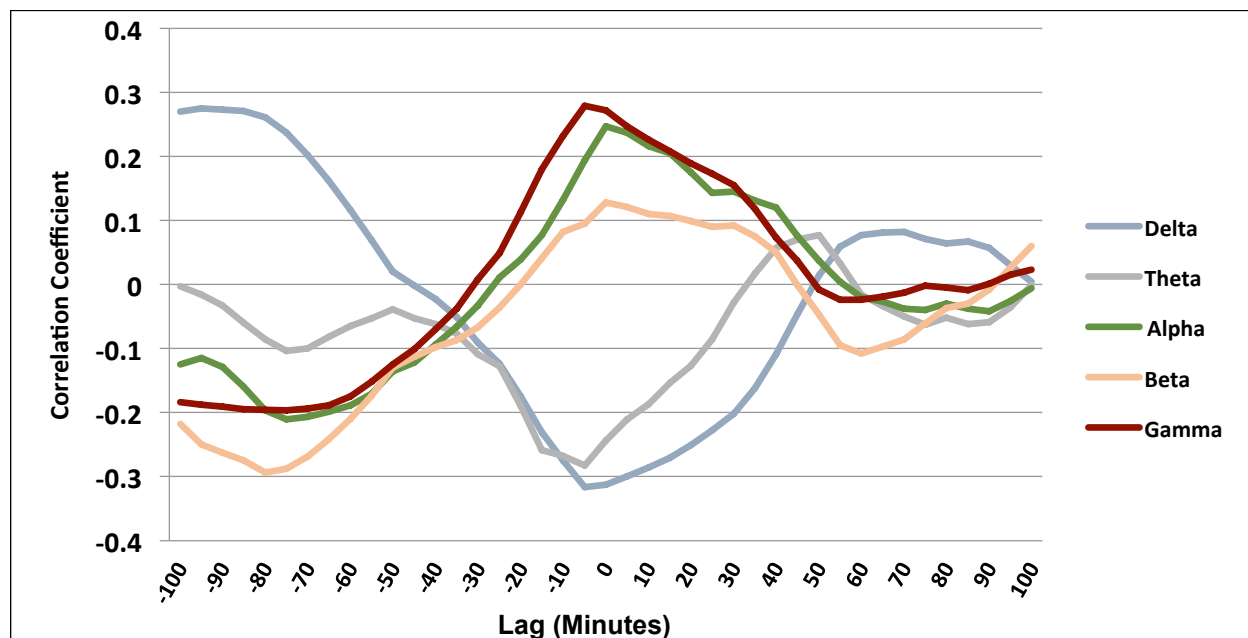


FIGURE XI: CROSS-CORRELATION FUNCTIONS FOR ONE SUBJECT ACROSS EEG BANDS

Lags were applied to glucose in five-minute increments up to ± 100 minutes (negative lag indicates glucose is leading EEG and positive lag indicates EEG leading glucose change). Most subjects exhibited multiple peaks at both positive and negative lags for all 5 EEG Bands.

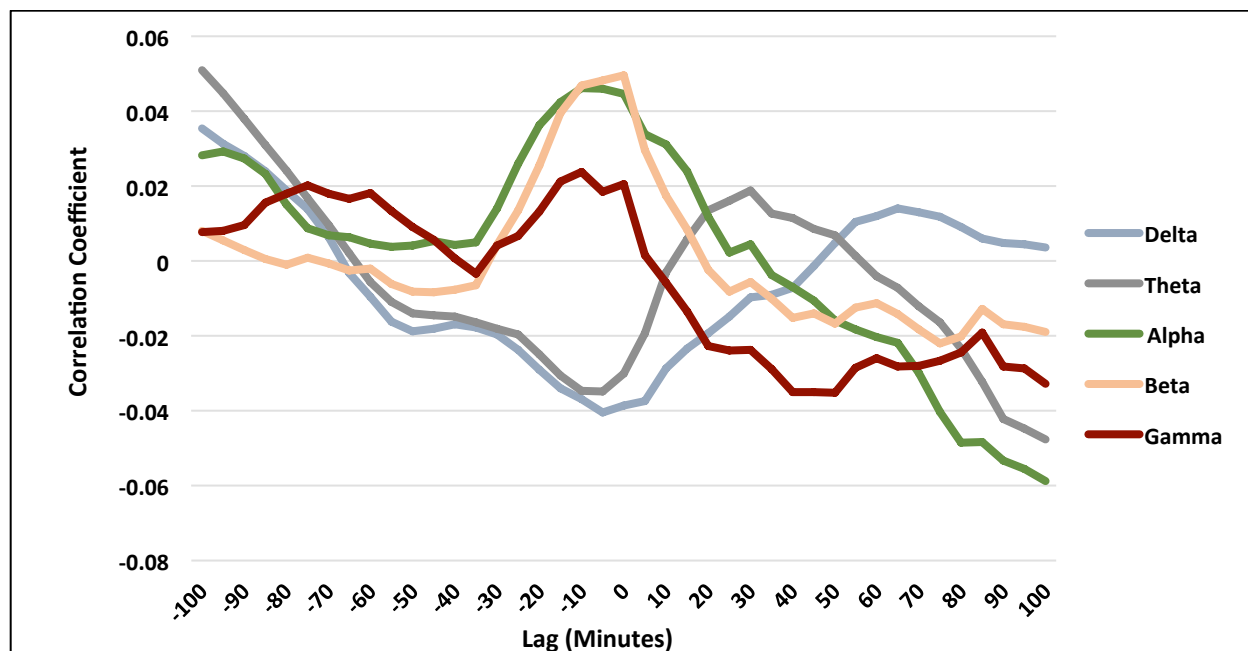


FIGURE XII: MEAN CROSS-CORRELATION FUNCTIONS ACROSS EEG BANDS

The sign of correlation coefficients were highly variable for subjects. Most subjects had an extreme value at or near a zero lag and the sign tended to be negative for Delta and Theta (associated with sleep) and positive for Alpha, Beta and Gamma (associated with wake).

Because the initial impulse response demonstrated that glucose fluctuations caused oppositely-directed effects on Alpha and Theta activity, the maximum cross-correlation coefficients of glucose versus EEG power in the Theta and Alpha Bands were assessed for those subjects who had a maximum value within the range of 0 ± 2 lags (± 10 minutes). As depicted in Figure XIII, for these subjects, the average cross correlation coefficients for Theta and Alpha were different from each other (Theta: -0.25 ± 0.42 [mean \pm SD] and Alpha: 0.35 ± 0.40 , $p = 0.05$).

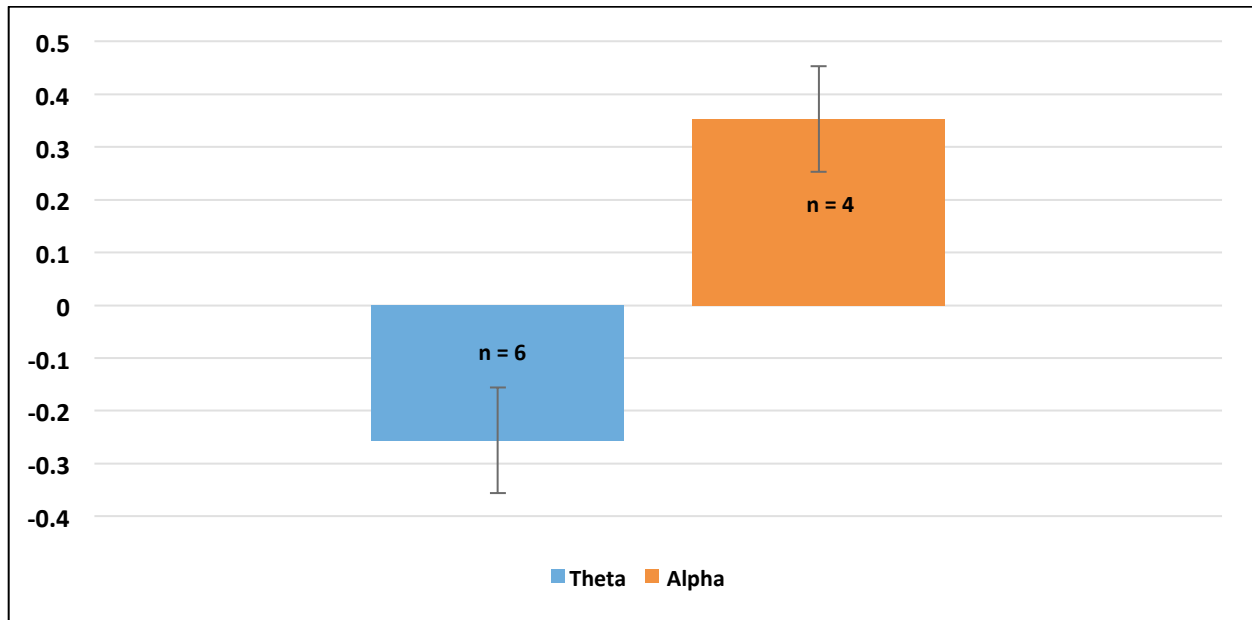


FIGURE XIII: PEAK CORRELATION COEFFICIENT FOR ALPHA AND THETA IN SUBJECTS WITH OPTIMAL LAG BETWEEN ± 10 MINUTES

Values were significantly different by un-paired t-test. Theta: -0.25 ± 0.42 and Alpha: 0.35 ± 0.40 , $p = 0.05$

4. Bivariate Correlation

Normalized Gamma power (high power associated with awakenings) was positively correlated with WASO ($r = 0.55$, $p = 0.003$) and negatively associated with SE ($r = -0.62$, $p = 0.001$).

Normalized Delta power was negatively associated with number of arousals (-0.45 , $p = 0.02$).

Normalized Theta power was negatively associated with number of awakenings (-0.42 , $p = 0.03$) as well as SSS score ($r = -0.38$, $p = 0.048$). HbA1c was negatively associated with number of arousals ($r = -0.52$, $p = 0.01$).

D. Discussion

In the present study we aimed to determine the relationship between glucose and brain activity assessed by quantitative EEG analysis in young adults with T1DM. Granger analysis supported our hypotheses that: 1) sleep EEG and glucose exert bidirectional causal influences and 2) these

relationships are EEG Band-specific. Across all 5 of EEG Bands, 70% to 100% of all subjects demonstrated a causal connection with glucose. Taken collectively, the present findings support the existence of both positive and negative feedback loops involving both glucose and brain activity in young adults with T1DM. Specifically, increasing glucose can drive changes in EEG activity consistent with arousal or awakening that, in turn, can cause either a further increase or a corrective decrease in glucose level. Cross-correlation function analysis revealed that interactions between glucose and EEG may occur on differing time scales, but that most subjects exhibited short-latency coupling with delays of ≤ 10 minutes. The bidirectional relationship between glucose level and brain activity during sleep identified in this study may have important implications for understanding glucose homeostasis and its management in young adults with T1DM.

Our findings support the view that increases in glucose can cause arousals or awakenings from sleep in young adults with T1DM. Both the average sign of significant VAR coefficients (Table 7) and the initial impulse response function (Figure X) demonstrated that increasing glucose frequently was causal to a shift from Theta Band to Alpha Band EEG power; a shift consistent with arousal or awakening. Results from cross-correlation function analysis support this interpretation and further suggest that the relationship between increases in glucose and sleep disruption most often have a short latency. As expected from the VAR coefficient and initial impulse response analyses, the cross correlation coefficients between glucose and EEG power exhibited opposite signs for the Alpha and Theta Bands (Figure XIII) in subjects with a peak correlation at a lag of ≤ 10 minutes. Also consistent with the interpretation that increasing glucose drives arousal or awakening, in subjects demonstrating Glucose \rightarrow EEG causality in the Delta Band the relationship was negative. In other words, increasing glucose decreases the Delta activity associated with deep sleep. The view that increases in glucose lead to short-latency disruptions in sleep is further supported by the finding that subjects with significant Granger coefficients for Glucose \rightarrow EEG causality in Alpha or Theta had a significantly higher number of

arousals from sleep than those who did not have significant Granger coefficients for either Band (39.4 ± 22.7 vs. 20.8 ± 10.0 , respectively).

It is also possible that a decrease in glucose leads to an increase in Theta and Delta and decrease in Alpha activity, suggesting a shift toward a deeper sleep. Indeed, multiple studies have shown that hypoglycemia induces EEG changes during wakefulness (135–137) and sleep (138,139) in people with T1DM. Tribi et al. (1996) found an increase in Theta and decrease in Alpha activity during induced hypoglycemia in 7 young adults (mean age 33 years) with T1DM (137). In a more recent study, Sejling and colleagues found similar results, EEG power in lower frequency Bands, most specifically the Theta Band, increased during induced hypoglycemia in 24 adults with T1DM while they were awake (151). Bendston and colleagues showed, in a small study of children with T1DM, that hypoglycemia (less than 2 mmol/L or 36 mg/dL) caused an increase in EEG power in the Delta and Theta Bands in 3 (out of 8) subjects (139) during sleep. Thus, consistent with our current findings based on Granger-causality analysis, decreasing glucose may lead to deepening of sleep.

Schultes et al. (2007) found that there was a decreased awakening response to hypoglycemia in adults with T1DM as compared to age-matched healthy controls (152). In a group of adolescents with T1DM, the occurrence of spontaneous hypoglycemia did not result in awakenings (153). A decrease in the epinephrine response to hypoglycemia induced by insulin-clamp has been reported in both children (94) and adults (93) with T1DM as compared to healthy controls. Further, a decreased awakening response to spontaneous hypoglycemia during sleep has been reported in children with T1DM (95). However, Pillar and colleagues reported that a rapid ($>25\text{mg/dL/hr}$) decrease in glucose levels was associated with awakenings from sleep in children with T1DM (105), suggesting the rate of change in glucose may play an important role in its impact on sleep processes. We cannot determine the time course between causal relationships reported in this study, thus it is possible that rate of change in glucose may be important in its effect on changes in sleep.

Additional interventional studies investigating the relationship between both the rate and direction of change in glucose values and their impact on EEG during sleep in people with T1DM are needed to fully understand the impact of glycemic variability on sleep continuity and depth. The present study is important in its demonstration of significant bidirectional causality between EEG and glucose during sleep in a naturalistic, non-interventional context. This important new evidence provides additional motivation to conduct interventional studies to more precisely determine the mechanisms underlying the observed causality.

The present Granger analysis also supports the conclusion that fluctuations in EEG power during sleep cause changes in glucose in young adults with T1DM. Specifically, we report that increases in high frequency (Beta Band) EEG during sleep can cause increases in glucose. Significant Granger coefficients for Beta EEG→Glucose changes were observed in over one-third of subjects. Moreover, the average sign of significant VAR coefficients and the average initial impulse response both were consistently positive, indicating that increases of Beta power caused increased glucose. We cannot determine mechanisms underlying this relationship from our study, but it is possible that this is due to impaired insulin sensitivity caused by increased wakefulness during the sleep period. It has been reported that sleep restriction leads to decreased insulin sensitivity the next morning in young adults with T1DM (92). In a recent study in nine children with T1DM, researchers showed that during sleep, spontaneous hyperglycemia was associated with an increase in EEG power, including Beta and Gamma Band powers (140). Our results extend these findings, suggesting that an increase in high frequency EEG during sleep may be causally linked to increased glucose levels in people with T1DM. Changes in Theta power were casually related to glucose changes in 15 subjects and on average, the direction of this relationship was opposite; increasing theta power was predictive of decreasing glucose. Theta power is increased during REM sleep; our findings support the previous report that REM sleep was associated with decreased concentrations of interstitial glucose in healthy individuals (71).

The sign of the VAR coefficients for EEG→Glucose causality in the Delta Band was more commonly positive, however the initial impulse response was close to zero (-0.04). It is well known that Delta power (a marker of slow wave sleep) has a normal ultradian cycling of around 90 - 120 minutes during the sleep period, which is stronger in the beginning of the night (154). Growth hormone is normally secreted during slow wave sleep which causes a decrease in insulin sensitivity (143). Thus, after a bout of slow wave sleep (or increased Delta activity), glucose levels may increase for a period of time. Our findings highlight a bi-directional relationship between EEG and glucose changes throughout one night of sleep. These relationships likely operate on different time scales through the night; rapid changes in glucose may drive arousals or awakenings; while changes in Delta power may result in increasing glucose levels over longer periods of time. Granger analysis does not provide information about the time-course of causal relationships.

Cross-correlation analysis can be helpful to identify the variability within the relationship between two signals across time. As illustrated in Figures 11 and 12, at short latencies, Band specific directionality was seen, with sleep related EEG (Delta and Theta power) exhibiting a negative relationship to glucose and wake related EEG (Alpha, Beta and Theta) exhibiting a positive relationship. However, we were not able to determine an optimal lag between glucose changes and EEG power in any of the Bands, likely due to the bi-directionality and potential time-varying nature of the relationship between glucose and EEG power. Indeed, as Figures 11 and 12 illustrate, all 5 Bands exhibited multiple local peaks in correlation over positive and negative lags. At periods where EEG is driving glucose changes, the cross-correlation is expected to have an extreme value at a positive lag and when glucose is driving EEG changes, the cross-correlation is expected to have an extreme value at a negative lag. The bidirectional relationship between glucose and EEG power throughout the night may be why we could not find a single optimal lag between glucose and EEG power; when averaged across the night, these opposite relationships decrease the correlation coefficient at all lags.

Delta and Theta Band activity are more prevalent during sleep whereas Alpha, Beta and Gamma Band activity are more prevalent during wakefulness. Investigating the correlation between normalized banded power and traditional measures of sleep continuity/disruption, we found, as expected, that less Delta power was associated with a higher number of arousals and lower Theta power was associated with an increased number of awakenings and higher levels of subjective sleepiness (SSS score) the next morning. We also found that HbA1c and number of arousals were significantly correlated, providing further support that disrupted sleep is related to poor overall glycemic control. Barone and colleagues reported a positive correlation between number of awakenings from sleep and HbA1c in adults with T1DM (90). Other authors have reported a negative relationship between HbA1c and time spent in slow wave sleep in children and adults with T1DM (86,155). The mechanism behind this may be due to impaired insulin sensitivity. Sleep fragmentation, achieved by causing EEG microarousals in healthy subjects, caused decreased insulin sensitivity (72). To our knowledge, the effect of microarousals on insulin sensitivity has not been studied in individuals with T1DM.

The small sample size and observational nature of our study do not allow us to fully determine causality. Further, EEG data were obtained in a laboratory setting, which is not the subjects' normal sleeping environment. Despite the variability in relationships between glucose and EEG in our sample, our findings demonstrate strong causal relationships between spontaneous fluctuations of EEG power and glucose, which may have implications for glycemic control in people with T1DM. Future research conducted in larger samples, including control groups and utilizing interventional designs will help to define the mechanistic basis of the observed causality and to further delineate the significance of these findings.

In summary, the current study provides evidence for a bidirectional causal relationship between brain activity during sleep and glucose changes in young adults with T1DM. Increasing glucose can drive changes in EEG activity consistent with arousal or awakening from sleep, and this, in turn, may drive

either a further increase or a corrective decrease in glucose level. Future studies are needed to define the long-term impacts of such nested interactions between glucose and brain activity in young adults with T1DM. Such understanding may be valuable to optimize diabetes management strategies.

V. RELATIONSHIP BETWEEN SLEEP, INFLAMMATORY MARKERS AND CORTISOL

A. Introduction

It is well known that Type 1 Diabetes Mellitus (T1DM) increases the risk of cardiovascular events (156) and cardiovascular disease (CVD). Over-activation of inflammatory processes (55,157) or of the Hypothalamic-Pituitary-Adrenal (HPA) axis (67,68) can contribute to the development of atherosclerotic CVD. People with T1DM have elevated levels of cortisol (65) and inflammatory cytokines such as interleukin-6 (IL-6) and tumor necrosis factor alpha (TNF- α) (158–160); derangements that could lead to CVD in these individuals.

Poor glycemic control, manifested as increased Hemoglobin A1c (HbA1c) is well known to be associated with increased incidence of CVD in T1DM (156). However, sleep disruption also may be an important contributor to development of CVD. Achieving normal sleep is one important component of health maintenance, including cardiovascular health. Disrupted sleep increases inflammatory cytokine and stress hormone levels (including cortisol), even in healthy individuals (79,161–163). People with T1DM have impaired sleep in comparison to healthy controls (86,103,141). This degraded sleep architecture may result in chronic inflammation, ultimately increasing CVD risk. It is important to understand if sleep plays a role in increased inflammation and activation of the HPA axis in individuals with T1DM, as this has not been systematically studied, and sleep is a potentially modifiable behavior. We hypothesized that sleep characteristics may mediate inflammation as well as cortisol levels in young adults with T1DM.

The aim of this study was to define the relationships between sleep, the inflammatory markers IL-6 and TNF- α , and cortisol in young adults with T1DM.

B. Methods

1. Subjects

Young adults aged 18-30 years, diagnosed with T1DM for at least five years and treated by insulin pump were recruited for the study. Individuals were excluded if they: were pregnant; worked night or rotating shifts; reported use of corticosteroids; were diagnosed with primary cardiovascular disease, retinopathy, nephropathy or peripheral neuropathy; had uncontrolled hypertension or thyroid disease; were diagnosed with a primary sleep disorder or reported chronic use of oral sleep medications; reported use of psychoactive medications (e.g. antidepressants) or illicit drugs (e.g. marijuana or cocaine); or reported severe metabolic instability (e.g. ketoacidosis, hypoglycemia or, hypoglycemic seizures) during the last 2 months.

2. Study Protocol

All procedures were approved by the institutional review board of the University of Illinois at Chicago. After informed consent was provided and inclusion/exclusion criteria were verified, a continuous glucose monitoring sensor (Guardian® REAL-Time System; Medtronic MiniMed) was placed in the abdominal subcutaneous tissue and an actigraphy monitor (Actiwatch2, Respironics) was placed on the non-dominant wrist. Subjects completed the Pittsburgh Sleep Quality Index (PSQI) (7) and Epworth Sleepiness Scale (ESS) (8) and answered questions about demographics. A sample of blood was drawn to measure hemoglobin A1c (HbA1c), a marker of glycemic control. Subjects then left the laboratory and spent three days and two nights carrying out their normal routine activity. On the third night, subjects underwent polysomnography (PSG) at the Sleep Science Center of University of Illinois Chicago. Lights out for each subject was between 10 pm and 11 pm and lights on was at 6 am, ensuring at least 7 hours of time in bed. Blood was collected from each subject immediately prior (within 10 minutes) to lights out, immediately after lights on (within 10 minutes), and again one hour (within five minutes) after lights on. Each sample was drawn with a 21-gauge needle from an antecubital vein while

subjects were either lying in bed or sitting comfortably in a chair. The samples were drawn into an ethylenediaminetetraacetic acid coated 10-ml tube. To separate the plasma, each blood sample was centrifuged (Eppendorf 5810 R™) at 1800 revolutions per minute for 12 minutes at 4° Celsius. The plasma was aliquoted into plastic tubes, labeled with subject ID number, sample number (time point of collection) and stored at -80° Celsius until the completion of the study.

3. PSG-Derived Sleep Measures

PSG comprised computer-based recording (Alice 5, Respironics) of: multiple EEG leads, bilateral referential electrooculogram, chin and anterior tibialis electromyogram, lead I electrocardiogram, respiratory movement of thorax and abdomen by piezoelectric strain gauges, airflow via nasal pressure cannula and oronasal thermistors and arterial oxygen saturation of hemoglobin by pulse oximeter. Each sleep study was scored using American Academy Sleep Medicine guidelines for visual scoring (149). Standard overnight summary variables were extracted from each PSG, including: sleep latency (SLAT), total sleep time (TST), sleep efficiency (SE), percentages of each sleep stage, arousal index (ARI), slow-wave sleep percent (SWS%), and wake after sleep onset (WASO, minutes). Apnea Hypopnea Index (AHI) was determined for each subject and subjects were excluded from analysis if they had an AHI ≥ 5 . An apnea was defined as a cessation in airflow for at least 10 seconds and a hypopnea was defined as a reduction in thoracoabdominal movement amplitude by $\geq 30\%$ combined with a 4% desaturation as measured by pulse oximeter (164).

4. Inflammatory Cytokine and Cortisol Assays

IL-6 and TNF- α were measured from plasma samples using commercially available high sensitivity enzyme-linked immunosorbent assay (ELISA) kits (Quantikine® High Sensitivity ELISA, R&D systems). Cortisol levels were measured using a commercially available competitive binding assay kit (Parameter™, R&D Systems). The mean lower limit of detection for TNF- α was reported to be 0.106 pg/ml and for IL-6 was 0.039 pg/ml. The average intra-assay coefficient of variation (CoV) was 5.4% for

TNF- α and 7.4% for IL-6. The average inter-assay CoV was 8.3% for TNF- α and 7.8% for IL-6 (165,166). The mean lower limit of detection for the cortisol assay was reported as 0.071 ng/mL. Average intra-assay CoV was 6.97% and the average inter-assay CoV was 13.6% for the cortisol assay (167). All three markers were run in duplicate and the average of the two values was taken.

5. Statistical Analysis

To normalize distributions and linearize relationships for statistical analysis, IL-6 and TNF- α were inverse (reciprocal) transformed and cortisol levels were square-root transformed. Mean and standard deviation data reported below are untransformed, whereas pairwise correlations and regressions are reported for the transformed variables. Repeated measures Analysis of Variance (ANOVA) was used to compare levels of IL-6, TNF- α , and cortisol between time points. Post-hoc pairwise contrasts between time points were tested using paired t-tests. To assess the effects of average glycemic control on inflammatory cytokines and cortisol, subjects were separated into two groups: those with "Poor" Control ($>7.0\%$) and those with "Good" Control ($\leq 7.0\%$) HbA1c (25). ANOVA using glycemic control (Good versus Poor) as a fixed effect and time (Pre-sleep; Awakening; 1-Hour Post Awakening) as a within subject repeated measure was performed to determine their effects on the inflammatory cytokine and cortisol measures. Pairwise comparisons were used to test specific contrasts. Greenhouse-Geisser correction was applied to the F statistic of all repeated measures reported. Unpaired t-tests were used to compare the difference in mean values of IL-6, TNF- α and cortisol between glycemic groups. The Pearson product-moment correlation coefficient was calculated between standard clinical measures of sleep (from PSG) and glycemic control with reciprocal values of IL-6, TNF- α , and square root values of cortisol at each time point.

All statistical analyses were performed using STATA[®] 14.0 (StataCorp[®]) and a p-value ≤ 0.05 indicated significance.

C. Results

1. Subjects and Sleep Characteristics

Blood was obtained from 27 of the 30 subjects enrolled. Two of these subjects exhibited an AHI ≥ 5 and were excluded from the analysis. Table 8 summarizes glycemic control as well as self-reported and PSG-derived measures of sleep and sleep quality of subjects included in the analysis (N = 25).

Characteristic	N = 24
Age (years)	23.8 (3.9)
Male (%)	11 (44.0)
Caucasian (%)	22 (88.0)
Diabetes Duration (years)	11.9 (4.4)
HbA1c (%)	7.8 (1.3)
BMI (kg/m ²)	26.0 (3.4)
PSQI (Range 0-21)	4.84 (2.3)
ESS (Range 0 – 24)	4.8 (2.7)
Total Sleep Time (min)	372.9 (43.0)
Sleep Efficiency (%)	81.3 (9.1)
Sleep Latency (min)	36.4 (18.9)
WASO (min)	53.0 (36.2)
Stage 1 Sleep (%)	6.3 (4.3)
Stage 2 Sleep (%)	50.7 (8.7)
Stage 3 Sleep (%)	21.2 (5.2)
REM Sleep (%)	21.8 (6.2)
Number of Awakenings (Total #)	24.3 (9.2)
Number of Arousals (Total #)	30.3 (20.2)
Apnea Hypopnea Index (# per hour)	0.88 (0.89)

TABLE 8: DEMOGRAPHIC, GLYCEMIC CONTROL AND SLEEP CHARACTERISTICS
Data are reported as Mean (SD); Male and Caucasian are reported as number (% of total).

2. Temporal Variations of IL-6, TNF- α and Cortisol

Table 9 provides the mean values for TNF- α , IL-6 and cortisol measured immediately before sleep, upon awakening and 1-hour post awakening for the entire group. Repeated measures ANOVA demonstrated a significant effect of time on TNF- α ($F = 68.41$, $p < 0.0001$), with values at awakening and 1-hour post awakening being significantly higher than pre-sleep ($p < 0.0001$ for each). Repeated measures ANOVA for cortisol showed the same pattern ($F = 54.25$, $p < 0.0001$), with cortisol significantly higher at awakening and 1-hour post awakening than pre-sleep ($p < 0.0001$ for each). Repeated measures ANOVA for IL-6 showed a significant effect of time ($F = 5.66$, $p < 0.009$); mean values were significantly lower at awakening and 1-hour post awakening than pre-sleep ($p = 0.014$ and $p = 0.003$, respectively).

	TNF- α (pg/mL)	IL-6 (pg/mL)	Cortisol (ng/mL)
Before Sleep	0.96 (0.48) n = 24	1.04 (0.59) n = 24	9.1 (7.2) n = 22
Awakening	1.4 (0.66) n = 24	0.85 (0.55) n = 24	61.2 (44.0) n = 23
1 Hr Post	1.6 (0.62) n = 23	0.74 (0.32) n = 23	82.42 (33.2) n = 22

TABLE 9: VALUES OF TNF- α , IL-6 AND CORTISOL BEFORE AND AFTER SLEEP

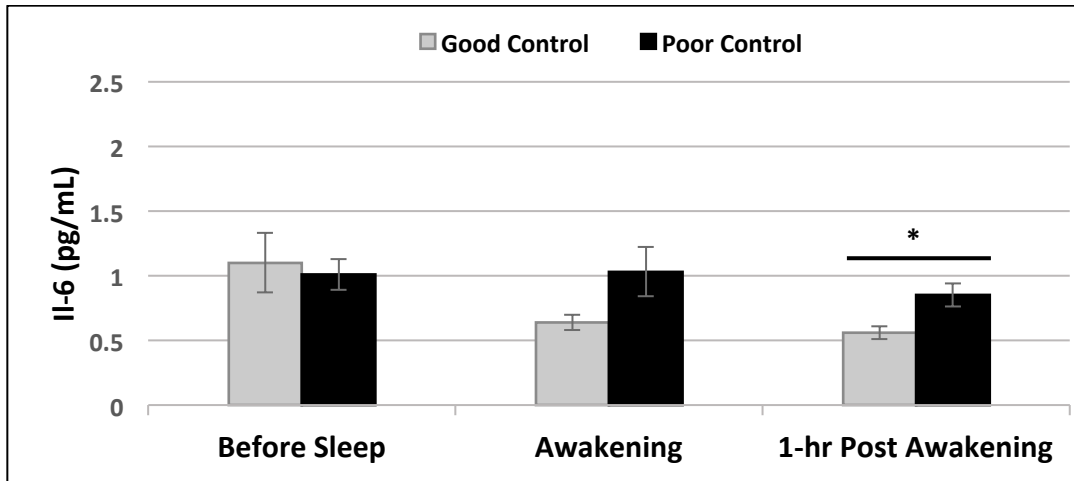
Values are mean (SD); * Indicates $p \leq 0.03$; # indicates $p \leq 0.0001$

TNF- α : Awakening and 1-hour post awakening significantly higher than pre-sleep ($p < 0.0001$); 1-hour post awakening significantly higher than awakening ($p = 0.01$, indicated with *); IL-6: Awakening and 1-hour post awakening significantly lower than pre-sleep ($p \leq 0.014$); Cortisol: Awakening and 1-hour post awakening significantly higher than pre-sleep ($p < 0.0001$).

3. IL-6, TNF- α and Cortisol in Relation to Average Glycemic Control

Repeated measures ANOVA demonstrated significant effects of HbA1c on TNF- α and IL-6 ($F = 4.89$, $p = 0.03$ and $F = 5.09$, $p = 0.03$, respectively), but no effect on cortisol level. Further, there was no significant interaction between HbA1c and sample time for TNF- α , IL-6 or cortisol. Figure XIV shows the differences in IL-6 (top panel, a) and TNF- α (bottom panel, b) values stratified according to HbA1c group. The Poor glycemic control group had significantly higher mean TNF- α levels upon awakening (Poor: 1.72 ± 0.78 [SD] pg/mL vs. Good: 1.11 ± 0.24 pg/mL, $p = 0.0004$) and 1-hour post awakening (Poor: 1.82 ± 0.66 pg/mL vs. Good: 1.25 ± 0.36 pg/mL, $p = 0.0042$). Further, the Poor glycemic control group exhibited significantly higher mean IL-6 values 1-hour post awakening (Poor: 0.85 ± 0.35 pg/mL vs. Good: 0.56 ± 0.15 pg/mL, $p = 0.011$). No significant differences were found between Poor and Good glycemic control for cortisol at any time point.

a.



b.

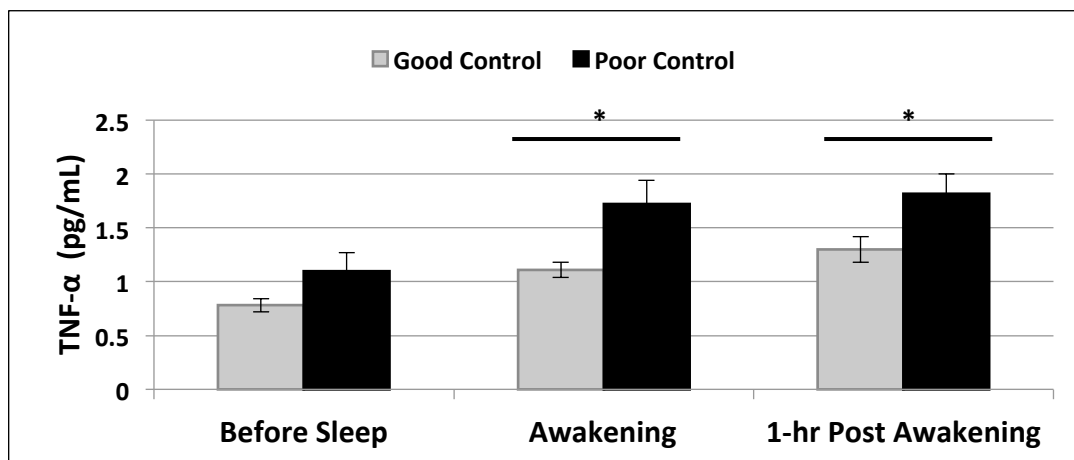


FIGURE XIV: PRE- AND POST-SLEEP IL-6 AND TNF- α IN SUBJECTS WITH GOOD VERSUS POOR GLYCEMIC CONTROL

Top Panel (a): Values of IL-6 between groups: The Poor Glycemic Control Group (HbA1c > 7.0%) had significantly higher values one hour post awakening as compared to the Good Glycemic Control Group (HbA1c \leq 7.0%). **Bottom Panel (b): Values of TNF- α between groups:** Both awakening and one hour post awakening values were higher for the Poor Glycemic Control Group as compared to the Good Glycemic Control Group.

4. Correlations of TNF- α , IL-6 and Cortisol with Sleep and Glycemic Control Measures

Table 10 provides the correlations between reciprocal values of IL-6 and TNF- α and square root values of cortisol for each time point with standard measures of sleep and glycemic control. A significant negative correlation was observed between (reciprocal) TNF- α and Hba1c at all time points (pre-sleep: $r = -0.66$, awakening $r = -0.77$, 1-hour post awakening: $r = -0.71$; $p \leq 0.0004$ for each). Further, a significant negative correlation was found between (reciprocal) TNF- α upon awakening and the number of arousals during the preceding sleep period ($r = -0.42$, $p = 0.04$). A negative correlation was observed between (reciprocal) IL-6 1-hour post awakening and both Hba1c ($r = -0.41$, $p = 0.05$) and number of arousals ($r = -0.54$ and $r = -0.53$, respectively; $p = 0.01$ for each). A significant positive correlation was found between (reciprocal) IL-6 upon awakening and number of awakenings during the preceding sleep period ($r = 0.48$, $p = 0.02$). Pre-sleep (reciprocal) IL-6 values were positively correlated with % of stage 3 sleep ($r = 0.45$, $p = 0.03$) and WASO ($r = 0.41$, $p = 0.05$). Awakening values of (square root) cortisol were positively associated with WASO ($r = 0.48$, $p = 0.02$). One hour post awakening (square root) cortisol was negatively correlated with number of arousals ($r = -0.54$, $p = 0.01$) and HbA1c (-0.46 , $p = 0.03$). Number of arousals and HbA1c were themselves positively correlated ($r = 0.52$, $p = 0.006$). Reciprocal TNF- α and IL-6 values were positively correlated ($r = 0.56$, $p = 0.006$) only at 1-hour post awakening.

	Reciprocal IL-6			Reciprocal TNF- α			Square Root Cortisol		
	T1	T2	T3	T1	T2	T3	T1	T2	T3
HbA1c (%)	-0.23	-0.27	-0.41*	-0.66[#]	-0.77[#]	-0.71[#]	0.07	-0.28	-0.46
Mean Glucose (mg/dL)	-0.22	-0.02	-0.08	-0.22	-0.24	-0.05	0.08	0.00	-0.29
CONGA-1 (mg/dL)	0.03	0.13	0.02	0.00	0.20	0.15	0.17	-0.13	-0.19
SD Glucose (mg/dL)	0.08	0.02	-0.11	0.15	0.13	0.15	0.19	0.06	-0.36
WASO (min)	0.41	0.37	0.26	0.12	0.22	0.14	-0.03	0.48*	0.15
% Stage 3	0.45*	0.32	0.35	0.17	0.23	0.18	-0.04	0.18	0.28
% Stage 2	0.00	-0.16	0.10	-0.09	-0.08	0.17	0.00	0.13	-0.18
% Stage 1	0.19	0.23	-0.08	-0.13	-0.21	-0.34	-0.03	-0.05	0.24
% REM	-0.52*	-0.21	-0.39	0.08	0.06	-0.16	0.06	-0.31	-0.14
# Arousals	-0.28	-0.54*	-0.53*	-0.26	-0.42*	-0.32	0.13	-0.09	-0.54*
# Awakenings	0.11	0.48	0.24	0.06	0.02	-0.03	-0.15	0.10	0.13
Sleep Latency (min)	0.18	0.11	0.15	-0.12	0.03	0.06	0.28	-0.13	-0.19
Sleep Efficiency (%)	-0.47*	-0.40	-0.36	-0.09	-0.21	-0.21	0.00	-0.35	-0.12
Total Sleep Time (min)	-0.40	-0.26	-0.19	0.06	-0.07	-0.04	0.00	-0.27	0.05

TABLE 10: CORRELATION TABLE OF PRE-SLEEP, AWAKENING AND 1-HOUR POST AWAKENING RECIPROCAL VALUES OF IL-6 AND TNF- α AND SQUARE ROOT VALUES OF CORTISOL WITH STANDARD MEASURES OF SLEEP AND GLYCEMIC CONTROL

[#] indicates $p < 0.0001$; * indicates $p < 0.05$

CONGA-1: Continuous Net Glycemic Action-1 Hour; SD Glucose: Standard Deviation of Glucose

D. Discussion

In the present study, we report significant pre-sleep to post-sleep changes of inflammatory cytokines and cortisol in a group of 18-30 year olds with T1DM. IL-6 levels were lower whereas cortisol and TNF- α levels were higher in the morning (Table 1). This, to our knowledge, is the first report of an increase in TNF- α levels after sleep in young adults with T1DM. For the entire subject group, higher inflammatory cytokine levels were significantly correlated to HbA1c as well as to PSG-derived measures of sleep disruption. Subjects with poor glycemic control exhibited higher levels of IL-6 and TNF- α than did those with good control. Sleep disturbance may play a role in mediating increased levels of inflammation and/or reduced glycemic control in young adults with T1DM.

Sleep disruption has been shown to impact TNF- α and IL-6 levels. Acute sleep deprivation has been reported to cause an increase in TNF- α levels with no effect on IL-6 levels in healthy men (77). In another study of total sleep deprivation, Scheerer et al. (2001) showed that IL-6 secretion was increased but TNF- α levels were not affected (78). Investigators have also reported that modest sleep restriction (6 hours of sleep) increased IL-6 levels and TNF- α levels in men, but only IL-6 levels in women (168). We report, in the present study, elevations in TNF- α after a night of normal undisturbed sleep in a group of young adults with T1DM. Additionally, a significant negative correlation was found between arousals and the reciprocal of IL-6 and TNF- α ; which indicates a positive correlation between IL-6 and TNF- α and number of arousals. This supports the view that sleep disruption may contribute to elevated inflammatory activity in young adults with T1DM.

Elevated levels of IL-6 and TNF- α have been reported in children (158) and adults (159) with T1DM as compared to controls. However, no studies, to our knowledge, have examined these levels in relation to the sleep period in people with T1DM. In the present study, we found a significant increase in the awakening and one hour post awakening levels of TNF- α as compared to pre-sleep values. In contrast, IL-6 levels were lower upon awakening and one hour after awakening in our sample. TNF- α values have been reported to not exhibit a circadian pattern (169,170), with stable levels seen throughout the 24-hour period. It has been reported that IL-6 exhibits a circadian pattern, with a peak around 5 am and a nadir around 8 am (171,172). The observed post-sleep decrease in IL-6 was driven by the good glycemic control group; the poor glycemic control group exhibited no decrease in IL-6. This finding suggests that the normal circadian pattern of IL-6 may be disrupted in individuals with poor glycemic control. It must be noted that HbA1c and number of arousals were themselves correlated, and when HbA1c was controlled by multiple regression, the relationship of arousals to TNF- α , was no longer significant. However, even after controlling for HbA1c, the relationship between number of arousals and IL-6 at awakening remained significant. Thus, it is possible poor glycemic control impacts both sleep

and inflammation in young adults with T1DM. Glycemic control has been implicated in changes in sleep architecture in T1DM(86). The lack of a control group in our study does not allow us to define any changes in sleep architecture associated with T1DM per se. However sleep parameters derived from the PSG were not different from those expected for this age group (154).

In addition to altered sleep architecture, glycemic control has been previously reported to be significantly correlated to inflammatory marker levels in adolescents and adults with T1DM (158,159,173). Here we extend this finding, reporting an effect of glycemic control on pre-post sleep changes in inflammatory markers in T1DM. TNF- α levels were significantly higher in the morning in the poor glycemic control versus the good glycemic control group. Despite the fact that IL-6 levels were lower for the entire group after sleep, the good glycemic control group drove the decrease. The poor glycemic control group did not have significantly lower IL-6 values in the morning and, further, had significantly higher levels 1 hour post awakening as compared to the good glycemic control group (Figure XIV). This finding, along with the positive correlation between number of arousals and morning values of IL-6, suggests that both glycemic control and altered sleep architecture play a role in increased inflammation in individuals with poor glycemic control.

The TNF- α and IL-6 values reported here are not elevated beyond what has been reported for healthy subjects (77,168,170). Further, they are similar to those reported by Mitrovic and colleagues (2014) in subjects with T1DM without complications (173), as well as Schram and colleagues (159). We do not have a control group for comparison of our values, however our IL-6 values were much lower than those reported in youth (mean age 15 years) in Snell-Borgeon's study (7.8 pg/ml) (158). They measured serum levels of IL-6 and we measured plasma levels; however large differences in serum and plasma levels are not expected. It has been reported that IL-6 values are higher in people 7-17 years old as compared to those greater than 18 (174), which may contribute to the differences in IL-6 levels observed here, versus those reported by Snell-Borgeon et al (158).

Cortisol, as expected, was elevated in the morning as compared to pre sleep values. It is well known that cortisol exhibits a peak plasma level in the early morning (175,176). Further, cortisol levels have been reported to rise in the first hour after awakening, known as the cortisol awakening response (177–179). Our findings support these reports, as cortisol levels were highest one hour after awakening. Elevated 24 hour urinary secretion of cortisol has been reported in people with T1DM (65), however the plasma values for our sample were within normal limits (180). Interestingly, awakening cortisol level was positively correlated to minutes of wake after sleep onset (WASO), but cortisol 1-hour after awakening was negatively correlated to number of arousals and HbA1c. The reasons behind these findings are unclear, however it is possible that individuals with longer awakenings through the night had more stress upon awakening resulting in elevation of awakening cortisol levels. In contrast, individuals whose sleep was more disrupted by arousals (more shifts to higher EEG frequencies but did not lead to awakenings) had a blunted cortisol awakening response. It has been reported that sleep restriction and insomnia result in lower morning levels of salivary cortisol (81,82). A recent study in children with T1DM reported that children with high HbA1c had significantly higher cortisol levels than those with low HbA1c (66). Our findings suggest the opposite, high HbA1c was associated with lower 1-hour post awakening cortisol levels. It is not clear what the mechanism behind a decrease in 1-hour post awakening cortisol levels and HbA1c could be, however it may be due to the relationship between increased arousals and lower cortisol levels as HbA1c and number of arousals were significantly correlated. Our findings support that in a small group with T1DM, cortisol secretion follows a normal pattern.

Our study has notable limitations. The sample size was small and lacks a control group, it was a homogenous group of subjects with T1DM and it was observational in nature. Further, sleep was measured in a laboratory setting, so it is possible that the relationships reported may be different for sleep in the home environment. Future interventional studies with larger sample sizes and control

groups conducted in a natural setting should further investigate the relationships reported in the present study.

In summary, we report increases in inflammatory marker TNF- α after sleep in a small group of young adults with T1DM. Further, notable differences were found between inflammatory profiles in those with good glycemic control compared to those with poor glycemic control. Arousals during the sleep period were significantly correlated with morning IL-6 and TNF- α , and morning cortisol levels were lower in those with poor glycemic control and with more arousals through the night. Our findings suggest that poor glycemic control and sleep disruption each may promote inflammation in young adults with T1DM. Understanding the relationships between sleep, inflammation and glycemic control is important to inform improved clinical management strategies that could decrease CVD development and improve quality of life in people with T1DM.

VI. DISCUSSION

A. Overview

The first aim of this dissertation study was to define sleep architecture and its relationship to glucose variability in young adults with Type 1 Diabetes Mellitus (T1DM). The findings detailed in chapters 2 - 4 support my *a priori* hypothesis that, in this population, changes in sleep and glucose exhibit biologically and statistically significant coupling that is both bi-directional and time-varying. Because it is a joint time-frequency transformation, Wavelet Coherence Analysis (WCA) is a powerful tool to identify coupling between two time series even when this coupling is time-varying and depends upon the speed of fluctuations in the underlying waveforms. WCA demonstrated that sleep and glucose fluctuations often are strongly coupled, but that this coupling varies with time and depends on fluctuation speed when sleep is measured either by actigraphy in the home environment (Chapter 2) or by PSG in the laboratory (Chapter 3). Despite its strengths, WCA is analogous to correlation analysis and does not provide information on potential causal relationships between two time series.

Using Granger analysis, I demonstrated that sleep and glucose changes are causally related and this is bi-directional (Chapter 4). Here, qEEG analysis was employed to provide a quantitative readout on the level of physiological arousal, including sleep depth, during the overnight PSG recordings. Delta Band EEG activity is characteristic of deep sleep; Theta Band activity is characteristic of light sleep or dreaming sleep; whereas Alpha, Beta and Gamma Band activities reflect wakefulness. Across all 5 of these EEG Bands, 70% to 100% of all subjects demonstrated a causal connection with glucose. In each Band, more subjects demonstrated significant causality with EEG driving glucose change than with glucose driving EEG change. However, in the Alpha and Theta EEG Bands, there were approximately equal numbers of subjects in each group. A small number of subjects demonstrated simultaneous bidirectional coupling during a single night (5 subjects for Alpha and 5 for Theta).

When assessing the sense of the relationship for instances of significant Granger causality, the VAR coefficient analysis and initial impulse response function analysis showed consistent patterns (Chapter 4). When changes in Beta or Delta Band EEG activity were driving changes in glucose, the relationship was positive (increasing EEG activity led to increasing glucose) and the converse was true for the Theta Band (increasing Theta EEG activity led to decreasing glucose). When glucose changes were driving EEG, an increase in glucose led to decreased Delta and Theta Band power and increased Alpha Band power. Cross-Correlation function analysis was also employed to identify any consistent time lag that was associated with the causal influences of glucose on EEG power or vice versa. The main finding was that all subjects exhibited a peak in the correlation function at or near a zero lag. In subjects with the global peak correlation observed at a lag of 0 ± 10 minutes, Alpha activity versus glucose demonstrated a positive correlation and Theta activity versus glucose demonstrated a negative correlation (Chapter 4), consistent with the findings from the VAR coefficient and initial impulse response analyses. Taken collectively, these findings support the view that increasing glucose can drive changes in EEG activity consistent with arousal or awakening from sleep, and that this change in behavioral state may, in turn, drive either a further increase or a corrective decrease in glucose level. This further supports the existence of both positive and negative feedback loops involving both glucose and brain activity in young adults with T1DM.

The second aim of this dissertation study was to quantitatively define the relationships among sleep, inflammatory cytokines, and endocrine stress markers measured before and after sleep in young adults with T1DM. I hypothesized that the inflammatory markers IL-6 and TNF- α , as well as cortisol would be elevated after sleep as compared to before sleep. The findings from my study support that TNF- α is elevated and IL-6 is decreased after sleep as compared to before sleep in a small group of young adults with T1DM. Cortisol was elevated in the morning as compared to before sleep in this group (Chapter 5). When comparing subjects with good ($\text{HbA1c} \leq 7.0\%$) versus poor ($\text{HbA1c} > 7.0\%$)

glycemic control, TNF- α levels were significantly higher upon awakening and one hour after awakening in those with poor glycemic control. Further, only subjects with good glycemic control demonstrated lower IL-6 levels after sleep, and the levels of IL-6 were significantly higher in those with poor versus good glycemic control one hour after awakening. Finally, increasing frequency of arousals during sleep was associated with increased morning IL-6 level, even after controlling for HbA1c. These findings argue that sleep disruption and poor glycemic control may each independently contribute to the increased inflammation and CVD risk seen in T1DM.

B. Glucose Variability as a Driver of Sleep Disruption

The findings from Granger analysis coupled with VAR coefficient and initial impulse response function analyses support the conclusion that when glucose drives EEG changes during sleep, increasing glucose causes a shift from sleep toward arousal or awakening; increasing Alpha and decreasing Delta and Theta Band EEG activity. Results from cross-correlation function analysis suggest that causal interactions with glucose driving brain activity during sleep most often occur within short latencies of ≤ 10 minutes. Further, coherence analysis demonstrated that Rapid fluctuations in glucose and EEG exhibited multiple intervals of significant coupling that were brief in duration, consistent with arousals or brief awakenings through the night. Decreased sleep quality has been reported in both adults and children with T1DM (83–85) and altered sleep architecture, specifically less slow wave sleep, has been reported in adults and adolescents with T1DM (86,141). My findings suggest that increases in glucose through the night may be one important mechanism contributing to disrupted sleep in people with T1DM. The number of nighttime arousals was significantly higher in subjects who had significant causality for Glucose driving EEG changes. Stage 2 sleep was higher and Stage 3 sleep was lower in these subjects as well, but the differences were not significant; mean glucose was also higher (not significant) in this group. Notably, no differences were observed for traditional measures of glucose variability (standard deviation of glucose or CONGA-1) for the overnight period between subjects who

had significant causality for Glucose driving EEG changes in the Theta or Alpha Bands versus those who did not. Overall variability may not be the important predictor of sleep disruption, it may be the rate of change in glucose during the night. Rapid decreases in glucose (>25 mg/dl/hr) were associated with increased awakenings from sleep in children with T1DM (105), but these authors did not assess the temporal relationship between rapid increases in glucose and awakenings. Thus, it is plausible that the rate of change in glucose during a sleep period may be an important factor causing sleep disruption.

Not all subjects exhibited significant causal coupling of glucose driving EEG changes throughout the study night. This may be due to the fact that on a given night, not all subjects experienced rapid glucose increases (or decreases) which could lead to an arousal or an awakening. In future studies, more than one study night will be needed to fully define the causal impact of glucose fluctuations as a source of awakenings or arousals from sleep in T1DM. Further, Granger analysis uses the glucose and EEG power from the entire night. Wavelet coherence showed that glucose and EEG changes exhibit time-varying coupling and this coupling is different for different fluctuation speeds. Thus, it may be that at certain points during the night, a glucose change is driving a change in EEG, but at other times a change in EEG is driving a change in glucose and when these patterns are averaged through the night, the relationship is diminished. Future interventional studies in which either sleep or glucose are controlled will help to fully define the mechanisms coupling glucose changes to ensuing EEG changes.

C. Sleep as a Driver of Glucose Variability

In this study, more than half of the subjects exhibited instances of EEG driving glucose changes during normal nocturnal sleep in the laboratory, suggesting that the sleep process may play an important role in regulating glucose throughout the night in individuals with T1DM. In previous studies, researchers have demonstrated that sleep significantly impacts metabolic control. Reduced insulin sensitivity has been reported in healthy subjects following one week of sleep restriction (73) or a single night of sleep fragmentation (increased arousals) (72). Similar findings have been reported in adults

with T1DM, where reduced insulin sensitivity was observed following a single night of sleep restriction to four hours (92). These previous studies examined the impact of experimental manipulations of the sleep process on glucose control. In contrast, this dissertation study quantified interactions between the spontaneous fluctuations of physiological arousal characteristic of normal sleep, and real time fluctuations in interstitial glucose concentration. Both VAR coefficient analysis and initial impulse response analysis identified that increasing EEG power in the Beta Band, characteristic of wakefulness, or in the Delta Band, observed during slow wave or deep sleep, resulted in increasing glucose levels. Conversely, increasing EEG power in the Theta Band, which is associated with light non-dreaming sleep as well as dreaming (REM) sleep, resulted in decreasing glucose.

Although the mechanisms underlying these causal impacts of brain activity on glucose cannot be determined from this observational study, several possibilities are supported by the literature. Brain metabolism has been reported to increase during REM sleep and decrease during NREM sleep (181,182). Thus, it is possible that when subjects experienced REM sleep in my study (manifested by increasing Theta Power), glucose levels declined. My findings are consistent with a previous report in which REM sleep was associated with decreased glucose measured by CGMS in healthy men (183). Growth hormone secretion is normally increased during slow wave sleep (increased Delta power) (143). Growth hormone decreases insulin sensitivity which could result in increasing glucose levels (70), consistent with my observation that increased Delta Band power was causally related to increasing glucose. Results from Granger Analysis do not give a time scale to the relationships noted. During normal sleep, there is an ultradian cycling between periods of REM and non-REM (NREM) sleep, characteristically progressing from onset (stage 1, light sleep) to deep slow wave sleep (high Delta power), followed by REM sleep (high Theta power) and a return to light sleep approximately every 60-120 minutes throughout the night (184). Future studies which control either sleep or glucose levels may help to provide insight on the time course by which these changes in glucose occur.

Increased Beta power, associated with wakefulness, resulted in increased glucose levels in my subjects. Increasing glucose may be due to increased sympathetic activation, e.g. increased epinephrine levels, pursuant to awakening or arousal. Awakening from sleep causes increased epinephrine levels (185) and epinephrine elevates glucose (186). Thus, increased awakening through the night may drive increasing glucose secondary to elevated epinephrine levels. It is also interesting to note that glucose variability, measured by CONGA-1, was significantly associated with coherence between rapid (Rapid Range) fluctuations of glucose and EEG power in the Gamma and Beta Bands. Thus, increasing awakenings may result in short-term increases in glucose level that contribute to elevated glucose variability.

Collectively, these findings highlight that even during a normal night of sleep, there are physiologic changes that can have potentially important impacts on glucose levels in young adults with T1DM.

D. Inflammation Is Altered by Sleep Processes and Glycemic Control

As reported in Chapter 5, TNF- α was increased in subjects post-sleep as compared to pre-sleep. There was also a significant effect of glycemic control; people with poor control (HbA1c > 7.0%) had higher levels of TNF- α in the morning. IL-6 levels decreased after sleep, however, this change was completely driven by the good glycemic control group. IL-6 level was equivalent before and after sleep for the poor glycemic control group and the one-hour post-awakening values of IL-6 were significantly higher in the poor control versus the good glycemic control group. A nadir in IL-6 secretion during the morning hours has been reported (171), but TNF- α has not been reported to exhibit a circadian pattern (169,170). Thus, my findings suggest the possibility that the sleep process *per se* results in perturbation of inflammation and this effect is more profound in people with poor glycemic control. Other investigators have reported associations between glycemic control and both TNF- α and IL-6 (158,159,173). However, the relationship between sleep and inflammation has not been systematically

investigated in young adults with T1DM. It is also interesting to note that the IL-6 level upon awakening was significantly associated with the number of arousals during the preceding night, even after adjusting for HbA1c level. This suggests an independent effect of disrupted sleep leading to increased inflammation the next day. If, over time, disrupted sleep leads to chronically elevated inflammatory processes, this could represent one source of accelerated CVD development in T1DM. It must be noted that the observed levels of IL-6 and TNF- α were not elevated beyond what is reported in the literature for healthy controls (169,171). Future studies with control groups and interventions controlling sleep or glucose are needed to determine the mechanisms behind the observed disruptions to inflammatory process. Despite this, my findings highlight the importance of investigating the role of sleep and interactions between sleep and glucose control in inflammation development in people with T1DM.

Cortisol was significantly elevated after sleep as compared to pre-sleep, which is a normal physiological finding. It is well known that cortisol secretion peaks in the early morning hours (175,176). Cortisol normally increases further during the first hour after awakening, a phenomenon known as the cortisol awakening response (177–179). My subjects with T1DM demonstrated an apparently normal cortisol awakening response, with the highest values of cortisol seen one hour after awakening. No differences in cortisol were noted between glycemic control groups. However, the lack of a control group does not allow a determination of whether the morning elevation in cortisol is abnormal for people with T1DM. Future studies with control groups are needed to determine if sleep in T1DM may mediate cortisol levels.

E. Sleep, Glucose Variability and Inflammation: A Vicious Cycle?

Figure XV provides a framework for synthesis and interpretation of all dissertation findings reported above. It is likely that the patterns of physiological arousal and the associated brain activity characteristic of the normal sleep process impact people with T1DM differently than non-diabetic controls. During a normal night of sleep, an individual will cycle between NREM and REM sleep. A bout

of slow wave sleep (high Delta power) can initiate an increase in glucose, likely through increased growth hormone secretion, which decreases insulin sensitivity. In people without diabetes, the pancreas maintains the glucose levels within normal ranges by increasing and decreasing insulin secretion in response to changes in glucose due to normal sleep. However, in an individual with T1DM who does not sense the initial increase in glucose and increase insulin secretion, these changes in glucose level due to sleep are unmasked, and the glucose level will continue to rise. As the sleep process cycles from slow wave sleep to REM sleep, the effects of brain activity on glucose will shift: Delta activity will decrease, decreasing growth hormone secretion, improving insulin sensitivity and allowing glucose level to drop; simultaneously, Theta activity will increase, brain glucose utilization will increase, and again glucose will drop. Through these pathways, as supported by the findings of this dissertation study, the normal cycling of NREM and REM sleep will drive larger glucose fluctuations in individuals with T1DM than in healthy individuals who can mount effective insulin and glucagon responses to control glucose.

Increasing glucose levels, especially ones that are more rapid in nature, may precipitate an arousal or awakening, manifested as increased Alpha, Beta and Gamma power and decreased Delta and Theta power. The arousal-related shift from Theta to Alpha and Beta power can result in positive feedback, driving a further increase in glucose. The arousal also decreases Delta power; decreasing growth hormone secretion; increasing insulin sensitivity; and initiating a corrective decrease of glucose. The net effect on glucose will depend on the relative strength of these parallel and offsetting pathways at any given time. If a net decrease in glucose is rapid in nature, this too may result in an awakening from sleep (105) and that awakening (shift to higher frequency EEG) may result in an increase in glucose, again depending on the relative strength of the parallel negative and positive feedback loops. Taken together, these factors suggest that the increased variability of glucose level typically observed in individuals with T1DM may be even more severe during sleep than during wakefulness, due to

increasing fluctuations of physiological arousal and concomitant brain activity. Simultaneously, these wider glucose fluctuations may be expected to drive fragmentation of sleep in individuals with T1DM.

One additional homeostatic pathway that may serve to dampen wide fluctuations in glucose and attendant sleep fragmentation in T1DM is cortisol secretion. Cortisol is a counter-regulatory hormone secreted when glucose level drops. Like growth hormone, increasing cortisol levels reduce insulin sensitivity, in turn initiating a corrective increase in glucose level. The level of physiological arousal also may influence cortisol secretion. I observed a negative association between morning cortisol levels and the number of arousals during the previous night of sleep; suggesting the possibility that in people with T1DM, when increasing glucose initiates an arousal from sleep, this may cause decreased cortisol secretion, in turn helping to decrease glucose level. The efficacy of this homeostatic pathway, again, will likely vary among individuals and even from night to night, depending on the balance of positive and negative feedback effects between glucose and physiological arousal.

As depicted in Figure XV, my findings also support the view that both poor glycemic control and sleep disruption can promote inflammatory processes, thereby increasing risks for CVD development (157). Hyperglycemia (158,173,187) and sleep disruption (77,170,171) are well recognized correlates of elevated inflammatory cytokines such as IL-6 and TNF- α . But it remains unclear to what extent these two factors are important in individuals with T1DM, and whether sleep fragmentation may serve as an important mediator of inflammatory responses secondary to glycemic variability. Granger analysis demonstrated that glucose fluctuations can be an important source of arousal/awakening from sleep and that sleep fragmentation, in turn, was significantly related to increased morning IL-6 levels, independent of average glycemic control (HbA1c). Moreover, morning IL-6 and TNF- α levels were significantly higher among individuals with poor glycemic control. Together, these observations argue that sleep fragmentation may be an important mediator of elevated inflammatory responses secondary to poor glycemic control.

Figure XV illustrates several other factors that may also play significant roles in disrupting sleep and glucose in individuals with T1DM. I identified a significant circadian pattern to the coupling between glucose and activity in my subjects, with a peak coherence observed around 5 pm. If an individual experiences a phase delay or advance, such as when traveling across time zones or staying up late and sleeping in on weekends, this may result in alteration of normal circadian coupling between activity in glucose, potentially exacerbating derangements of nighttime glucose homeostasis and disruptions of sleep. Lifestyle choices including daytime food and alcohol intake as well as physical activity can have delayed impacts on glucose metabolism that can later occur during the night, resulting in sleep disturbances. Further, self-management of T1DM may include setting an alarm to check blood sugar in the middle of the night (especially if the individual ate or drank something which he or she knows can have a delayed impact on glucose level) causing planned sleep disruption, with potentially negative attendant effects on glucose homeostasis and inflammatory processes. Thus, common patterns of behavior for individuals with T1DM may further exacerbate the sleep disruptions caused by nighttime glucose variations characteristic of this disorder. It is evident that there is a need to determine the clinical implications of lifestyle as well as clinical self-management behaviors on sleep in individuals with T1DM. It is possible that these behaviors can be modified to ultimately improve sleep, glycemic control and longevity in people with T1DM.

F. Conclusions and Implications

Findings from my study highlight that there is a bi-directional and time varying relationship between sleep and glucose in young adults with T1DM. Glucose fluctuations can drive changes in sleep and sleep disruption can drive changes in glucose. Further, restriction or disruption of the sleep process may exacerbate inflammation in people with T1DM. This dissertation provides evidence that interactions between sleep and glucose fluctuations are regulated by multiple nested feedback loops with the potential to exert vicious cycle interactions with attendant elevations of glycemic variability and

sleep disruption. In turn, these disturbances each can contribute to increased inflammation, potentially accelerating the incidence or progression of CVD in individuals with T1DM.

Future studies aimed at delineating the mechanisms behind the relationships reported in this study are critical to guide clinical interventions intended to improve glycemic control and further decrease CVD development in T1DM. For example, if we can understand the time delay by which changes in the sleep process result in increasing or decreasing glucose, we can optimize insulin delivery to minimize these changes. Studies to define the impact of lifestyle and self-management related sleep disruptions are needed, because these behaviors are potentially modifiable. Modifying behaviors may result in improved sleep quality through less sleep disruption, ultimately improving glycemic control and decreasing inflammation.

In summary, my findings highlight an important role for sleep in both glucose homeostasis and inflammation in young adults with T1DM. These findings lay the essential foundation to develop future mechanistic studies yielding information essential to improve clinical management of T1DM and ultimately quality of life for these individuals.

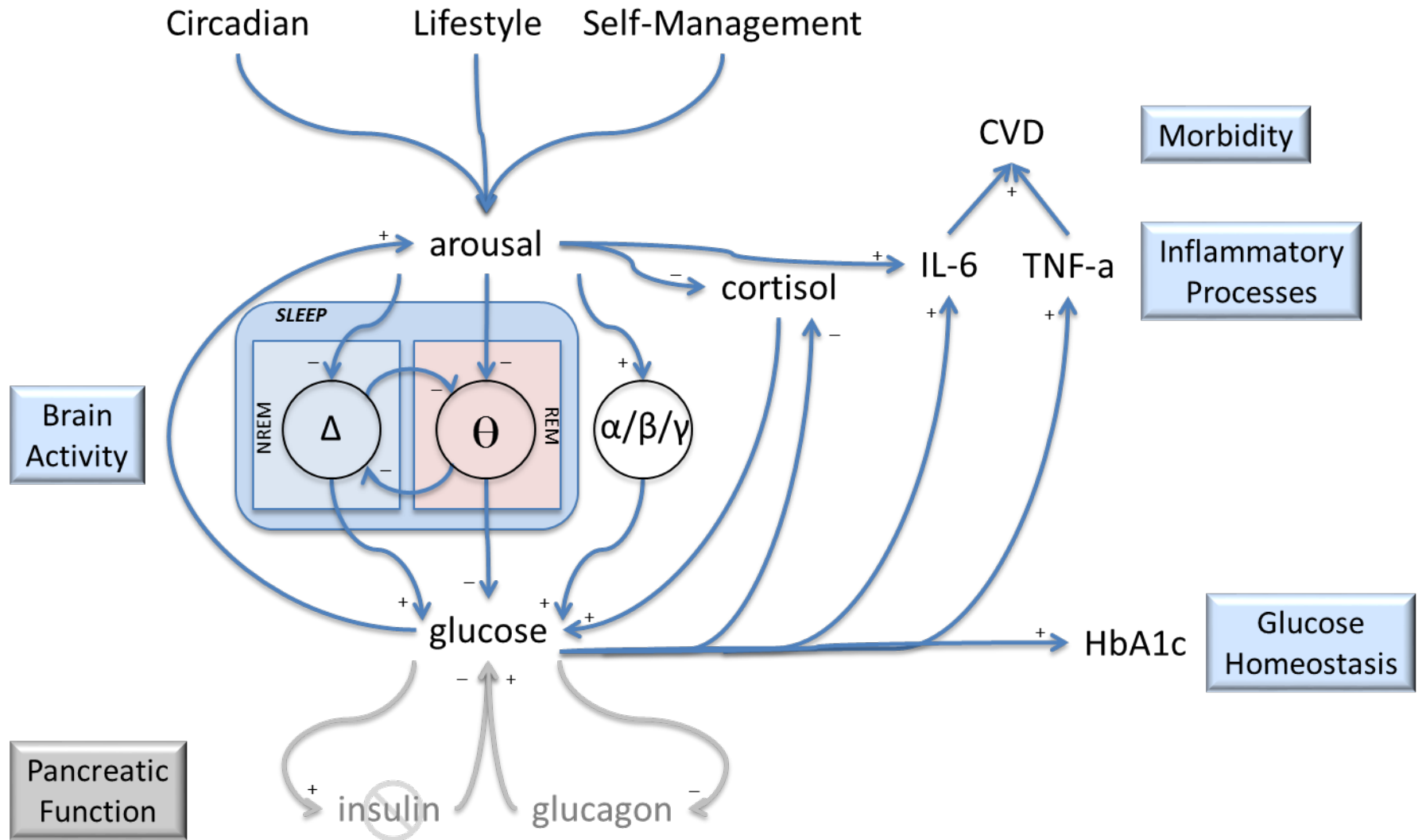


FIGURE XV. SCHWARZ FARABI FRAMEWORK

- The central aspect is level of physiological arousal, specifically during sleep, which is influenced by many factors for those with T1DM, including circadian influences, lifestyle choices and self-management decisions. Level of arousal is reflected in brain activity, which can be separated into Delta (Δ), Theta (Θ), Alpha (α), Beta (β) and gamma (γ) activity using qEEG analysis. Delta and Theta activity are characteristic of sleep; Delta patterns predominate during deep sleep, Theta activity is higher during REM, or dreaming sleep. Delta and Theta activity are suppressed by heightened levels of arousal and when arousal level drops, this inhibition dissipates and sleep begins. Sleep proceeds with an orderly ultradian alternation between NREM and REM sleep until arousal again suppresses Delta and Theta activity while simultaneously increasing Alpha, Beta and Gamma activity. My data support that increasing Delta activity increases glucose levels possibly due to increasing growth hormone and decreasing insulin sensitivity. Conversely, increased Theta activity characteristic of REM sleep can drive a decrease in glucose, possibly due to increased glucose utilization rate seen in REM sleep. My data also support that high frequency brain activity (Beta and Gamma) associated with arousal or awakening also increases glucose levels.
- Each of these influences of brain activity on glucose is expected to manifest more clearly in individuals with T1DM, because the normal primary homeostatic systems responsible for maintaining constant glucose levels, insulin and glucagon secretion from the pancreas are absent or impaired. This leads to a situation where circulating glucose levels become much more variable, as is characteristic of T1DM. My data also demonstrate that increasing glucose drives increasing arousal level. This lays a foundation for multiple possible feedback loops involving glucose and arousal state. Delta activity provides a negative-feedback, or homeostatic loop; a spontaneous increase in glucose reduces Delta activity, which provides a decrease of glucose back toward baseline (“correcting” the increase). The same increase of glucose (causing an arousal) will lead to a parallel decrease of Theta activity which will have the opposite effect – a further increase of glucose, providing a positive-feedback. Similarly, increased glucose will increase high frequency EEG, again driving a further increase of glucose. So there exists the potential for both “vicious cycles” of increasing (or decreasing) glucose, as well as at least one homeostatic feedback loop involving brain activity. The net effect will depend on the relative strength of these feedback loops, which may vary as a function of time. Another important feedback loop may remain active, even in those with T1DM: the counterregulatory response of cortisol. Hypoglycemia triggers secretion of cortisol, impairing insulin sensitivity and allowing glucose level to rise, or “correct”. Again, this is a negative feedback homeostatic loop controlling glucose, which may complement the Delta activity homeostatic feedback loop. My data also support that increasing arousal level (number of arousals during sleep) may lead to reduced cortisol level. The net effect of a spontaneous increase of glucose would be a “corrective” decrease of glucose back toward baseline. Thus, again, we see that the regulatory interaction between physiological arousal and glucose encompasses multiple positive and multiple negative nested feedback loops – and the strength of each loops may be time varying.
- A central hypothesis of this work is that disturbances of sleep and arousal processes represent a mediating factor linking glucose variability to elevated inflammatory processes in T1DM. My data in fact, support this hypothesis. Not only do glucose variations have the potential to perturb sleep and arousal state, but increased arousals in the form of sleep fragmentation are associated with elevated IL-6 levels even after controlling for glucose. Thus, part of the impact of glucose variability on inflammation may be exerted indirectly by sleep fragmentation driving elevated biomarker levels. It is possible this is due to increased sympathetic nerve activation (sympathoexcitation) which has been reported by other studies of sleep fragmentation.
- It is important to recognize that various elements of this system may be operating on intrinsically different time scales. For example, HbA1c provides a convenient and accessible measure of average glucose level over a period of several months. Whereas circadian influences occur daily, cyclical alternations of NREM and REM sleep occur on a period of one to two hours and arousals from sleep may last only seconds. Also, increases of glucose (manifested as high HbA1c) also are associated with increased levels of inflammatory markers, and this interaction probably occurs over a period of hours to days. Conversely, elevated inflammatory states lead to increased risks for cardiovascular disease and morbidity that may play out over a period of years.

CITED LITERATURE

1. Maahs DM, West NA, Lawrence JM, Mayer-Davis EJ. Chapter 1: Epidemiology of Type 1 Diabetes. *Endocrinol Metab Clin North Am*. 2010 Sep;39(3):481–97.
2. Juvenile Diabetes Research Foundation. Type 1 Diabetes Facts [Internet]. JDRF. 2015. Available from: <http://jdrf.org/about/fact-sheets/type-1-diabetes-facts/>
3. Centers for Disease Control. National Diabetes Statistics Report: Estimates of Diabetes and Its Burden in the United States, 2014. Atlanta, GA: U.S. Department of Health and Human Services; 2014.
4. Lipman TH, Levitt Katz LE, Ratcliffe SJ, Murphy KM, Aguilar A, Rezvani I, et al. Increasing incidence of type 1 diabetes in youth: twenty years of the Philadelphia Pediatric Diabetes Registry. *Diabetes Care*. 2013 Jun;36(6):1597–603.
5. The Writing Group for the SEARCH for Diabetes in Youth Study Group. Incidence of Diabetes in Youth in the United States. *JAMA J Am Med Assoc*. 2007 Jun 27;297(24):2716–24.
6. Vehik K, Hamman RF, Lezotte D, Norris JM, Klingensmith G, Bloch C, et al. Increasing Incidence of Type 1 Diabetes in 0- to 17-Year-Old Colorado Youth. *Diabetes Care*. 2007 Mar 1;30(3):503–9.
7. Dabelea D, Mayer-Davis EJ, Saydah S, Imperatore G, Linder B, Divers J, et al. Prevalence of type 1 and type 2 diabetes among children and adolescents from 2001 to 2009. *JAMA*. 2014 May 7;311(17):1778–86.
8. Alberts B, Johnson A, Lewis J, Raff M, Roberts K, Walter P. T Cells and MHC Proteins. 2002 [cited 2015 Nov 6]; Available from: <http://www.ncbi.nlm.nih.gov/books/NBK26926/>
9. Kishiyama J. Disorders of the Immune System. In: *Pathophysiology of Disease*. 6th ed. New York: McGraw-Hill Lange; 2010.
10. Atkinson MA. The pathogenesis and natural history of type 1 diabetes. *Cold Spring Harb Perspect Med*. 2012 Nov;2(11).
11. Taplin CE, Barker JM. Autoantibodies in type 1 diabetes. *Autoimmunity*. 2008 Feb;41(1):11–8.
12. Atkinson MA, Eisenbarth GS, Michels AW. Type 1 diabetes. *The Lancet*. 2014 Jan 10;383(9911):69–82.
13. Nokoff N, Rewers M. Pathogenesis of type 1 diabetes: lessons from natural history studies of high-risk individuals. *Ann N Y Acad Sci*. 2013 Apr;1281:1–15.
14. Kawasaki E. ZnT8 and type 1 diabetes. *Endocr J*. 2012;59(7):531–7.
15. Knip M, Korhonen S, Kulmala P, Veijola R, Reunanen A, Raitakari OT, et al. Prediction of type 1 diabetes in the general population. *Diabetes Care*. 2010 Jun;33(6):1206–12.

16. Wenzlau JM, Juhl K, Yu L, Moua O, Sarkar SA, Gottlieb P, et al. The cation efflux transporter ZnT8 (Slc30A8) is a major autoantigen in human type 1 diabetes. *Proc Natl Acad Sci U S A*. 2007 Oct 23;104(43):17040–5.
17. Concannon P, Rich SS, Nepom GT. Genetics of type 1A diabetes. *N Engl J Med*. 2009 Apr 16;360(16):1646–54.
18. Rønningen KS. Type 1 diabetes: prospective cohort studies for identification of the environmental trigger. *Arch Immunol Ther Exp (Warsz)*. 2013 Dec;61(6):459–68.
19. Rønningen KS, Norris JM, Knip M. Environmental Trigger(s) of Type 1 Diabetes: Why Is It So Difficult to Identify? *BioMed Res Int [Internet]*. 2015 [cited 2015 Aug 23];2015. Available from: <http://www.ncbi.nlm.nih.gov/pmc/articles/PMC4396126/>
20. Bergamin CS, Dib SA. Enterovirus and type 1 diabetes: What is the matter? *World J Diabetes*. 2015 Jun 25;6(6):828–39.
21. Tauriainen S, Oikarinen S, Oikarinen M, Hyöty H. Enteroviruses in the pathogenesis of type 1 diabetes. *Semin Immunopathol*. 2011 Jan;33(1):45–55.
22. Eringsmark Regnéll S, Lernmark A. The environment and the origins of islet autoimmunity and Type 1 diabetes. *Diabet Med J Br Diabet Assoc*. 2013 Feb;30(2):155–60.
23. TEDDY Study Group. The Environmental Determinants of Diabetes in the Young (TEDDY) Study. *Ann N Y Acad Sci*. 2008 Dec;1150:1–13.
24. Eisenbarth GS. Type I diabetes mellitus. A chronic autoimmune disease. *N Engl J Med*. 1986 May 22;314(21):1360–8.
25. American Diabetes Association. Standards of medical care in diabetes-2015 abridged for primary care providers. *Clin Diabetes Publ Am Diabetes Assoc*. 2015 Apr;33(2):97–111.
26. Scrimgeour L, Cobry E, McFann K, Burdick P, Weimer C, Slover R, et al. Improved glycemic control after long-term insulin pump use in pediatric patients with type 1 diabetes. *Diabetes Technol Ther*. 2007 Oct;9(5):421–8.
27. Misso ML, Egberts KJ, Page M, O’Connor D, Shaw J. Continuous subcutaneous insulin infusion (CSII) versus multiple insulin injections for type 1 diabetes mellitus. *Cochrane Database Syst Rev*. 2010;(1):CD005103.
28. Plotnick LP, Clark LM, Brancati FL, Erlinger T. Safety and effectiveness of insulin pump therapy in children and adolescents with type 1 diabetes. *Diabetes Care*. 2003 Apr;26(4):1142–6.
29. Steineck I, Cederholm J, Eliasson B, Rawshani A, Eeg-Olofsson K, Svensson A-M, et al. Insulin pump therapy, multiple daily injections, and cardiovascular mortality in 18,168 people with type 1 diabetes: observational study. *BMJ*. 2015;350:h3234.
30. Giacco F, Brownlee M. Oxidative Stress and Diabetic Complications. *Circ Res*. 2010 Oct 29;107(9):1058–70.

31. Du X, Matsumura T, Edelstein D, Rossetti L, Zsengellér Z, Szabó C, et al. Inhibition of GAPDH activity by poly(ADP-ribose) polymerase activates three major pathways of hyperglycemic damage in endothelial cells. *J Clin Invest*. 2003 Oct 1;112(7):1049–57.
32. Chung SSM, Ho ECM, Lam KSL, Chung SK. Contribution of polyol pathway to diabetes-induced oxidative stress. *J Am Soc Nephrol JASN*. 2003 Aug;14(8 Suppl 3):S233–6.
33. Dunlop M. Aldose reductase and the role of the polyol pathway in diabetic nephropathy. *Kidney Int*. 2000 Sep;58(S77):S3–12.
34. Inoguchi T, Sonta T, Tsubouchi H, Etoh T, Kakimoto M, Sonoda N, et al. Protein Kinase C–Dependent Increase in Reactive Oxygen Species (ROS) Production in Vascular Tissues of Diabetes: Role of Vascular NAD(P)H Oxidase. *J Am Soc Nephrol*. 2003 Aug 1;14(suppl 3):S227–32.
35. Shanmugam N, Reddy MA, Guha M, Natarajan R. High Glucose-Induced Expression of Proinflammatory Cytokine and Chemokine Genes in Monocytic Cells. *Diabetes*. 2003 May 1;52(5):1256–64.
36. Pieper GM, Riaz-ul-Haq null. Activation of nuclear factor-kappaB in cultured endothelial cells by increased glucose concentration: prevention by calphostin C. *J Cardiovasc Pharmacol*. 1997 Oct;30(4):528–32.
37. Du XL, Edelstein D, Dimmeler S, Ju Q, Sui C, Brownlee M. Hyperglycemia inhibits endothelial nitric oxide synthase activity by posttranslational modification at the Akt site. *J Clin Invest*. 2001 Nov;108(9):1341–8.
38. Ahmed N. Advanced glycation endproducts--role in pathology of diabetic complications. *Diabetes Res Clin Pract*. 2005 Jan;67(1):3–21.
39. Peppas M, Uribarri J, Vlassara H. Glucose, Advanced Glycation End Products, and Diabetes Complications: What Is New and What Works. *Clin Diabetes*. 2003 Oct 1;21(4):186–7.
40. Goldin A, Beckman JA, Schmidt AM, Creager MA. Advanced Glycation End Products Sparking the Development of Diabetic Vascular Injury. *Circulation*. 2006 Aug 8;114(6):597–605.
41. Lee MY, Griendling KK. Redox Signaling, Vascular Function, and Hypertension. *Antioxid Redox Signal*. 2008 Jun;10(6):1045–59.
42. Capellini VK, Celotto AC, Baldo CF, Olivon VC, Viaro F, Rodrigues AJ, et al. Diabetes and vascular disease: basic concepts of nitric oxide physiology, endothelial dysfunction, oxidative stress and therapeutic possibilities. *Curr Vasc Pharmacol*. 2010 Jul;8(4):526–44.
43. Soedamah-Muthu SS, Fuller JH, Mulnier HE, Raleigh VS, Lawrenson RA, Colhoun HM. High risk of cardiovascular disease in patients with type 1 diabetes in the U.K.: a cohort study using the general practice research database. *Diabetes Care*. 2006 Apr;29(4):798–804.
44. Klein BEK, Klein R, McBride PE, Cruickshanks KJ, Palta M, Knudtson MD, et al. Cardiovascular disease, mortality, and retinal microvascular characteristics in type 1 diabetes: Wisconsin epidemiologic study of diabetic retinopathy. *Arch Intern Med*. 2004 Sep 27;164(17):1917–24.

45. Ferranti SD de, Boer IH de, Fonseca V, Fox CS, Golden SH, Lavie CJ, et al. Type 1 Diabetes Mellitus and Cardiovascular Disease: A Scientific Statement From the American Heart Association and American Diabetes Association. *Diabetes Care*. 2014 Oct 1;37(10):2843–63.
46. Mannucci E, Dicembrini I, Lauria A, Pozzilli P. Is glucose control important for prevention of cardiovascular disease in diabetes? *Diabetes Care*. 2013 Aug;36 Suppl 2:S259–63.
47. Conget I, Giménez M. Glucose control and cardiovascular disease: is it important? No. *Diabetes Care*. 2009 Nov;32 Suppl 2:S334–6.
48. Hirsch IB. Glycemic Variability: It's Not Just About A1C Anymore! *Diabetes Technol Ther*. 2005 Oct;7(5):780–3.
49. Quagliaro L, Piconi L, Assaloni R, Martinelli L, Motz E, Ceriello A. Intermittent High Glucose Enhances Apoptosis Related to Oxidative Stress in Human Umbilical Vein Endothelial Cells: The Role of Protein Kinase C and NAD(P)H-Oxidase Activation. *Diabetes*. 2003 Sep 5;52(11):2795–804.
50. Piconi L, Quagliaro L, Da Ros R, Assaloni R, Giugliano D, Esposito K, et al. Intermittent high glucose enhances ICAM-1, VCAM-1, E-selectin and interleukin-6 expression in human umbilical endothelial cells in culture: the role of poly(ADP-ribose) polymerase. *J Thromb Haemost*. 2004 Aug;2(8):1453–9.
51. Kilpatrick ES. The Effect of Glucose Variability on the Risk of Microvascular Complications in Type 1 Diabetes. *Diabetes Care*. 2006 Jul 1;29(7):1486–90.
52. Kilpatrick ES, Rigby AS, Atkin SL. Effect of Glucose Variability on the Long-Term Risk of Microvascular Complications in Type 1 Diabetes. *Diabetes Care*. 2009 Jun 23;32(10):1901–3.
53. Wentholt IME, Kulik W, Michels RPJ, Hoekstra JBL, DeVries JH. Glucose fluctuations and activation of oxidative stress in patients with type 1 diabetes. *Diabetologia*. 2007 Nov 10;51(1):183–90.
54. Peña AS, Couper JJ, Harrington J, Gent R, Fairchild J, Tham E, et al. Hypoglycemia, but not Glucose Variability, Relates to Vascular Function in Children with Type 1 Diabetes. *Diabetes Technol Ther*. 2012 Feb 7;120207092523006.
55. Libby P. Inflammation and Atherosclerosis. *Circulation*. 2002 Mar 5;105(9):1135–43.
56. Berg AH, Scherer PE. Adipose tissue, inflammation, and cardiovascular disease. *Circ Res*. 2005 May 13;96(9):939–49.
57. Fiorentino TV, Priolella A, Zuo P, Folli F. Hyperglycemia-induced oxidative stress and its role in diabetes mellitus related cardiovascular diseases. *Curr Pharm Des*. 2013;19(32):5695–703.
58. Lin Y, Berg AH, Iyengar P, Lam TKT, Giacca A, Combs TP, et al. The Hyperglycemia-induced Inflammatory Response in Adipocytes THE ROLE OF REACTIVE OXYGEN SPECIES. *J Biol Chem*. 2005 Feb 11;280(6):4617–26.

59. Wang W-T, Lee P, Yeh H-W, Smirnova IV, Choi I-Y. Effects of acute and chronic hyperglycemia on the neurochemical profiles in the rat brain with streptozotocin-induced diabetes detected using in vivo ¹H MR spectroscopy at 9.4 T. *J Neurochem*. 2012 May;121(3):407–17.
60. Gogitidze Joy N, Hedrington MS, Briscoe VJ, Tate DB, Ertl AC, Davis SN. Effects of Acute Hypoglycemia on Inflammatory and Pro-atherothrombotic Biomarkers in Individuals With Type 1 Diabetes and Healthy Individuals. *Diabetes Care*. 2010 Jul;33(7):1529–35.
61. Lechleitner M, Koch T, Herold M, Dzien A, Hoppichler F. Tumour necrosis factor-alpha plasma level in patients with type 1 diabetes mellitus and its association with glycaemic control and cardiovascular risk factors. *J Intern Med*. 2000 Jul;248(1):67–76.
62. Basu S, Larsson A, Vessby J, Vessby B, Berne C. Type 1 Diabetes Is Associated With Increased Cyclooxygenase- and Cytokine-Mediated Inflammation. *Diabetes Care*. 2005 Jun 1;28(6):1371–5.
63. Snell-Bergeon JK, Nadeau K. Cardiovascular disease risk in young people with type 1 diabetes. *J Cardiovasc Transl Res*. 2012 Aug;5(4):446–62.
64. Walker BR. Glucocorticoids and cardiovascular disease. *Eur J Endocrinol Eur Fed Endocr Soc*. 2007 Nov;157(5):545–59.
65. Dekker MJHJ, Koper JW, van Aken MO, Pols HAP, Hofman A, de Jong FH, et al. Salivary Cortisol Is Related to Atherosclerosis of Carotid Arteries. *J Clin Endocrinol Metab*. 2008 Jul 29;93(10):3741–7.
66. Cameron OG, Thomas B, Tiongco D, Hariharan M, Greden JF. Hypercortisolism in diabetes mellitus. *Diabetes Care*. 1987 Oct;10(5):662–4.
67. Dacou-Voutetakis C, Peppas-Patrikiou M, Dracopoulou M. Urinary free cortisol and its nyctohemeral variation in adolescents and young adults with IDDM: relation to endothelin 1 and indices of diabetic angiopathy. *J Pediatr Endocrinol Metab JPEM*. 1998;11(3):437–45.
68. Mosbah AAAE-R, Abd-Ellatif NAB, Sorour EI. Influence of serum cortisol levels on glycemic control in children with type 1 diabetes. *J Egypt Soc Parasitol*. 2011 Dec;41(3):777–84.
69. Sassin JF, Parker DC, Mace JW, Gotlin RW, Johnson LC, Rossman LG. Human growth hormone release: relation to slow-wave sleep and sleep-walking cycles. *Science*. 1969 Aug 1;165(3892):513–5.
70. Rizza RA, Mandarino LJ, Gerich JE. Effects of Growth Hormone on Insulin Action in Man: Mechanisms of Insulin Resistance, Impaired Suppression of Glucose Production, and Impaired Stimulation of Glucose Utilization. *Diabetes*. 1982 Aug 1;31(8):663–9.
71. Bialasiewicz P, Pawlowski M, Nowak D, Loba J, Czupryniak L. Decreasing concentration of interstitial glucose in REM sleep in subjects with normal glucose tolerance. *Diabet Med*. 2009 Apr;26(4):339–44.
72. Stamatakis KA, Punjabi NM. Effects of Sleep Fragmentation on Glucose Metabolism in Normal Subjects. *Chest*. 2009 Jun 19;137(1):95–101.

73. Buxton OM, Pavlova M, Reid EW, Wang W, Simonson DC, Adler GK. Sleep Restriction for 1 Week Reduces Insulin Sensitivity in Healthy Men. *Diabetes*. 2010 Jun 28;59(9):2126–33.
74. González-Ortiz M, Martínez-Abundis E, Balcázar-Muñoz BR, Pascoe-González S. Effect of sleep deprivation on insulin sensitivity and cortisol concentration in healthy subjects. *Diabetes Nutr Metab*. 2000 Apr;13(2):80–3.
75. Born J, Lange T, Hansen K, Mölle M, Fehm HL. Effects of sleep and circadian rhythm on human circulating immune cells. *J Immunol Baltim Md 1950*. 1997 May 1;158(9):4454–64.
76. Irwin MR, Wang M, Ribeiro D, Cho HJ, Olmstead R, Breen EC, et al. Sleep Loss Activates Cellular Inflammatory Signaling. *Biol Psychiatry*. 2008 Sep;64(6):538–40.
77. Chennaoui M, Sauvet F, Drogou C, Van Beers P, Langrume C, Guillard M, et al. Effect of one night of sleep loss on changes in tumor necrosis factor alpha (TNF- α) levels in healthy men. *Cytokine*. 2011 Nov;56(2):318–24.
78. Shearer W, Reuben J, Mullington J, Price N, Lee B, Smith E, et al. Soluble TNF- α receptor 1 and IL-6 plasma levels in humans subjected to the sleep deprivation model of spaceflight . *J Allergy Clin Immunol*. 2001 Jan;107(1):165–70.
79. Leproult R, Copinschi G, Buxton O, Van Cauter E. Sleep loss results in an elevation of cortisol levels the next evening. *Sleep*. 1997 Oct;20(10):865–70.
80. Fernandez-Mendoza J, Vgontzas AN, Calhoun SL, Vgontzas A, Tsaoussoglou M, Gaines J, et al. Insomnia symptoms, objective sleep duration and hypothalamic-pituitary-adrenal activity in children. *Eur J Clin Invest*. 2014 May;44(5):493–500.
81. Backhaus J, Junghanns K, Hohagen F. Sleep disturbances are correlated with decreased morning awakening salivary cortisol. *Psychoneuroendocrinology*. 2004 Oct;29(9):1184–91.
82. Omisade A, Buxton OM, Rusak B. Impact of acute sleep restriction on cortisol and leptin levels in young women. *Physiol Behav*. 2010 Apr;99(5):651–6.
83. Perfect MM, Elkins GR, Lyle-Lahroud T, Posey JR. Stress and quality of sleep among individuals diagnosed with diabetes. *Stress Health*. 2010 Feb;26(1):61–74.
84. van Dijk M, Donga E, van Dijk JG, Lammers GJ, van Kralingen KW, Dekkers OM, et al. Disturbed subjective sleep characteristics in adult patients with long-standing type 1 diabetes mellitus. *Diabetologia*. 2011 Aug;54(8):1967–76.
85. Caruso NC, Radovanovic B, Kennedy JD, Couper J, Kohler M, Kavanagh PS, et al. Sleep, executive functioning and behaviour in children and adolescents with type 1 diabetes. *Sleep Med*. 2014 Dec;15(12):1490–9.
86. Perfect MM, Patel PG, Scott RE, Wheeler MD, Patel C, Griffin K, et al. Sleep, glucose, and daytime functioning in youth with type 1 diabetes. *Sleep*. 2012 Jan;35(1):81–8.

87. Jauch-Chara K, Schultes B. Sleep and the response to hypoglycaemia. *Best Pract Res Clin Endocrinol Metab.* 2010 Oct;24(5):801–15.
88. Happe S, Treptau N, Ziegler R, Harms E. Restless legs syndrome and sleep problems in children and adolescents with insulin-dependent diabetes mellitus type 1. *Neuropediatrics.* 2005 Apr;36(2):98–103.
89. Bächle C, Lange K, Stahl-Pehe A, Castillo K, Holl RW, Giani G, et al. Associations between HbA1c and depressive symptoms in young adults with early-onset type 1 diabetes. *Psychoneuroendocrinology.* 2015 May;55:48–58.
90. Barone MTU, Wey D, Schorr F, Franco DR, Carra MK, Lorenzi Filho G, et al. Sleep and glycemic control in type 1 diabetes. *Arch Endocrinol Metab.* 2015 Feb;59(1):71–8.
91. Borel A-L, Pépin J-L, Nasse L, Baguet J-P, Netter S, Benhamou P-Y. Short Sleep Duration Measured by Wrist Actimetry Is Associated With Deteriorated Glycemic Control in Type 1 Diabetes. *Diabetes Care.* 2013 Oct 1;36(10):2902–8.
92. Donga E, van Dijk M, van Dijk JG, Biermasz NR, Lammers G-J, van Kralingen K, et al. Partial sleep restriction decreases insulin sensitivity in type 1 diabetes. *Diabetes Care.* 2010 Jul;33(7):1573–7.
93. Banarer S, Cryer PE. Sleep-Related Hypoglycemia-Associated Autonomic Failure in Type 1 Diabetes Reduced Awakening From Sleep During Hypoglycemia. *Diabetes.* 2003 May 1;52(5):1195–203.
94. Jones TW, Porter P, Sherwin RS, Davis EA, O'Leary P, Frazer F, et al. Decreased Epinephrine Responses to Hypoglycemia during Sleep. *N Engl J Med.* 1998 Jun 4;338(23):1657–62.
95. Diabetes Research in Children Network (DirecNet) Study Group*. Impaired overnight counterregulatory hormone responses to spontaneous hypoglycemia in children with type 1 diabetes. *Pediatr Diabetes.* 2007 Aug;8(4):199–205.
96. Juvenile Diabetes Research Foundation Continuous Glucose Monitoring Study Group. Prolonged Nocturnal Hypoglycemia Is Common During 12 Months of Continuous Glucose Monitoring in Children and Adults With Type 1 Diabetes. *Diabetes Care.* 2010 Mar 3;33(5):1004–8.
97. Ahmet A, Dagenais S, Barrowman NJ, Collins CJ, Lawson ML. Prevalence of Nocturnal Hypoglycemia in Pediatric Type 1 Diabetes: A Pilot Study Using Continuous Glucose Monitoring. *J Pediatr.* 2011 Aug;159(2):297–302.e1.
98. Beregszàsi M, Tubiana-Rufi N, Benali K, Noël M, Bloch J, Czernichow P. Nocturnal hypoglycemia in children and adolescents with insulin-dependent diabetes mellitus: Prevalence and risk factors. *J Pediatr.* 1997 Jul;131(1):27–33.
99. Kaufman FR, Austin J, Neinstein A, Jeng L, Halvorson M, Devoe DJ, et al. Nocturnal hypoglycemia detected with the continuous glucose monitoring system in pediatric patients with type 1 diabetes. *J Pediatr.* 2002 Nov;141(5):625–30.

100. Brod M, Pohlman B, Wolden M, Christensen T. Non-severe nocturnal hypoglycemic events: experience and impacts on patient functioning and well-being. *Qual Life Res Int J Qual Life Asp Treat Care Rehabil.* 2013 Jun;22(5):997–1004.
101. Brod M, Christensen T, Bushnell DM. Impact of nocturnal hypoglycemic events on diabetes management, sleep quality, and next-day function: results from a four-country survey. *J Med Econ.* 2012;15(1):77–86.
102. Porter PA, Byrne G, Stick S, Jones TW. Nocturnal hypoglycaemia and sleep disturbances in young teenagers with insulin dependent diabetes mellitus. *Arch Dis Child.* 1996 Aug;75(2):120–3.
103. Matyka KA, Crawford C, Wiggs L, Dunger DB, Stores G. Alterations in sleep physiology in young children with insulin-dependent diabetes mellitus: Relationship to nocturnal hypoglycemia. *J Pediatr.* 2000 Aug;137(2):233–8.
104. Radan I, Rajer E, Ursic Bratina N, Neubauer D, Krzisinik C, Battelino T. Motor activity during asymptomatic nocturnal hypoglycemia in adolescents with type 1 diabetes mellitus. *Acta Diabetol.* 2004 Jun;41(2):33–7.
105. Pillar G, Schusheim G, Weiss R, Malhotra A, McCowen KC, Shlitner A, et al. Interactions between hypoglycemia and sleep architecture in children with type 1 diabetes mellitus. *J Pediatr.* 2003 Feb;142(2):163–8.
106. Amaral FG, Turati AO, Barone M, Scialfa JH, do Carmo Buonfiglio D, Peres R, et al. Melatonin synthesis impairment as a new deleterious outcome of diabetes-derived hyperglycemia. *J Pineal Res.* 2014 Aug 1;57(1):67–79.
107. Coomans CP, van den Berg SAA, Lucassen EA, Houben T, Pronk ACM, van der Spek RD, et al. The suprachiasmatic nucleus controls circadian energy metabolism and hepatic insulin sensitivity. *Diabetes.* 2013 Apr;62(4):1102–8.
108. Summa KC, Turek FW. Chronobiology and obesity: Interactions between circadian rhythms and energy regulation. *Adv Nutr Bethesda Md.* 2014 May;5(3):312S – 9S.
109. Trümper BG, Reschke K, Molling J. Circadian variation of insulin requirement in insulin dependent diabetes mellitus the relationship between circadian change in insulin demand and diurnal patterns of growth hormone, cortisol and glucagon during euglycemia. *Horm Metab Res Horm Stoffwechselforschung Horm Métabolisme.* 1995 Mar;27(3):141–7.
110. Van Cauter E, Blackman JD, Roland D, Spire JP, Refetoff S, Polonsky KS. Modulation of glucose regulation and insulin secretion by circadian rhythmicity and sleep. *J Clin Invest.* 1991 Sep;88(3):934–42.
111. Houmard JA, Tanner CJ, Slentz CA, Duscha BD, McCartney JS, Kraus WE. Effect of the volume and intensity of exercise training on insulin sensitivity. *J Appl Physiol Bethesda Md* 1985. 2004 Jan;96(1):101–6.

112. Quirk H, Blake H, Tennyson R, Randell TL, Glazebrook C. Physical activity interventions in children and young people with Type 1 diabetes mellitus: a systematic review with meta-analysis. *Diabet Med.* 2014 Oct 1;31(10):1163–73.
113. Bally L, Laimer M, Stettler C. Exercise-associated glucose metabolism in individuals with type 1 diabetes mellitus. *Curr Opin Clin Nutr Metab Care.* 2015 Jul;18(4):428–33.
114. A Grinsted, Moore, J.C., Jevrejeva, S. Application of the cross wavelet transform and wavelet coherence to geophysical time series. *online Processes in Geophysics, European Geosciences Union (EGU).* 2004;11(5/6):561–6.
115. Islam M.R. MRI. Wavelets, its Application and Technique in signal and image processing. *Global Journal of Computer Science and Technology.* 2011;11(4).
116. Neu A, Behret F, Braun R, Herrlich S, Liebrich F, Loesch-Binder M, et al. Higher glucose concentrations following protein- and fat-rich meals - the Tuebingen Grill Study: a pilot study in adolescents with type 1 diabetes. *Pediatr Diabetes.* 2014 Oct 20;
117. Sonnenberg GE, Kemmer FW, Berger M. Exercise in type 1 (insulin-dependent) diabetic patients treated with continuous subcutaneous insulin infusion. Prevention of exercise induced hypoglycaemia. *Diabetologia.* 1990 Nov;33(11):696–703.
118. McMahon SK, Ferreira LD, Ratnam N, Davey RJ, Youngs LM, Davis EA, et al. Glucose requirements to maintain euglycemia after moderate-intensity afternoon exercise in adolescents with type 1 diabetes are increased in a biphasic manner. *J Clin Endocrinol Metab.* 2007 Mar;92(3):963–8.
119. Davey RJ, Howe W, Paramalingam N, Ferreira LD, Davis EA, Fournier PA, et al. The effect of midday moderate-intensity exercise on postexercise hypoglycemia risk in individuals with type 1 diabetes. *J Clin Endocrinol Metab.* 2013 Jul;98(7):2908–14.
120. Silveira APS, Bentes CM, Costa PB, Simão R, Silva FC, Silva RP, et al. Acute effects of different intensities of resistance training on glycemic fluctuations in patients with type 1 diabetes mellitus. *Res Sports Med Print.* 2014;22(1):75–87.
121. Hinshaw L, Dalla Man C, Nandy DK, Saad A, Bharucha AE, Levine JA, et al. Diurnal pattern of insulin action in type 1 diabetes: implications for a closed-loop system. *Diabetes.* 2013 Jul;62(7):2223–9.
122. Tatò F, Tatò S, Beyer J, Schrezenmeir J. Circadian variation of basal and postprandial insulin sensitivity in healthy individuals and patients with type-1 diabetes. *Diabetes Res Edinb Scotl.* 1991 May;17(1):13–24.
123. Hanlon EC, Van Cauter E. Quantification of sleep behavior and of its impact on the cross-talk between the brain and peripheral metabolism. *Proc Natl Acad Sci U S A.* 2011 Sep 13;108 Suppl 3:15609–16.
124. Nuwer M. Assessment of digital EEG, quantitative EEG, and EEG brain mapping: report of the American Academy of Neurology and the American Clinical Neurophysiology Society. *Neurology.* 1997 Jul;49(1):277–92.

125. Carney P, Fisher N, Ditto W, Geyer J. Quantitative Sleep Monitoring. In: Quantitative EEG Analysis Methods and Clinical Applications. Norwood, MA: Artech House; 2009. p. 257–88.
126. Klonoff DC. A review of continuous glucose monitoring technology. *Diabetes Technol Ther.* 2005 Oct;7(5):770–5.
127. Torrence C, Compo GP. A Practical Guide to Wavelet Analysis. *Bull Am Meteorol Soc.* 1998 Jan;79(1):61.
128. Buysse DJ, Reynolds CF 3rd, Monk TH, Berman SR, Kupfer DJ. The Pittsburgh Sleep Quality Index: a new instrument for psychiatric practice and research. *Psychiatry Res.* 1989 May;28(2):193–213.
129. Johns MW. A new method for measuring daytime sleepiness: the Epworth sleepiness scale. *Sleep.* 1991 Dec;14(6):540–5.
130. Delorme A, Makeig S. EEGLAB: an open source toolbox for analysis of single-trial EEG dynamics including independent component analysis. *J Neurosci Methods.* 2004 Mar 15;134(1):9–21.
131. EEGLAB - Open Source Matlab Toolbox for Electrophysiological Research [Internet]. [cited 2015 Oct 17]. Available from: <http://sccn.ucsd.edu/eeglab/>
132. M. Sifuzzaman MRI. Application of Wavelet Transform and its Advantages Compared to Fourier Transform. *J Phys Sci.* 2009;13.
133. Gjedde A, Marrett S, Vafae M. Oxidative and nonoxidative metabolism of excited neurons and astrocytes. *J Cereb Blood Flow Metab Off J Int Soc Cereb Blood Flow Metab.* 2002 Jan;22(1):1–14.
134. Mergenthaler P, Lindauer U, Dienel GA, Meisel A. Sugar for the brain: the role of glucose in physiological and pathological brain function. *Trends Neurosci.* 2013 Oct;36(10):587–97.
135. Pramming S, Thorsteinsson B, Stigsby B, Binder C. Glycaemic threshold for changes in electroencephalograms during hypoglycaemia in patients with insulin dependent diabetes. *Br Med J Clin Res Ed.* 1988 Mar 5;296(6623):665–7.
136. Juhl CB, Højlund K, Elsborg R, Poulsen MK, Selmar PE, Holst JJ, et al. Automated detection of hypoglycemia-induced EEG changes recorded by subcutaneous electrodes in subjects with type 1 diabetes--the brain as a biosensor. *Diabetes Res Clin Pract.* 2010 Apr;88(1):22–8.
137. Tribl G, Howorka K, Heger G, Anderer P, Thoma H, Zeitlhofer J. EEG topography during insulin-induced hypoglycemia in patients with insulin-dependent diabetes mellitus. *Eur Neurol.* 1996;36(5):303–9.
138. Snogdal LS, Folkestad L, Elsborg R, Remvig LS, Beck-Nielsen H, Thorsteinsson B, et al. Detection of hypoglycemia associated EEG changes during sleep in type 1 diabetes mellitus. *Diabetes Res Clin Pract.* 2012 Oct;98(1):91–7.
139. Bendtson I, Gade J, Rosenfalck AM, Thomsen CE, Wildschjødtz G, Binder C. Nocturnal electroencephalogram registrations in type 1 (insulin-dependent) diabetic patients with hypoglycaemia. *Diabetologia.* 1991 Oct;34(10):750–6.

140. Rachmiel M, Cohen M, Heymen E, Lezinger M, Inbar D, Gilat S, et al. Hyperglycemia is associated with simultaneous alterations in electrical brain activity in youths with type 1 diabetes mellitus. *Clin Neurophysiol Off J Int Fed Clin Neurophysiol*. 2015 Jul 26;
141. Jauch-Chara K, Schmid SM, Hallschmid M, Born J, Schultes B. Altered neuroendocrine sleep architecture in patients with type 1 diabetes. *Diabetes Care*. 2008 Jun;31(6):1183–8.
142. Dijk D-J, Hayes B, Czeisler CA. Dynamics of electroencephalographic sleep spindles and slow wave activity in men: effect of sleep deprivation. *Brain Res*. 1993 Oct 29;626(1–2):190–9.
143. Davidson JR, Moldofsky H, Lue FA. Growth hormone and cortisol secretion in relation to sleep and wakefulness. *J Psychiatry Neurosci JPN*. 1991 Jul;16(2):96–102.
144. Cappuccio FP, Cooper D, D’Elia L, Strazzullo P, Miller MA. Sleep duration predicts cardiovascular outcomes: a systematic review and meta-analysis of prospective studies. *Eur Heart J*. 2011 Jun;32(12):1484–92.
145. Bressler SL, Seth AK. Wiener-Granger causality: a well established methodology. *NeuroImage*. 2011 Sep 15;58(2):323–9.
146. Granger CWJ. Investigating Causal Relations by Econometric Models and Cross-spectral Methods. *Econometrica*. 1969 Aug 1;37(3):424–38.
147. Barnett L, Seth AK. The MVGC multivariate Granger causality toolbox: a new approach to Granger-causal inference. *J Neurosci Methods*. 2014 Feb 15;223:50–68.
148. Barnett L, Seth AK. The MVGC Multivariate Granger Causality Toolbox: A New Approach to Granger-causal Inference.
149. Garcia E. A tutorial on correlation coefficients. 2010; Available from: <http://web.simmons.edu/~benoit/lis642/a-tutorial-on-correlation-coefficients.pdf>
150. Sejling A-S, Kjær TW, Pedersen-Bjergaard U, Diemar SS, Frandsen CSS, Hilsted L, et al. Hypoglycemia-associated changes in the electroencephalogram in patients with type 1 diabetes and normal hypoglycemia awareness or unawareness. *Diabetes*. 2015 May;64(5):1760–9.
151. Schultes B, Jauch-Chara K, Gais S, Hallschmid M, Reiprich E, Kern W, et al. Defective Awakening Response to Nocturnal Hypoglycemia in Patients with Type 1 Diabetes Mellitus. *PLoS Med*. 2007;4(2):e69.
152. Trang T Ly TWJ. Hypoglycemia Does Not Change the Threshold for Arousal from Sleep in Adolescents with Type 1 Diabetes. *Diabetes Technol Amp Ther*. 2012;14(2):101–4.
153. Kryger MH, Roth T, Dement WC. *Principles and Practice of Sleep Medicine*. 5th ed. St. Louis, MO: Elsevier Saunders; 2011.
154. Feupe SF, Frias PF, Mednick SC, McDevitt EA, Heintzman ND. Nocturnal continuous glucose and sleep stage data in adults with type 1 diabetes in real-world conditions. *J Diabetes Sci Technol*. 2013 Sep;7(5):1337–45.

155. Kannel WB, McGee DL. Diabetes and cardiovascular risk factors: the Framingham study. *Circulation*. 1979 Jan 1;59(1):8–13.
156. Hansson GK. Inflammation, atherosclerosis, and coronary artery disease. *N Engl J Med*. 2005 Apr 21;352(16):1685–95.
157. Snell-Bergeon JK, West NA, Mayer-Davis EJ, Liese AD, Marcovina SM, D'Agostino RB Jr, et al. Inflammatory markers are increased in youth with type 1 diabetes: the SEARCH Case-Control study. *J Clin Endocrinol Metab*. 2010 Jun;95(6):2868–76.
158. Schram MT, Chaturvedi N, Schalkwijk CG, Fuller JH, Stehouwer CDA, EURODIAB Prospective Complications Study Group. Markers of inflammation are cross-sectionally associated with microvascular complications and cardiovascular disease in type 1 diabetes?the EURODIAB Prospective Complications Study. *Diabetologia*. 2005 Feb 4;48(2):370–8.
159. Devaraj S, Glaser N, Griffen S, Wang-Polagruto J, Miguelino E, Jialal I. Increased monocytic activity and biomarkers of inflammation in patients with type 1 diabetes. *Diabetes*. 2006 Mar;55(3):774–9.
160. Frey DJ, Fleshner M, Wright KP. The effects of 40 hours of total sleep deprivation on inflammatory markers in healthy young adults. *Brain Behav Immun*. 2007 Nov;21(8):1050–7.
161. Irwin M. Effects of Sleep and Sleep Deprivation on Catecholamine And Interleukin-2 Levels in Humans: Clinical Implications. *J Clin Endocrinol Metab*. 1999 Jun 1;84(6):1979–85.
162. Meier-Ewert HK, Ridker PM, Rifai N, Regan MM, Price NJ, Dinges DF, et al. Effect of sleep loss on C-Reactive protein, an inflammatory marker of cardiovascular risk. *J Am Coll Cardiol*. 2004 Feb;43(4):678–83.
163. Iber C, Ancoli-Israel S, Chesson A, Quan S. *The AASM manual for the scoring of sleep and associated events*. 1st ed. Westchester, IL: American Academy of Sleep Medicine; 2007.
164. Meoli AL, Casey KR, Clark RW, Coleman JA Jr, Fayle RW, Troell RJ, et al. Hypopnea in sleep-disordered breathing in adults. *Sleep*. 2001 Jun 15;24(4):469–70.
165. R&D Systems. Quantikine HS ELISA: Human TNF- α Immunoassay Product Datasheet [Internet]. Minneapolis, MN; 2015. Available from: https://www.rndsystems.com/products/human-tnf-alpha-quantikine-hs-elisa_hsta00d
166. R&D Systems. Quantikine HS ELISA: Human IL-6 Immunoassay Product Datasheet [Internet]. Minneapolis, MN; 2015. Available from: https://www.rndsystems.com/products/human-il-6-quantikine-elisa-kit_d6050
167. R&D Systems. Parameter Cortisol Product Datasheet [Internet]. Minneapolis, MN; 2015. Available from: https://www.rndsystems.com/products/cortisol-parameter-abetaay-kit_kge008
168. Vgontzas AN. Adverse Effects of Modest Sleep Restriction on Sleepiness, Performance, and Inflammatory Cytokines. *J Clin Endocrinol Metab*. 2004 May 1;89(5):2119–26.

169. Togo F, Natelson BH, Adler GK, Ottenweller JE, Goldenberg DL, Struzik ZR, et al. Plasma cytokine fluctuations over time in healthy controls and patients with fibromyalgia. *Exp Biol Med* Maywood NJ. 2009 Feb;234(2):232–40.
170. Fatima G, Mahdi AA, Das SK, Anjum B, Verma NS, Kumar P, et al. Lack of Circadian Pattern of Serum TNF- α and IL-6 in Patients with Fibromyalgia Syndrome. *Indian J Clin Biochem*. 2012 Oct;27(4):340–3.
171. Vgontzas AN, Bixler EO, Lin H-M, Prolo P, Trakada G, Chrousos GP. IL-6 and Its Circadian Secretion in Humans. *Neuroimmunomodulation*. 2005;12(3):131–40.
172. Vgontzas AN. Circadian Interleukin-6 Secretion and Quantity and Depth of Sleep. *J Clin Endocrinol Metab*. 1999 Aug 1;84(8):2603–7.
173. Mitrović M, Popović ĐS, Naglić DT, Paro JN, Ilić T, Zavišić BK. Markers of inflammation and microvascular complications in type 1 diabetes. *Cent Eur J Med*. 2014 Aug 16;9(6):748–53.
174. Kleiner G, Marcuzzi A, Zanin V, Monasta L, Zauli G, Kleiner G, et al. Cytokine Levels in the Serum of Healthy Subjects, Cytokine Levels in the Serum of Healthy Subjects. *Mediat Inflamm Mediat Inflamm*. 2013 Mar 7;2013, 2013:e434010.
175. Hellman L, Nakada F, Curti J, Weitzman ED, Kream J, Roffwarg H, et al. Cortisol Is Secreted Episodically by Normal Man. *J Clin Endocrinol Metab*. 1970 Apr 1;30(4):411–22.
176. Weitzman ED, Fukushima D, Nogeire C, Roffwarg H, Gallagher TF, Hellman L. Twenty-four Hour Pattern of the Episodic Secretion of Cortisol in Normal Subjects. *J Clin Endocrinol Metab*. 1971 Jul 1;33(1):14–22.
177. Rea MS, Figueiro MG, Sharkey KM, Carskadon MA, Rea MS, Figueiro MG, et al. Relationship of Morning Cortisol to Circadian Phase and Rising Time in Young Adults with Delayed Sleep Times, Relationship of Morning Cortisol to Circadian Phase and Rising Time in Young Adults with Delayed Sleep Times. *Int J Endocrinol Int J Endocrinol*. 2012 Oct 22;2012, 2012:e749460.
178. Pruessner JC, Wolf OT, Hellhammer DH, Buske-Kirschbaum A, von Auer K, Jobst S, et al. Free Cortisol Levels after Awakening: A Reliable Biological Marker for the Assessment of Adrenocortical Activity. *Life Sci*. 1997 Nov;61(26):2539–49.
179. Clow A, Hucklebridge F, Stalder T, Evans P, Thorn L. The cortisol awakening response: more than a measure of HPA axis function. *Neurosci Biobehav Rev*. 2010 Sep;35(1):97–103.
180. Serum Cortisol: Reference Range, Interpretation, Collection and Panels. 2015 Sep 18 [cited 2015 Oct 12]; Available from: <http://emedicine.medscape.com/article/2088826-overview>
181. Madsen PL, Schmidt JF, Wildschjødtz G, Friberg L, Holm S, Vorstrup S, et al. Cerebral O₂ metabolism and cerebral blood flow in humans during deep and rapid-eye-movement sleep. *J Appl Physiol Bethesda Md* 1985. 1991 Jun;70(6):2597–601.

182. Madsen PL, Holm S, Vorstrup S, Friberg L, Lassen NA, Wildschjødzt G. Human Regional Cerebral Blood Flow During Rapid-Eye-Movement Sleep. *J Cereb Blood Flow Metab.* 1991 May;11(3):502–7.
183. Bialasiewicz P, Pawlowski M, Nowak D, Loba J, Czupryniak L. Decreasing concentration of interstitial glucose in REM sleep in subjects with normal glucose tolerance. *Diabet Med.* 2009 Apr;26(4):339–44.
184. Colten HR, Altevogt BM, Research I of M (US) C on SM and. *Sleep Physiology.* 2006 [cited 2015 Oct 31]; Available from: <http://www.ncbi.nlm.nih.gov/books/NBK19956/>
185. Dodt C, Breckling U, Derad I, Fehm HL, Born J. Plasma epinephrine and norepinephrine concentrations of healthy humans associated with nighttime sleep and morning arousal. *Hypertension.* 1997 Jul;30(1 Pt 1):71–6.
186. Soman VR, Shamoan H, Sherwin RS, Ziegler WH. Effects of Physiological Infusion of Epinephrine in Normal Humans: Relationship between the Metabolic Response and β -Adrenergic Binding. *J Clin Endocrinol Metab.* 1980 Feb 1;50(2):294–7.
187. Heier M, Margeirsdottir HD, Brunborg C, Hanssen KF, Dahl-Jørgensen K, Seljeflot I. Inflammation in childhood type 1 diabetes; influence of glycemic control. *Atherosclerosis.* 2015 Jan;238(1):33–7.
188. Wiener N. *The Theory of Prediction.* In: *Modern Mathematics for Engineers.* New York: McGraw-Hill; 1956.
189. Bressler SL, Seth AK. Wiener–Granger Causality: A well established methodology. *NeuroImage.* 2011 Sep 15;58(2):323–9.
190. Geweke J. Measurement of Linear Dependence and Feedback Between Multiple Time Series. *J Am Stat Assoc.* 1982 Jun 1;77(378):304–13.
191. Seth AK, Barrett AB, Barnett L. Granger Causality Analysis in Neuroscience and Neuroimaging. *J Neurosci.* 2015 Feb 25;35(8):3293–7.
192. Barnett L, Barrett AB, Seth AK. Granger causality and transfer entropy are equivalent for Gaussian variables. *Phys Rev Lett.* 2009 Dec 4;103(23):238701.
193. Friston K, Moran R, Seth AK. Analysing connectivity with Granger causality and dynamic causal modelling. *Curr Opin Neurobiol.* 2013 Apr;23(2):172–8.
194. Kirchgassner G, Wolters J, Hassler U. Granger Causality. In: *Introduction to Modern Time Series Analysis.* 2nd ed. Berlin: Springer Berlin Heidelberg; 2013. p. 99–125.
195. Bourke P. Cross Correlation [Internet]. 1996 [cited 2015 Oct 5]. Available from: <http://paulbourke.net/miscellaneous/correlate/>

196. Rowell D. Signal Processing: Continuous and Discrete [Internet]. 2008. Available from: <http://ocw.mit.edu/courses/mechanical-engineering/2-161-signal-processing-continuous-and-discrete-fall-2008/study-materials/laplace.pdf>
197. Meko D. Lagged Correlation [Internet]. 2015. Available from: http://www.ltrr.arizona.edu/~dmeko/notes_10.pdf
198. Chatfield C. The Analysis of Time Series, An Introduction. 6th ed. Boca Raton, FL: Chapman & Hall; 2004.
199. Lachaux J-P, Lutz A, Rudrauf D, Cosmelli D, Le Van Quyen M, Martinerie J, et al. Estimating the time-course of coherence between single-trial brain signals: an introduction to wavelet coherence. *Neurophysiol Clin Clin Neurophysiol*. 2002 Jun;32(3):157–74.
200. Bordeianu CC, Landau RH, Paez MJ. Wavelet analyses and applications. *Eur J Phys*. 2009;30(5):1049.
201. Lequin RM. Enzyme Immunoassay (EIA)/Enzyme-Linked Immunosorbent Assay (ELISA). *Clin Chem*. 2005 Dec 1;51(12):2415–8.
202. Aydin S. A short history, principles, and types of ELISA, and our laboratory experience with peptide/protein analyses using ELISA. *Peptides*. 2015 Apr 20;
203. Yorde DE, Sasse EA, Wang TY, Hussa RO, Garancis JC. Competitive enzyme-linked immunoassay with use of soluble enzyme/antibody immune complexes for labeling. I. Measurement of human choriogonadotropin. *Clin Chem*. 1976 Aug;22(8):1372–7.
204. O’Kennedy R, Byrne M, O’Fagain C, Berns G. Experimental section: A review of enzyme-immunoassay and a description of a competitive enzyme-linked immunosorbent assay for the detection of immunoglobulin concentrations. *Biochem Educ*. 1990 Jul 1;18(3):136–40.
205. Gan SD, Patel KR. Enzyme Immunoassay and Enzyme-Linked Immunosorbent Assay. *J Invest Dermatol*. 2013 Sep;133(9):e12.
206. Kato K, Hamaguchi Y, Okawa S, Ishikawa E, Kobayashi K. Use of rabbit antibody IgG bound onto plain and aminoalkylsilyl glass surface for the enzyme-linked sandwich immunoassay. *J Biochem (Tokyo)*. 1977 Jul;82(1):261–6.
207. Sandwich ELISA [Internet]. [cited 2015 Oct 12]. Available from: <http://www.elisa-antibody.com/ELISA-Introduction/ELISA-types/sandwich-elisa>

APPENDICES

Appendix A

Detailed Methods for Statistical Approach of Determining Relationships between EEG Power and Glucose during PSG Study and Activity and Glucose over 60 hour Study Period

Introduction:

This appendix provides additional information for each of the three main analyses used to determine the relationship between changes in EEG and glucose variations in young adults with T1DM. Three complementary analyses were used, Granger Analysis, Cross-Correlation Function Analysis and Wavelet Coherence Analysis. Wavelet coherence was also applied to 60-hours of continuous glucose and activity data collected during the study. Details are provided for this analysis in the wavelet coherence section as well.

Pre-processing for EEG data

Six EEG derivations were recorded: two frontal (F3/A2 and F4/A1), two central (C3/A2 and C4/A1) and two occipital (O1/A2 and O2/A1). All EEG signals were bandpass filtered (0 to 200 Hz) and digitized 500 times per second. For analysis purposes, EEG data collected during the PSG were imported to Matlab utilizing the EEGLab plugin (130,131). For each EEG derivation, we determined power in the Delta (0.5 - 4.0 Hz), Theta (4.03 - 8.0 Hz), Alpha (8.03 - 15.0 Hz), Beta (15.03 - 30.0 Hz), and Gamma (30.03 - 80.0 Hz) Bands as well as two ratios between high and low EEG frequency Bands: $[\text{Alpha}/(\text{Delta} + \text{Theta})]$ and $[(\text{Alpha} + \text{Beta} + \text{Gamma})/(\text{Delta} + \text{Theta})]$ as follows. For each 30-second EEG epoch the Fast Fourier Transform (FFT) periodogram was calculated and the absolute and normalized (% total) power as well as the standard deviation of the absolute and normalized power were calculated for each Band. For each Band, these values were averaged over 10 consecutive 30-second epochs to provide a statistically consistent estimate of absolute and normalized EEG power for each Band every 5-minutes; allowing for temporal alignment with the simultaneous interstitial glucose measurements provided by the CGMS. Temporal alignment between EEG and glucose signals was performed using high-resolution time stamps provided by both the Alice5 and CGMS devices.

A. Wiener-Granger Causality Analysis

Originally described in 1956 by Norbert Weiner (188) and operationalized by Clive Granger in 1969 (146), Wiener-Granger Causality (WGC) is a statistical approach of causality (189). The WGC coefficient is calculated via linear vector autoregressive (VAR) modeling using standard linear regression, such as ordinary least squares regression (189,190). The best model order is determined using information criteria, such as the Akaike information criteria or Bayesian information criteria AIC or BIC, respectively). The WGC coefficient of the model is calculated to determine statistical significance. A statistically significant WGC means that variable x, “Wiener-Granger Causes” y; in other words, the variability of the error estimates for y are significantly less when x (at the specified model order) is included in the regression as compared to when x is not included. The WGC coefficient can never be negative (190). The magnitude of the WGC coefficient can be interpreted as the rate of information transfer, in bits-per unit-time; in other words, the higher the WGC coefficient, the faster the rate of information transfer from variable x to variable y (189,191,192). A popular model in econometric

analysis, Wiener Granger Causality has been used in neuroscience and neuroimaging (191,193). The WGC coefficient is calculated using the following equations (146,147):

First the vector autoregressive model of order p is calculated:

$$U_t = \sum_{k=1}^p A_k * U_{t-k} + \varepsilon_t + C$$

U is the universe of variables. A_k is the n x n matrix of the regression coefficients, ε_t are the residuals covariance matrix and C is a constant array of dimension n.

In the simplest case, and assuming that we wish to test unconditional G-causality, U is split into two jointly distributed multivariate processes, X and Y:

$$U_t = \begin{pmatrix} X_t \\ Y_t \end{pmatrix}$$

Considering the potential G-causality of Y on X, the full VAR model is:

$$X_t = \sum_{k=1}^p A_{xx,k} * X_{t-k} + \sum_{k=1}^p A_{xy,k} * Y_{t-k} + \varepsilon_{x,t} + C$$

Dependence of X on past Y values is summarized by the coefficients $A_{xy,k}$.

The reduced (autoregressive) model (if $A_{xy,1} = A_{xy,2} = A_{xy,\dots} = 0$, signifying no dependence of X on past values of Y) include only past values of X to predict X:

$$X_t = \sum_{k=1}^p A'_{xx,k} * X_{t-k} + \varepsilon_{x,t} + C$$

The reduced regression coefficients are $A'_{xx,k}$

$$F_{y \rightarrow x} = \ln \frac{|\Sigma'_{xx}|}{|\Sigma_{xx}|}$$

$F_{y \rightarrow x}$ is the G-causality coefficient from Y to X. Σ'_{xx} and Σ_{xx} are the residual covariance matrices of the VAR models from the full and restricted models. $F_{y \rightarrow x}$ tells us if the full model (with past Y included) is a better model than the reduced regression.

The WGC analysis makes the assumptions that the signals assessed are stationary and stochastic; further, the data needs to be long enough to model the AR model orders specified (146,194). A stationary process is one in which the mean, variance and autocorrelation of the process are constant throughout time. A stochastic, or random, process is one in which the collection of variables within the

process evolves randomly over time (the direction of the evolution of the process is random over time)(194).

The MVGC toolbox for MatLab (147) was used to execute the Granger Analysis for the EEG and glucose data. The code provided with the toolbox was modified for use with the glucose and EEG data. Average power along with normalized power as well as the standard deviation of these powers of all five Bands as well as the activation ratios for each of the six EEG channels was calculated. It was hypothesized that there was a bidirectional relationship between glucose changes and EEG changes during sleep. Thus, both directions of WGC were assessed; A WGC coefficient was calculated for the effect of a change in glucose on EEG power in each Band (termed in the text as “G→E causality”) as well as the effect of a change in EEG power in each Band on a change in glucose (termed “E→G causality” in the text). The MVGC toolbox tests for strict stationarity of the data by checking the spectral radius of the data. If the spectral radius was ≥ 1 , stationarity was rejected and causality calculations were not performed. The regression type specified for the VAR modeling was ordinary least squares. A maximum order of 20 was used for each calculation and the AIC was used to determine the best fitting model. A maximum model order of 20 was set because 100 minutes was approximately 25% of the total recording time and the temporal relationship between glucose and EEG changes was hypothesized to be rapid in nature. Statistical significance of the WGC coefficient was determined using the chi-squared analysis with a p-value of 0.05. The glucose and EEG power time series of only the models with a statistically significant WGC were imported into STATA. Using the model order specified by the significant WGC, VAR models were run to assess the net sign of the significant coefficients in the model between EEG and glucose (as suggested by Barnett, L. in personal communication 2015).

Below is the Matlab Code, “SWAGEEGgcfinal.m” used to run the WGC analysis for each subject.

```
%% Multivariate Granger Causality
% Last updated 10/5/15 by SS Farabi
%
% *_Note_*: Do _not_ pre-filter your data prior to GC estimation, _except_
% possibly to improve stationarity (e.g notch-filtering to eliminate line noise
% or high-pass filtering to suppress low-frequency transients). Pre-filtering
% (of stationary data) may seriously degrade Granger-causal inference! If you
% want (time-domain) GC over a limited frequency range, rather calculate
% "band-limited" GC; to do this, calculate frequency-domain GCs over the full
% frequency range, then integrate over the desired frequency band [3]; see
% <smvgc_to_mvgc.html |smvgc_to_mvgc|>.
%
%% References
%
% [1] L. Barnett and A. K. Seth,
% <http://www.sciencedirect.com/science/article/pii/S0165027013003701 The MVGC
% Multivariate Granger Causality Toolbox: A New Approach to Granger-causal
% Inference>, _J. Neurosci. Methods_ 223, 2014
% [ <matlab:open('mvgc_preprint.pdf') preprint> ].
%
% [2] A. B. Barrett, L. Barnett and A. K. Seth, "Multivariate Granger causality
% and generalized variance", _Phys. Rev. E_ 81(4), 2010.
%
% [3] L. Barnett and A. K. Seth, "Behaviour of Granger causality under
```

```

% filtering: Theoretical invariance and practical application", _J. Neurosci.
% Methods_ 201(2), 2011.
%
% (C) Lionel Barnett and Anil K. Seth, 2012. See file license.txt in
% installation directory for licensing terms.
%
%% Parameters

ntrials = 1;      % number of trials
nobs    = length(avpower(1,:)); % number of observations per trial

regmode = 'OLS'; % VAR model estimation regression mode ('OLS', 'LWR' or
empty for default)
icregmode = 'LWR'; % information criteria regression mode ('OLS', 'LWR' or
empty for default)

morder = 'AIC'; % model order to use ('AIC', 'BIC' or supplied numerical
value)
momax = 20; % maximum model order for model order estimation
ncondvars = 0; %number of conditioning variables

acmaxlags = []; % maximum autocovariance lags (empty for automatic
calculation)

tstat = 'chi2'; % statistical test for MVGC: 'F' for Granger's F-test
(default) or 'chi2' for Geweke's chi2 test
alpha = 0.05; % significance level for significance test
mhtc = 'None'; % multiple hypothesis test correction (see routine
'significance')

fs = 1/300; % sample rate (Hz)
fres = []; % frequency resolution (empty for automatic calculation)

seed = 0; % random seed (0 for unseeded)

%% Input data into test variable |X| (see below and <mvgchelp.html#4 Common
variable names and data structures>).

%figfile = input('file header for figure output = ','s');
%NOTE: uncomment line above if saved fig files are desired.

clear mean;
filename = input('Please enter the name of the stats output file ".gc" > ',
's');
outfile = sprintf('%s.gc',filename);
fmode = input('Do you want to append (enter "a") or overwrite (enter "w") data
in these files? ','s');
if fmode ~= 'w'
    if fmode ~= 'a'
        display('Warning: invalid file mode specified; data will be appended to
file %s\n', outfile);
        fmode = 'a';
    end
end
end

```

```

fout = fopen(outfile, fmode);
if fmode == 'w'

fprintf(fout, 'sid\tch\tstat\tband\tfgcc\tfgcp\tfpsig\trgcc\trgcp\trpsig\torder\
n');
end

% above code initializes file which will hold the EEG→Glucose and Glucose→EEG
WGC
% the model order and the significance of the coefficient

startchan = input('Please input the starting channel number >');
endchan = input('Please input the ending channel number >');
% if ((endchan-startchan)>3)
%     fprintf('Cannot process more than 4 channels. Resetting ending channel to
%d\n',startchan+3);
%     endchan = startchan+3;
% end

clear statistic; %%holds the statistic specified
statistic(1,:) = 'AVP ';
statistic(2,:) = 'nAVP';
statistic(3,:) = 'SDP ';
statistic(4,:) = 'nSDP';

clear bands; %%holds the power bands specified
bands(1,:) = 'Delta';
bands(2,:) = 'Theta';
bands(3,:) = 'Alpha';
bands(4,:) = 'Beta ';
bands(5,:) = 'Gamma';
bands(6,:) = 'AR1  ';
bands(7,:) = 'AR2  ';

for chanidx = startchan:1:endchan %%indexes over channels 1-6 for AVP, nAVP, SD
and nSD, respectively
    for j = 1:1:4
        if j==1
            testpower = avpower;
        end
        if j==2
            testpower = avnpower;
        end
        if j==3
            testpower = sdpower;
        end
        if j==4
            testpower = sdnpower;
        end
        for k = 1:1:7
            X = testpower((chanidx-1)*7+k : (chanidx-1)*7+k,:);
            X(2,:) = Sensor;
            morder = 'AIC'; %%tests model order using AIC

```

```

%% Model order estimation (<mvgc_schema.html#3 |A2|>)

% Calculate information criteria up to specified maximum model
order.

ptic('\n*** tsdata_to_infocrit\n');
[AIC,BIC,moAIC,moBIC] = tsdata_to_infocrit(X,momax,icregmode);
ptoc('*** tsdata_to_infocrit took ');

% Plot information criteria.
%(NOTE: Uncomment next 3 lines if plots desired)

%figure((chanidx-1)*2+1); clf;
%plot_tsdata([AIC BIC]',{'AIC','BIC'},1/fs);
%title('Model order estimation');

fprintf('\nbest model order (AIC) = %d\n',moAIC);
fprintf('best model order (BIC) = %d\n',moBIC);

% Select model order.

if strcmpi(morder,'AIC')
    morder = moAIC;
    fprintf('\nusing AIC best model order = %d\n',morder);
elseif strcmpi(morder,'BIC')
    morder = moBIC;
    fprintf('\nusing BIC best model order = %d\n',morder);
else
    fprintf('\nusing specified model order = %d\n',morder);
end

%% VAR model estimation (<mvgc_schema.html#3 |A2|>)

% Estimate VAR model of selected order from data.

ptic('\n*** tsdata_to_var... ');
[A,SIG] = tsdata_to_var(X,morder,regmode);
ptoc;

% Check for failed regression

if(isbad(A))
    fprintf('VAR estimation failed');
    fprintf(fout,'\n');
    continue;
end

% NOTE: at this point we have a model and are finished with the
data! - all
% subsequent calculations work from the estimated VAR parameters A
and SIG.

%% Autocovariance calculation (<mvgc_schema.html#3 |A5|>)

```

```

        % The autocovariance sequence drives many Granger causality
calculations (see
        % next section). Now we calculate the autocovariance sequence G
according to the
        % VAR model, to as many lags as it takes to decay to below the
numerical
        % tolerance level, or to acmaxlags lags if specified (i.e. non-
empty).

        ptic('*** var_to_autocov... ');
[G,info] = var_to_autocov(A,SIG,acmaxlags);
        ptoc;

        % The above routine does a LOT of error checking and issues useful
diagnostics.
        % If there are problems with your data (e.g. non-stationarity,
colinearity,
        % etc.) there's a good chance it'll show up at this point - and the
diagnostics
        % may supply useful information as to what went wrong. It is thus
essential to
        % report and check for errors here.

        var_info(info,false); % report results (but don't bail out on
error)

        if(info.rho>1)
            fprintf(fout,'\n');
            continue;
        end

        %% Granger causality calculation: time domain (<mvgc_schema.html#3
|A13|>)

        % Calculate time-domain pairwise-conditional causalities - this
just requires
        % the autocovariance sequence.

        ptic('*** autocov_to_pwcgc... ');
F = autocov_to_pwcgc(G);
        ptoc;

        % Check for failed GC calculation

        if(isbad(F,false))
            fprintf('GC calculation failed');
            fprintf(fout,'\n');
            continue;
        end

        % Significance test using theoretical null distribution, adjusting
for multiple
        % hypotheses.

        pval = mvgc_pval(F,morder,nobs,ntrials,1,1,ncondvars,tstat); % take
careful note of arguments!

```

```

sig = significance(pval,alpha,mhtc);

% Plot time-domain causal graph, p-values and significance.

% figh = figure((chanidx-1)*2+2); clf;
% subplot(1,3,1);
% plot_pw(F);
% title(['Pairwise-conditional GC; Subject = ' sid]);
% subplot(1,3,2);
% plot_pw(pval);
% title(['p-values; Channel = ' num2str(chan(chanidx))]);
% subplot(1,3,3);
% plot_pw(sig);
%title(['Significant at p = ' num2str(alpha)]);
%figout = sprintf('%s-%s',figfile,num2str(chan(chanidx)));
%savefig(figh,figout);

fpsig = (pval(2,1)<0.05);
rpsig = (pval(1,2)<0.05);

fprintf(fout, '%s\t%d\t%s\t%s\t%5.4f\t%5.4f\t%d\t%5.4f\t%5.4f\t%d\t%d\n', sid, cha
n(chanidx), statistic(j, :), bands(k, :), F(2, 1), pval(2, 1), fpsig, F(1, 2), pval(1, 2), rp
sig, morder);
    if fpsig+rpsig>0
        datafile=sprintf('%s-%d-%d-%d.xdat', sid, chanidx, j, k);
        fdout=fopen(datafile, 'w');
        for dc = 1:length(X(1, :))
            fprintf(fdout, '%5.4f\t%4.1f\t%d\n', X(1, dc), X(2, dc), dc);
        end
        fclose(fdout);
    end

% For good measure we calculate Seth's causal density (cd) measure
- the mean
% pairwise-conditional causality. We don't have a theoretical
sampling
% distribution for this.

cd = mean(F(~isnan(F)));

fprintf('\ncausal density = %f\n', cd);

%% Granger causality calculation: frequency domain
(<mvgc_schema.html#3 |A14|>)

% Calculate spectral pairwise-conditional causalities at given
frequency
% resolution - again, this only requires the autocovariance
sequence.

ptic('\n*** autocov_to_spwgc... ');
f = autocov_to_spwgc(G, fres);
ptoc;

% Check for failed spectral GC calculation

```

```

if(isbad(f,false))
    fprintf('spectral GC calculation failed');
    fprintf(fout, '\n');
    continue;
end

% Plot spectral causal graph.

%figure(3); clf;
%plot_spw(f,fs);

%% Granger causality calculation: frequency domain -> time-domain
(<mvgc_schema.html#3 |A15|>)

% Check that spectral causalities average (integrate) to time-
domain
% causalities, as they should according to theory.

fprintf('\nchecking that frequency-domain GC integrates to time-
domain GC... \n');
Fint = smvgc_to_mvgc(f); % integrate spectral MVGCs
mad = maxabs(F-Fint);
madthreshold = 1e-5;
if mad < madthreshold
    fprintf('maximum absolute difference OK: = %.2e (<
%.2e)\n',mad,madthreshold);
else
    fprintf(2,'WARNING: high maximum absolute difference = %e.2 (>
%.2e)\n',mad,madthreshold);
end

end
end
end
fclose(fout);

```

B. Cross-Correlation Function Analysis

The cross-correlation function provides the correlation coefficient between a time series, x , and shifted (past or future) values of time series y . The maximum coefficient is found at the positive or negative shift-value (lag) where alignment of the two signals provides the strongest correlation (195,196). Cross-Correlation is similar to WGC analysis in that it can be applied to two time series to assess the relationship between the signals at various lags. It also assumes that the signals are stochastic and stationary. The sign of the correlation coefficient at each lag provides information about the direction of the association between the two time series. The cross-correlation coefficient does not determine predictability as the WGC analysis does, however it can provide information as to whether there is periodicity in the relationship between two signals. Peaks (or troughs) of the cross-correlation coefficient at multiple lags would indicate periodicity within the two signals. The cross-correlation is calculated by first determining the co-variance function of two time series using the following equation (197,198):

$$c_{xy}(k) = \frac{1}{N} \sum_{t=1}^{N-k} (x_t - \bar{x})(y_{t+k} - \bar{y}) \quad [k = 0, 1, \dots (N - 1)]$$

$$c_{xy}(k) = \sum_{t=1-k}^{N-k} (x_t - \bar{x})(y_{t+k} - \bar{y}) \quad [k = -1, -2, \dots - (N - 1)]$$

N is the series length, \bar{x} and \bar{y} are the means of the two time series, x_t and y_t , and k is the lag applied to one of the time series, in this case y . The function is then determined using the equation (197,198):

$$r_{xy}(k) = \frac{c_{xy}(k)}{\sqrt{c_{xx}(0)c_{yy}(0)}}$$

$c_{xx}(0)$ and $c_{yy}(0)$ are the sample variances of the time series x_t and y_t .

Since it was hypothesized that the relationship between EEG and glucose may be bidirectional and periodic, lags of -20 to 20 (-100 minutes to 100 minutes) applied to glucose were assessed. An upper limit of 100 minutes was used as it was hypothesized that the relationship between glucose and EEG during sleep would be rapid in nature. The cross-correlation coefficients were determined for glucose with: average power, normalized average power, standard deviation of average power and standard deviation of normalized average power for each of the power Bands as well as the two activation ratios for all 6 channels in each subject.

Cross-correlation coefficients are not additive and cannot be added to determine a mean or standard error (150). Thus as suggested by Garcia, (2010) the cross-correlation coefficients were transformed to Z Fisher statistics, which allow for determining the mean of the coefficients and comparison among subjects as well as comparison to zero (150).

Below is the actual Matlab Code, "SWAGEEGcorrfinal.m" used to run the WGC analysis for each subject.

```

%% last updated by S. Farabi 10/5/2015
%%cross correlation coefficient determination for EEG and glucose

sid = input('Please enter the subject ID> ','s');
filename = input('Please enter the name of the ".cor" and ".corstat" files for output>
','s');
fmode = input('Do you want to append (enter "a") or overwrite (enter "w") data in
these files? ','s');
outfile = sprintf('%s.cor',filename);
outfile2 = sprintf('%s.corstat',filename);
if fmode ~= 'w'
    if fmode ~= 'a'
        display('Warning: invalid file mode specified; data will be appended to file
%s\n', outfile);
        fmode = 'a';
    end
end
fout10 = fopen(outfile,fmode);
fout11 = fopen(outfile2,fmode);
fprintf(fout10,'SID\tChan\tBand\tLag\tAV\ttnAV\tSD\ttnSD\n');
fprintf(fout11,'SID\tChan\tBand\tAV\tAVlag\ttnAV\ttnAVlag\tSD\tSDlag\ttnSD\ttnSDlag\n');
%.cor and .corstat will hold all of the correlations at each lag assessed
%and then the best correlation and at what lag it occurs respectively

mlag = input('Please enter maximum number of lags for analysis >');
%input how many correlation lags (pos and neg) you want to look at
clear bands
%holder for each of power bands
bands(1,:) = 'Delta   ';
bands(2,:) = 'Theta   ';
bands(3,:) = 'Alpha   ';
bands(4,:) = 'Beta    ';
bands(5,:) = 'Gamma   ';
bands(6,:) = 'AR1    ';
bands(7,:) = 'AR2    ';

clear xc nxc sdx nsdx; %clears holders for 4 statistics
nchan = length(chan); %counter for how many channels
xc = zeros(7*nchan,(mlag*2)+1);
nxc = zeros(7*nchan,(mlag*2)+1);
sdx = zeros(7*nchan,(mlag*2)+1);
nsdx = zeros(7*nchan,(mlag*2)+1);

if length(avpower(1,:)) < length(Sensor) %ensures that avpower will be the same length
as Sensor
    maxlength = length(avpower(1,:));
    glucose = Sensor([1:maxlength]);
else
    glucose = Sensor;
end

for chanidx = 1:1:nchan %%determines cross-correlation by channel for each statistic
(av power, normalized av power and std. deviations)

```

```

for i = 1:1:7
    [xc(i+(chanidx-1)*7,:), lags] = xcorr(avpower(i+(chanidx-1)*7,:)-
mean(avpower(i+(chanidx-1)*7,:),glucose-mean(glucose)),mlag,'coeff');
    [sdx(i+(chanidx-1)*7,:), lags] = xcorr(sdpower(i+(chanidx-1)*7,:)-
mean(sdpower(i+(chanidx-1)*7,:),glucose-mean(glucose)),mlag,'coeff');
    [nxc(i+(chanidx-1)*7,:), lags] = xcorr(avnpower(i+(chanidx-1)*7,:)-
mean(avnpower(i+(chanidx-1)*7,:),glucose-mean(glucose)),mlag,'coeff');
    [nsdx(i+(chanidx-1)*7,:), lags] = xcorr(sdnpower(i+(chanidx-1)*7,:)-
mean(sdnpower(i+(chanidx-1)*7,:),glucose-mean(glucose)),mlag,'coeff');
    xcmax = 0;
    nxcmax = 0;
    sdxmax = 0;
    nsdxmax = 0;
    xcbestlag = 0;
    nxcbestlag = 0;
    sdxcbestlag = 0;
    nsdxcbestlag = 0;
    xcmaxs = 0;
    nxcmaxs = 0;
    sdxcmxs = 0;
    nsdxcmxs = 0;
    xcbestlags = 0;
    nxcbestlags = 0;
    sdxcbestlags = 0;
    nsdxcbestlags = 0;
%this part will determine if correlation at current lag is higher than
%previous lag by looking at absolute value of the correlation
    for lagidx = 1:1:mlag*2+1 %will determine if correlation at current lag is
higher than previous lag and will print to file if is

fprintf(fout10, '%s\t%d\t%s\t%d\t%4.3f\t%4.3f\t%4.3f\t%4.3f\n',sid,chan(chanidx),bands(
i,:),lags(lagidx),xc(i+(chanidx-1)*7,lagidx),nxc(i+(chanidx-
1)*7,lagidx),sdx(i+(chanidx-1)*7,lagidx),nsdx(i+(chanidx-1)*7,lagidx));
    if abs(xc(i+(chanidx-1)*7,lagidx)) > xcmax
        xcmax = abs(xc(i+(chanidx-1)*7,lagidx));
        xcmaxs = xc(i+(chanidx-1)*7,lagidx);
        xcbestlag = lags(lagidx);
    end
    if abs(nxc(i+(chanidx-1)*7,lagidx)) > nxcmax
        nxcmax = abs(nxc(i+(chanidx-1)*7,lagidx));
        nxcmaxs = nxc(i+(chanidx-1)*7,lagidx);
        nxcbestlag = lags(lagidx);
    end
    if abs(sdx(i+(chanidx-1)*7,lagidx)) > sdxmax
        sdxmax = abs(sdx(i+(chanidx-1)*7,lagidx));
        sdxcmxs = sdx(i+(chanidx-1)*7,lagidx);
        sdxcbestlag = lags(lagidx);
    end
    if abs(nsdx(i+(chanidx-1)*7,lagidx)) > nsdxmax
        nsdxmax = abs(nsdx(i+(chanidx-1)*7,lagidx));
        nsdxcmxs = nsdx(i+(chanidx-1)*7,lagidx);
        nsdxcbestlag = lags(lagidx);
    end
end
end

```


C. Wavelet Coherence

Wavelet coherence is useful for identifying time varying and frequency specific coupling between two time series (signals). Wavelet coherence analysis relies on wavelet transformation of signals from the time domain into a joint time-frequency domain. This approach is particularly advantageous over traditional Fourier transformation when the underlying time series is not stationary. Briefly, wavelet transformation decomposes a signal into a family of components, each having the same sampling rate as the original signal but with each component representing a different time scale. This wavelet decomposition process is thus analogous to applying a “filter bank” to the underlying signal. Wavelet coherence involves computing the time-varying coupling, or coherence, between two signals that have undergone wavelet decomposition. The result is a matrix providing the coherence coefficient – which is analogous to the squared correlation coefficient – as a function of time and time scale (or equivalently, frequency) (132,199,200).

Wavelet transformation requires that you choose a specific wavelet function. According to Torrence and Compo (1998), there are four components of the wavelet to consider when picking a wavelet function: 1) orthogonal or non-orthogonal, 2) complex or real 3) width and 4) shape (127). A frequently recommended wavelet is the Morlet wavelet (115). This wavelet is non-orthogonal (which provides more smooth curves to the wavelet) and complex (provides amplitude and phase), has a width of $\sqrt{2}$ *scale which provides a balance between time and frequency localization of the wavelet and its shape is smooth (127). The Morlet wavelet function is defined as:

$$\psi_0(\eta) = \pi^{-1/4} e^{-i\omega_0\eta} e^{-\frac{1}{2}\eta^2} \quad (114)$$

Where η is time (without dimensions) and ω_0 is frequency and has a value of 6 for the Morlet (114,127). A set of scales needs to be chosen for the wavelet transform (127). For the coherence between EEG power and glucose in the overnight PSG, we used a set of 48 scales that ranged from 2 to 30.2040 (10 to 151.02 minutes). Thus, we had 48 periods ranging from 2.06 to 31.20 (10.6 to 156.01 minutes). For the 60 hour analysis of coherence between glucose and activity, we used a set of 84 scales that ranged from 2 to 241.632 (10 to 1208.16 minutes) and had periods ranging from 2.06 to 249.616 (10.6 to 1248.08 minutes). Using the continuous wavelet transform, the wavelet is stretched in time by varying its scale and is used to determine the wavelet power in a time series using the following equations, (114):

$$W_n^X(s) = \sqrt{\frac{\delta t}{s}} \sum_{n'=1}^N x_{n'} \varphi_0\left[(n' - n) \frac{\delta t}{s}\right]$$

where δt specifies uniform time steps, s is the scale and the wavelet power is defined as

$$|W_n^X(s)|^2$$

The cross wavelet transform can then be determined for two time series, x_t and y_t . The equation to determine the cross-wavelet transform is defined as (114,127):

$$W^{xy} = W^x W^{y*}$$

* is the complex conjugation (equal real part but opposite in sign). The wavelet power from the cross-wavelet transform is defined as:

$$|W^{xy}|$$

Wavelet coherence is the determination of the areas of two wavelets with common power. It can be thought of as a cross-correlation between two wavelets in time and frequency. The equations to derive cross wavelet coherence are as follows (114,127):

$$R_n^2(s) = \frac{|S(s^{-1}W_n^{XY}(s))|^2}{S(s^{-1}|W_n^X(s)|^2) * S(s^{-1}|W_n^Y(s)|^2)}$$

S is the smoothing operator. It is recommended that the smoothing operator has a similar track to the wavelet. For the Morlet wavelet the smoothing operator is defined as (114,127):

$$S_{scale} W|_n = (W_n(s) * c_2 \Pi(0.6s))|_n$$

c_2 is a normalization constant and Π is the rectangular function (value of 0 outside of [-0.5:0.5] and value of 1 between [-0.5:0.5]). 0.6 is the scale decorrelation length for the Morlet (114,127).

There are errors at the beginning and end of the spectrum in calculation of power as one assumption is that the data are cyclic (periodic) (127). The cone of influence (COI) is calculated to provide the region of the wavelet power spectrum which has values which cannot be trusted due to these circular convolution effects. This is calculated at each period by taking the width using the width of wavelet function $(\sqrt{2} * scale)^2$ for each side (127). Only wavelet power values outside the COI were considered for the analysis.

Wavelet transformation was carried out on the average power and normalized average power, standard deviation of average power and normalized power of all five EEG Bands for each of the five channels as well as the two activation ratios and on the glucose for the entire PSG recording. The wavelet coherence was determined between glucose and each Band of EEG as well as the two activation ratios.

To determine statistical significance of computed coherence values, Monte Carlo Simulation (500 iterations) was performed as recommended by both Grinsted and Torrence and Compo (114,127). The phase angle (in degrees) between the two time series was also determined as a function of time and period (114) and then we converted these for reporting to a phase delay in minutes: phase delay (minutes) = (period * phase (in degrees) * 5 minutes) / 360.

We utilized the wavelet coherence toolbox for Matlab provided by Grinsted and colleagues (114) to carry out the procedures. The wavelet chosen was the Morlet. A document was generated to provide the period and phase at which statistically significant coherence occurred. Another document was generated for the epoch number onset and offset of statistically significant coherence (intervals of significance).

Below is the Matlab code, titled "SWAGEEGhere.m" written to perform the analysis for the PSG study to determine coherence between EEG Power and Glucose. Following that is the code, titled "rsq60hour.m" for the 60 hour coherence data.

1. SWAGEEGhere.m

```
%last updated by S. Farabi 9/4/15

sid = input('Please enter the subject ID> ','s');

filename = input('Output file name: ','s');
fmode = input('Do you want to append (enter "a") or overwrite (enter "w") data
in these files? ','s');
if fmode ~= 'w'
    if fmode ~= 'a'
        display('Warning: invalid file mode specified; data will be appended to
file %s\n', outfile);
        fmode = 'a';
    end
end

filename1 = sprintf('%s.coh',filename);
filename2 = sprintf('%s.bcoh',filename);
filename3 = sprintf('%s.drp',filename);
[fout,errmsg] = fopen(filename1, fmode);
[fout2,errmsg] = fopen(filename3, fmode);
[fout10,errmsg] = fopen(filename2, fmode);
%.coh will provide the stastically significant coherence by channel, power
%band & coherence band,.bcoh file will provide average coherence in and out
%of COI, mean phase by channel, power band & coherence band, .drp provides
%the onset, offset and percent of COI that statistically significant drops
%occur in each channel, power band and coherence band

bw = input('Color (enter 0) or Black and White (enter 1) plot?>');

clear bands; % provides holder for each power band
bands(1,:) = 'Delta      ';
bands(2,:) = 'Theta      ';
bands(3,:) = 'Alpha      ';
bands(4,:) = 'Beta       ';
bands(5,:) = 'Gamma      ';
bands(6,:) = 'A/(D+T)    ';
bands(7,:) = '(A+B+G)/(D+T)';

clear blabs; %holder for naming of figures (i.e D=Delta, 6=AR1)
blabs(1,:) = 'D';
blabs(2,:) = 'T';
blabs(3,:) = 'A';
blabs(4,:) = 'B';
blabs(5,:) = 'G';
blabs(6,:) = '1';
blabs(7,:) = '2';

clear statistic; % holds the four statistics from the power bands created
```

```

(average power, normalized average and standard deviations of averages
statistic(1,:) = 'AVP ';
statistic(2,:) = 'nAVP';
statistic(3,:) = 'SDP ';
statistic(4,:) = 'nSDP';

cbands = [1 19 39 48]; %coherence band cut points (upper limits)
nbands = 3; %how many bands you want to create

clear mean; %prevents error message when calculating mean rsq

nchan = length(chan);

fprintf(fout, 'SubID\tStatistic\tChannel\tBand\t Period\t Epoch\t Coher\t
Sig95\t Phase\t COI\t Exclude?\n');
fprintf(fout2, 'Subject\tStatistic\tChannel\tBand\tPeriod\tOnset\tOffset\tPerce
nt COI\n');
fprintf(fout10, 'Subject\tStatistic\tChannel\tBand\tCohBand\tAvRsq\tAvrsqnc\tAvP
hase\n');

for statidx = 1:1:4
    if statidx == 1
        poweract = avpower;
    end
    if statidx == 2
        poweract = avnpower;
    end
    if statidx == 3
        poweract = sdpower;
    end
    if statidx == 4
        poweract = sdnpower;
    end

    for chanidx = 1:1:nchan %will iterate through statistic in each powerband
for each channel
        for v = 1:1:7
            figh=figure('Position',[100,100,600,850]);
            subplot(2,1,1); %creates a plot with raw data
            [ax,p1,p2]=plotyy(1:1:length(poweract((chanidx-
1)*7+v,:)),poweract((chanidx-1)*7+v,:),1:1:length(Sensor),Sensor);
            xlim(ax(1),[0, length(poweract((chanidx-1)*7+v,:))]);
            xlim(ax(2),[0, length(poweract((chanidx-1)*7+v,:))]);
            ylabel(ax(1),bands(v,:));
            ylabel(ax(2),'Sensor Glucose');

            subplot(2,1,2); %creation of coherence plot; uses morlet function
('db8') to create the plot; wtcnc is a .m file which provides the coherence
plot without a color bar. wtcncp.m provides a plot without the phase arrows
            [rsq,period,scale,coi,sig95,phase]=wtcnc(Sensor,poweract((chanidx-
1)*7+v,:), 'MakeFigure',1, 'BlackandWhite',bw); %creates variables with the mean
coherence at every single point assessed at every frequency
            phasedeg = phase*180/3.14159;

            title(bands(v,:));

```

```

    figfile = sprintf('%s-%s-%d-%s-
coh.fig',sid,statistic(statidx,:),chan(chanidx),blabs(v));
    figlabel = sprintf('Filename = %s',figfile);
    text(0,730,figlabel,'Units','pixels');
    xlabel('Epoch Number (5-min increments)');

    savefig(figh,figfile);
    close all;

    dim = size(sig95);

    for i=1:1:dim(1)
        for j=1:1:dim(2)
            if(sig95(i,j)) >= 1
                fprintf(fout,'%s\t%s\t%d\t%s\t %5.3f\t %0.0f\t %5.4f\t
%5.4f\t %5.2f\t %5.3f\t
%0.0f\n',sid,statistic(statidx,:),chan(chanidx),bands(v,:), period(i), j,
rsq(i,j), sig95(i,j), phasedeg(i,j), coi(j), (period(i)>coi(j)));
            end
        end
    end
    fprintf(fout,'\n');

    %%%

    mrsq = zeros(nbands,1);
    mrsqnc = zeros(nbands,1);
    mphase = zeros(nbands,1);
    sumrsq = zeros(dim(1),1);
    numrsq = zeros(dim(1),1);
    numphase = zeros(dim(1),1);
    sumphase = zeros(dim(1),1);
    sumrsqnc = zeros(dim(1),1);
    numrsqnc = zeros(dim(1),1);
    avgphase = zeros(dim(1),1);
    avgrsq = zeros(dim(1),1);
    avgrsqnc = zeros(dim(1),1);
    meanrsq = zeros(nbands,1);
    meanphase = zeros(nbands,1);

    for l=1:1:dim(1)
        for j=1:1:dim(2)

            if period (l) <= coi(j)
                sumrsq(l) = sumrsq(l) + rsq(l,j);
                numrsq(l) = numrsq(l) + 1;
                sumphase(l) = sumphase(l) + phase(l,j);
                numphase(l) = numphase(l) + 1;

            else
                sumrsqnc(l) = sumrsqnc(l) + rsq(l,j);
                numrsqnc(l) = numrsqnc(l) + 1;
            end
        end
    end

```

```

end

for s=1:1:dim(1)
    avgrsq(s) = sumrsq(s)/numrsq(s);
    avgrsqnc(s) = sumrsqnc(s)/numrsqnc(s);
    avgphase(s) = sumphase(s)/numphase(s);
end

for h=1:1:nbands
    if h==1
        mrsq(h) = mean(avgrsq([cbands(h):cbands(h+1)]));
        mrsqnc(h) = mean(avgrsqnc([cbands(h):cbands(h+1)]));
        mphase(h) = mean(avgphase([cbands(h):cbands(h+1)]));
    end
    if h > 1
        mrsq(h) = mean(avgrsq([(cbands(h)+1):cbands(h+1)]));
        mrsqnc(h) =
mean(avgrsqnc([(cbands(h)+1):cbands(h+1)]));
        mphase(h) =
mean(avgphase([(cbands(h)+1):cbands(h+1)]));
    endthe

fprintf(fout10, '%s\t%s\t%d\t%s\t%d\t%4.3f\t%4.3f\t%4.3f\n', sid, statistic(statid
x), chan(chanidx), bands(v,:), h, mrsq(h), mrsqnc(h), mphase(h));

end

%%%

newdrop = 0;
drpon = 0;
drpoff = 0;
for i=1:1:dim(2)
    drpband = 'Low';
    if i > drpoff
        for j=1:1:19
            if sig95(j,i) >= 1 && period(j) <= coi(i)
                newdrop = 1;
                drpon = i;
                k = 1;
                while max(sig95(1:19,i+k)) >= 1 && period(1) <=
coi(i+k)
                    k = k+1;
                end
                if i+k-1 > drpoff
                    drpoff = i+k-1;
                end
            end
        end
    end
end
if newdrop == 1

```

```

fprintf(fout2, '%s\t%s\t%d\t%s\t%s\t%0.0f\t%0.0f\t%4.2f\n', sid, statistic(statidx
), chan(chanidx), bands(v,:), drpband, drpon, drpoff, 100*(drpoff-
drpon+1)/(0.876*dim(2)));
        newdrop = 0;
    end
end

newdrop = 0;
drpon = 0;
drpoff = 0;
for i=1:1:dim(2)
    drpband = 'Mid';
    if i > drpoff
        for j=20:1:39
            if sig95(j,i) >= 1 && period(j) <= coi(i)
                newdrop = 1;
                drpon = i;
                k = 1;
                while max(sig95(20:39,i+k)) >=1 && period(20)
<= coi(i+k)
                    k = k+1;
                end
                if i+k-1 > drpoff
                    drpoff = i+k-1;
                end
            end
        end
    end
    if newdrop == 1

fprintf(fout2, '%s\t%s\t%d\t%s\t%s\t%0.0f\t%0.0f\t%4.2f\n', sid, statistic(statidx
), chan(chanidx), bands(v,:), drpband, drpon, drpoff, 100*(drpoff-
drpon+1)/(0.639*dim(2)));
        newdrop = 0;
    end
end

newdrop = 0;
drpon = 0;
drpoff = 0;
for i=1:1:dim(2)
    drpband = 'High';
    if i > drpoff
        for j=40:1:48
            if sig95(j,i) >= 1 && period(j) <= coi(i)
                newdrop = 1;
                drpon = i;
                k = 1;
                while max(sig95(40:48,i+k)) >=1 && period(40)
<= coi(i+k)
                    k = k+1;
                end
                if i+k-1 > drpoff
                    drpoff = i+k-1;
                end
            end
        end
    end

```



```

643;112 216 377 491 635;...
    74 210 355 497 631;46 157 350 452 630;49 139 329 438 634;52 190 362 490
632;74 175 368 465 633;68 225 355 442 632;58 167 328 464 625;70 150 349 451
623;42 164 328 450 639;...
    73 162 350 454 625;68 172 355 458 621;71 177 330 436 619;58 136 352 442
619;45 161 341 453 628];

for q=1:1:length(names)
    load(names(q,:));
    fname = names(q,:);
    display(fname);
    subnum = q;

    for l = 1:1:6
        if l < 5
            glusnip = Sensor([stateon(subnum,l):stateon(subnum,l+1)]);
            actsnip = dsmtotact([stateon(subnum,l):stateon(subnum,l+1)]);
            nbandaug = -2;
        end
        if l == 5
            glusnip = Sensor([stateon(subnum,l):length(Sensor)]);
            actsnip = dsmtotact([stateon(subnum,l):length(Sensor)]);
            nbandaug = -2;
        end
        if l == 6
            glusnip = Sensor;
            actsnip = dsmtotact;
            nbandaug = 0;
        end

        figh(v)=figure('Position',[100,100,700,1000]);
        subplot(2,1,1);
        [ax,p1,p2]=plotyy(1:1:length(actsnip),actsnip, 1:1:length(glusnip),
glusnip);
        xlim(ax(1),[0, length(actsnip)]);
        xlim(ax(2),[0, length(actsnip)]);
        ylabel(ax(1),'activity');
        ylabel(ax(2),'Sensor Glucose');

        subplot (2,1,2);

[rsq,period,scale,coi,sig95,phase]=wtcncnp(glusnip,actsnip,'MakeFigure',1,'Blac
kandWhite',cbw);
        phasedeg = phase*180/3.14159;
        figname=sprintf('%s-%d',names(q,[1:6]),i);
        savefig(figname);
        close all;

        for p = 1:1:1

            dim = size(sig95);
            cbands(nbands+1) = dim(1);

```

```

mrsq = zeros(nbands+nbandaug,1);
mrsqnc = zeros(nbands+nbandaug,1);
mphase = zeros(nbands+nbandaug,1);
sumrsq = zeros(dim(1),1);
numrsq = zeros(dim(1),1);
numphase = zeros(dim(1),1);
sumphase = zeros(dim(1),1);
sumrsqnc = zeros(dim(1),1);
numrsqnc = zeros(dim(1),1);
avgphase = zeros(dim(1),1);
avgrsq = zeros(dim(1),1);
avgrsqnc = zeros(dim(1),1);
meanrsq = zeros(nbands+nbandaug,1);
meanphase = zeros(nbands+nbandaug,1);

for l=1:1:dim(1)
    for j=1:1:dim(2)

if period (l) <= coi(j)
    sumrsq(l) = sumrsq(l) + rsq(l,j);
    numrsq(l) = numrsq(l) + 1;
    sumphase(l) = sumphase(l) + phase(l,j);
    numphase(l) = numphase(l) + 1;

else
    sumrsqnc(l) = sumrsqnc(l) + rsq(l,j);
    numrsqnc(l) = numrsqnc(l) + 1;
end
end

end

for s=1:1:dim(1)
    avgrsq(s) = sumrsq(s)/numrsq(s);
    avgrsqnc(s) = sumrsqnc(s)/numrsqnc(s);
    avgphase(s) = sumphase(s)/numphase(s);
end

for h=1:1:nbands+nbandaug
    if h < nbands+nbandaug
        mrsq(h) = mean(avgrsq([cbands(h),cbands(h+1)]));
        mrsqnc(h) = mean(avgrsqnc([cbands(h),cbands(h+1)]));
        mphase(h) = mean(avgphase([cbands(h),cbands(h+1)]));
    else
        mrsq(h) = mean(avgrsq([cbands(h),dim(1)]));
        mrsqnc(h) = mean(avgrsqnc([cbands(h),dim(1)]));
        mphase(h) = mean(avgphase([cbands(h),dim(1)]));
    end

fprintf(fout10, '%s\t%d\t%d\t%.2f\t%.3f\t%.3f\n', fname, i, h, mrsq(h), mrsqnc(h),

```

```

mphase(h));

    end

    dim = size(sig95);

    newdrop = 0;
    drpon = 0;
    drpoff = 0;
    for i=1:1:dim(2)
        drpband = '1';
        if i > drpoff
            for j=1:1:19
                if sig95(j,i) >= 1 && period(j) <= coi(i)
                    newdrop = 1;
                    drpon = i;
                    k = 1;
                    while max(sig95(1:19,i+k)) >=1 && period(1) <= coi(i+k)
                        k = k+1;
                    end
                    if i+k-1 > drpoff
                        drpoff = i+k-1;
                    end
                end
            end
        end
        if newdrop == 1
            meanphase = 0;
            for k = drpon:1:drpoff
                for l=1:1:19
                    meanphase = (meanphase + phasedeg(l,k));
                end
            end
            meanphase = (meanphase)/((drpoff-drpon+1)*12);
        end
        fprintf(fout2, '%s\t%s\t%s\t%0.0f\t%0.0f\t%4.2f\t%5.2f\n', filename, bands(v,:), dr
        pband, drpon, drpoff, 100*(drpoff-drpon+1)/(0.8925*dim(2)), meanphase);
        newdrop = 0;
    end
end

newdrop = 0;
drpon = 0;
drpoff = 0;
for i=1:1:dim(2)
    drpband = '2';
    if i > drpoff
        for j=20:1:31
            if sig95(j,i) >= 1 && period(j) <= coi(i)
                newdrop = 1;
                drpon = i;
                k = 1;
            end
        end
    end
end

```

```

                                while max(sig95(20:31,i+k)) >=1 && period(20) <=
coi(i+k)
                                k = k+1;
                                end
                                if i+k-1 > drpoff
                                    drpoff = i+k-1;
                                end
                                end
                                end
                                if newdrop == 1
                                    meanphase = 0;
                                    for k = drpon:1:drpoff
                                        for l=20:1:31
                                            meanphase = (meanphase + phasedeg(l,k));
                                        end
                                    end
                                    end
                                    meanphase = (meanphase)/((drpoff-drpon+1)*12);

fprintf(fout2, '%s\t%s\t%s\t%0.0f\t%0.0f\t%4.2f\t%5.2f\n', filename, bands(v,:), dr
pband, drpon, drpoff, 100*(drpoff-drpon+1)/(0.8065*dim(2)), meanphase);
                                newdrop = 0;
                                end
                                end
                                end

                                newdrop = 0;
                                drpon = 0;
                                drpoff = 0;
                                for i=1:1:dim(2)
                                    drpband = '3';
                                    if i > drpoff
                                        for j=32:1:43
                                            if sig95(j,i) >= 1 && period(j) <= coi(i)
                                                newdrop = 1;
                                                drpon = i;
                                                k = 1;
                                                while max(sig95(32:43,i+k)) >=1 && period(32) <=
coi(i+k)
                                                    k = k+1;
                                                    end
                                                    if i+k-1 > drpoff
                                                        drpoff = i+k-1;
                                                    end
                                                    end
                                                    end
                                                    if newdrop == 1
                                                        meanphase = 0;
                                                        for k = drpon:1:drpoff
                                                            for l=32:1:43
                                                                meanphase = (meanphase + phasedeg(l,k));
                                                            end
                                                        end
                                                        end
                                                        meanphase = (meanphase)/((drpoff-drpon+1)*12);

fprintf(fout2, '%s\t%s\t%s\t%0.0f\t%0.0f\t%4.2f\t%5.2f\n', filename, bands(v,:), dr

```

```

pband,drpon,drpoff,100*(drpoff-drpon+1)/(0.5484*dim(2)),meanphase);
    newdrop = 0;
    end
end
end

newdrop = 0;
drpon = 0;
drpoff = 0;
for i=1:1:dim(2)
    drpband = '4';
    if i > drpoff
        for j=44:1:55
            if sig95(j,i) >= 1 && period(j) <= coi(i)
                newdrop = 1;
                drpon = i;
                k = 1;
                while max(sig95(44:55,i+k)) >=1 && period(44) <=
coi(i+k)
                    k = k+1;
                end
                if i+k-1 > drpoff
                    drpoff = i+k-1;
                end
            end
        end
        if newdrop == 1
            meanphase = 0;
            for k = drpon:1:drpoff
                for l=44:1:55
                    meanphase = (meanphase + phasedeg(l,k));
                end
            end
            meanphase = (meanphase)/((drpoff-drpon+1)*(12));
        end
    end
end

fprintf(fout2,'%s\t%s\t%s\t%0.0f\t%0.0f\t%4.2f\t%5.2f\n',filename,bands(v,:),dr
pband,drpon,drpoff,100*(drpoff-drpon+1)/(0.526*dim(2)),meanphase);
    newdrop = 0;
    end
end

if l ==6
    newdrop = 0;
    drpon = 0;
    drpoff = 0;
    for i=1:1:dim(2)
        drpband = '5';
        if i > drpoff
            for j=56:1:67
                if sig95(j,i) >= 1 && period(j) <= coi(i)
                    newdrop = 1;
                    drpon = i;
                    k = 1;
                    while max(sig95(56:67,i+k)) >=1 && period(56) <=

```

```

coi(i+k)
        k = k+1;
        end
        if i+k-1 > drpoff
            drpoff = i+k-1;
        end
    end
end
if newdrop == 1
    meanphase = 0;
    for k = drpon:1:drpoff
        for l=56:1:67
            meanphase = (meanphase + phasedeg(l,k));
        end
    end
    meanphase = (meanphase)/((drpoff-drpon+1)*12);

fprintf(fout2, '%s\t%s\t%s\t%0.0f\t%0.0f\t%4.2f\t%5.2f\n', filename, bands(v,:), dr
pband, drpon, drpoff, 100*(drpoff-drpon+1)/(0.5484*dim(2)), meanphase);
    newdrop = 0;
end
end
end

newdrop = 0;
drpon = 0;
drpoff = 0;
for i=1:1:dim(2)
    drpband = '6';
    if i > drpoff
        for j=67:1:84
            if sig95(j,i) >= 1 && period(j) <= coi(i)
                newdrop = 1;
                drpon = i;
                k = 1;
                while max(sig95(67:84,i+k)) >=1 && period(67) <=
coi(i+k)
                    k = k+1;
                    end
                    if i+k-1 > drpoff
                        drpoff = i+k-1;
                    end
                end
            end
        end
        if newdrop == 1
            meanphase = 0;
            for k = drpon:1:drpoff
                for l=44:1:84
                    meanphase = (meanphase + phasedeg(l,k));
                end
            end
            meanphase = (meanphase)/((drpoff-drpon+1)*(12));

fprintf(fout2, '%s\t%s\t%s\t%0.0f\t%0.0f\t%4.2f\t%5.2f\n', filename, bands(v,:), dr
pband, drpon, drpoff, 100*(drpoff-drpon+1)/(0.526*dim(2)), meanphase);

```

```
                newdrop = 0;
            end
        end
    end
end

end

clear avgrsq;
clear mrsq;
clear avgrsqnc;
clear mrsqnc;
clear cvrsqnc;
clear cvrsq;
clear mean;

fprintf(fout10, '\n');

end
```

Appendix B Validation of Matlab Code

A. Validation of FFT-Based Banded Power Computations: SWAGFFT300bands.m

1. Create and Plot Simulated EEG Data: testSWAGFFT300bands.m

```
time=.002:.002:300; %create 500/s time base

% create sinwave combinations for 5 simulated EEG channels, with one sine
% component in each EEG band
ch1 =
sin(6.283*time*2)+sin(6.283*time*6)+sin(6.283*time*12)+sin(6.283*time*20)+sin(6
.283*time*40);
ch2 =
2*sin(6.283*time*2)+2*sin(6.283*time*6)+sin(6.283*time*12)+sin(6.283*time*20)+s
in(6.283*time*40);
ch3 =
3*sin(6.283*time*2)+3*sin(6.283*time*6)+sin(6.283*time*12)+sin(6.283*time*20)+s
in(6.283*time*40);
ch4 =
4*sin(6.283*time*2)+4*sin(6.283*time*6)+sin(6.283*time*12)+sin(6.283*time*20)+s
in(6.283*time*40);
ch5 =
5*sin(6.283*time*2)+5*sin(6.283*time*6)+sin(6.283*time*12)+sin(6.283*time*20)+s
in(6.283*time*40);

% fill the EEG.data structure with simulated sinewave data in channels 1-5
for i = 1:1:97
EEG.data(1,:,i) = ch1(:);
EEG.data(2,:,i) = ch2(:);
EEG.data(3,:,i) = ch3(:);
EEG.data(4,:,i) = ch4(:);
EEG.data(5,:,i) = ch5(:);
end

% plot channels to verify waveforms
figh=figure('Position',[100,100,600,850]); subplot(5,1,1);
plot(time,EEG.data(1,:,1));
xlim([0 10]);
title('Channel 1');
subplot(5,1,2);
plot(time,EEG.data(2,:,1));
title('Channel 2');
xlim([0 10]);
subplot(5,1,3);
plot(time,EEG.data(3,:,1));
title('Channel 3');
xlim([0 10]);
subplot(5,1,4);
plot(time,EEG.data(4,:,1));
title('Channel 4');
xlim([0 10]);
subplot(5,1,5);
plot(time,EEG.data(5,:,1));
title('Channel 5');
xlim([0 10]);
```

```
xlabel('Time (seconds)');

% save plot
savefig(figh,'Simulated EEG Test Plot');
```

2. Run SWAGFFT300bands to Verify Output:

```
>> SWAGFFT300bands
Please enter the channel numbers or ranges for analysis >5 4 3 2 1
Name of file to save graph for first specified analysis channel >Simulated EEG
FFT Test Plot
Please enter the first epoch for analysis >1
Please enter number of epochs for analysis >97
>> SWAGEEGcorr
Please enter the subject ID> SimTest
Please enter the name of the ".cor" and ".corstat" files for output> Simulated
EEG Corr Test
Do you want to append (enter "a") or overwrite (enter "w") data in these files?
w
Please enter maximum number of lags for analysis >20
>>
```

3. Confirm Results Generated by SWAGFFT300bands.m

Ensure graph depicts results for simulated EEG channel #5, as it was entered first.

As expected, all banded power values and their ratios are constant over time.

As expected, Delta power and Theta power are equal ($375 \mu\text{V}^2$) and Alpha, Beta and Gamma power are equal ($15 \mu\text{V}^2$).

Simulated Delta and Theta sine waves each have an amplitude of 5 versus 1 for Alpha, Beta and Gamma. Converting from amplitude to power confirms the expected ratio of 25 (5-squared).

For normalized power, we expect the value of Delta and Theta to be:

$$375/(375+375+15+15+15) = 0.471$$

For normalized power, we expect the value of Alpha, Beta and Gamma to be:

$$15/(375+375+15+15+15) = 0.019$$

These values also are confirmed by the plot above.

We expect the activation ratio to be:

$$15+15+15/(375+375+15+15+15) = 0.057$$

Because all power values are invariant over time, we expect the standard deviation of power and normalized power to be zero. This is confirmed by the plot above, which demonstrates that all values are constant with a value of less than 10^{-7} , which represents rounding error.

B. Validation of EEG/Glucose Cross Correlation Analysis: SWAGEEGcorr.m

1. Create and plot simulated average and sd power; absolute and normalized:

```
testSWAGEEGcorr.m
time=0:300:28800; %create 500/s time base
clear glucose;
```

```

% create sinwave simulated EEG power and Glucose
for i = 1:1:5
    avpower((i-1)*7 + 1,:) = sin(6.28*time/1500);
    avpower((i-1)*7 + 2,:) = sin(6.28*time/3000);
    avpower((i-1)*7 + 3,:) = sin(6.28*time/4500);
    avpower((i-1)*7 + 4,:) = sin(6.28*time/6000);
    avpower((i-1)*7 + 5,:) = sin(6.28*time/7500);
    avpower((i-1)*7 + 6,:) = sin(6.28*time/9000);
    avpower((i-1)*7 + 7,:) = sin(6.28*time/10500);
    avnpower((i-1)*7 + 1,:) = sin(6.28*time/1500);
    avnpower((i-1)*7 + 2,:) = sin(6.28*time/3000);
    avnpower((i-1)*7 + 3,:) = sin(6.28*time/4500);
    avnpower((i-1)*7 + 4,:) = sin(6.28*time/6000);
    avnpower((i-1)*7 + 5,:) = sin(6.28*time/7500);
    avnpower((i-1)*7 + 6,:) = sin(6.28*time/9000);
    avnpower((i-1)*7 + 7,:) = sin(6.28*time/10500);
    sdpower((i-1)*7 + 1,:) = sin(6.28*time/1500);
    sdpower((i-1)*7 + 2,:) = sin(6.28*time/3000);
    sdpower((i-1)*7 + 3,:) = sin(6.28*time/4500);
    sdpower((i-1)*7 + 4,:) = sin(6.28*time/6000);
    sdpower((i-1)*7 + 5,:) = sin(6.28*time/7500);
    sdpower((i-1)*7 + 6,:) = sin(6.28*time/9000);
    sdpower((i-1)*7 + 7,:) = sin(6.28*time/10500);
    sdnpower((i-1)*7 + 1,:) = sin(6.28*time/1500);
    sdnpower((i-1)*7 + 2,:) = sin(6.28*time/3000);
    sdnpower((i-1)*7 + 3,:) = sin(6.28*time/4500);
    sdnpower((i-1)*7 + 4,:) = sin(6.28*time/6000);
    sdnpower((i-1)*7 + 5,:) = sin(6.28*time/7500);
    sdnpower((i-1)*7 + 6,:) = sin(6.28*time/9000);
    sdnpower((i-1)*7 + 7,:) = sin(6.28*time/10500);
    glucose(i,:) = sin(6.28*time/(1500*i));
end
Sensor = sin(6.28*time/1500);

% plot channels to verify waveforms
figh=figure('Position',[100,100,600,850]);
subplot(4,1,1);
plot(time,transpose(avpower));
title('avpower');
subplot(4,1,2);
plot(time,transpose(avnpower));
title('avnpower');
subplot(4,1,3);
plot(time,transpose(sdpower));
title('sdpower');
subplot(4,1,4);
plot(time,transpose(sdnpower));
title('sdnpower');
xlabel('Time (seconds)');

% save plot
savefig(figh,'Simulated Power Correlation Test Plot');

2. Run SWAGEEGcorr.m to verify output
>> SWAGEEGcorrTest

```

```

Please enter the subject ID> testsub
Please enter the name of the ".cor" and ".corstat" files for output>
EEGCorrTest
Do you want to append (enter "a") or overwrite (enter "w") data in these files?
w
Please enter maximum number of lags for analysis >20

```

3. Confirm results generated by SWAGEEGcorr.m

Ascending power bands for avpower, avnpower, sdpower and sdnpower (1 through 7) were given sine wave periods of 5, 10, 15, 20, 25, 30 and 35 points (at 1 per 5-min sampling frequency).

For correlations, glucose was given a sine wave period of 5*channel# for analysis purposes.

Thus plots for each channel (1 through 5) should reflect sign wave oscillatory correlation with one band oscillating between +1 at zero lag through -1 at period/2 lags and back to +1 with a period equal to the underlying sine wave period.

All other bands should demonstrate low (near zero) correlation oscillating at the "beat frequency" between the two sine waves.

These findings are confirmed by graphical output.

C. Validation of Wavelet Coherence Computations: SWAGEEGhere.m

1. Conceptual Approach

Consider the case of a single-input single-output linear time-invariant system, given by:

$$y(t) = \beta x(t) + N(t)$$

Where: $y(t)$ is the output
 $x(t)$ is the input
 $N(t)$ is additive noise

Then, the coherence function between x and y is given by:

$$\gamma^2(f) = 1/(1+G_{NN}(f)/G_{XX}(f))$$

Where: γ^2 is the squared coherence
 $G_{NN}(f)$ is the power spectral density of $N(t)$
 $G_{XX}(f)$ is the power spectral density of $x(t)$

In the simplest case:

$$x(t) = \beta \sin(2\pi * t * f_0) \text{ and}$$

$$G_{XX}(f) \text{ scales as } \beta^2 \text{ for } f = f_0 \text{ and}$$

$$G_{XX}(f) = 0 \text{ for all } f \neq f_0$$

Thus, by adding uniform white noise to the sinusoidal input $x(t)$ we can achieve a predictable degradation of coherence, ranging from

$$\gamma^2(f) = 1 \text{ for } G_{NN}(f_0) = 0 \text{ to}$$

$\gamma^2(f)$ approaching 0 as $G_{NN}(f_0)$ approaches infinity

2. Create simulated data for a single EEG and single glucose channel as above:

```

randcoheretest.m
time=0:300:28800; %create 1/300s time base with 97 values
r1 = rand(1,97); %generates random variable between 0 and 1 with length of time
base

for i = 1:1:100 % generate 100 additional realizations of random noise to get
mean and SD stats
    rn=rand(1,97)-.5;
    [rnpeeg,f]=periodogram(rn,[],97,1/300);
    mrnpeeg(i)=mean(rnpeeg);
end
meanrnpeeg=mean(mrnpeeg); %mean power of simulated EEG
sdrnpeeg=std(mrnpeeg); % SD of of mean power for simulated EEG realizations

% create sinewave simulated EEG power and Glucose using r1 random noise to
% degrade signal to noise ratio in simulated EEG realizations

Sensor = sin(6.28*time/3000);

for i = 1:1:1
    avpower((i-1)*7 + 1,:) = sin(6.28*time/3000)+1*(r1-.5);
    avpower((i-1)*7 + 2,:) = sin(6.28*time/3000)+5*(r1-.5);
    avpower((i-1)*7 + 3,:) = sin(6.28*time/3000)+10*(r1-.5);
    avpower((i-1)*7 + 4,:) = sin(6.28*time/3000)+15*(r1-.5);
    avpower((i-1)*7 + 5,:) = sin(6.28*time/3000)+20*(r1-.5);
    avpower((i-1)*7 + 6,:) = sin(6.28*time/3000)+25*(r1-.5);
    avpower((i-1)*7 + 7,:) = sin(6.28*time/3000)+50*(r1-.5);
end

% plot channels to verify waveforms
figh=figure('Position',[100,100,600,850]);
plot(time,transpose(avpower));
title('simulated avpower');
hold
plot(time,glucose);

[rlpeeg,f]=periodogram(rn,[],97,1/300); %get actual power density spectrum for
random noise realization
[Speeg,f]=periodogram(Sensor,[],97,1/300); %get actual power density spectrum
for sinewave glucose
ratio(1)=rlpeeg(11)/Speeg(11); %get ratio of noise power to signal power at
frequency of 1/3000 (point 11)
ratio(2)=25*rlpeeg(11)/Speeg(11);
ratio(3)=100*rlpeeg(11)/Speeg(11);
ratio(4)=225*rlpeeg(11)/Speeg(11);
ratio(5)=400*rlpeeg(11)/Speeg(11);
ratio(6)=625*rlpeeg(11)/Speeg(11);
ratio(7)=2500*rlpeeg(11)/Speeg(11);

```

```

for i = 1:1:7 %predicted coherence based on actual observed Sensor and
simulated EEG power at f=1/3000
    precoh(i)=1/(1+ratio(i));
end

savefig(figh,'SNR Simulation Data');

```

3. Run SWAGEEGhere.m to confirm output

```

>> SWAGEEGhere
Please enter the subject ID> foobar
Output file name: foobar
Do you want to append (enter "a") or overwrite (enter "w") data in these
files? w
Color (enter 0) or Black and White (enter 1) plot?>0
>>

```

Visual inspection confirms that for low levels of noise (Delta and Theta bands above) a single band of high and significant coherence is detected over the full recording period.

This band of significant coherence is centered at a period of 10, or 3000 seconds, which is part of the “middle” bands of frequencies used for droplet and mean coherence analyses. This also confirms prediction, because the period of the sine wave used for simulations was 3000s (or 10 sample points).

As expected, with increasing noise power from Delta through AR2 bands, the mean coherence diminishes even at a period of 10. For the AR2 band, into which noise with a range of ± 50 was added to the sine wave with an amplitude of 1, no significant coherence is observed at any time or period.

4. Quantify relationship between predicted and observed coherence

Coheretest.m

```

time=0:300:28800; %create 1/300s time base with 97 values
r1 = rand(1,97); %generates random variable between 0 and 1 with length of time base

for j = 1:1:500 % generate 500 realizations of random noise to get mean and SD
stats
    r1=rand(1,97)-.5;
    [r1peeg,f]=periodogram(r1,[],97,1/300); %get actual power density spectrum for
random noise realization
    [Speeg,f]=periodogram(Sensor,[],97,1/300); %get actual power density spectrum
for sinewave glucose

    ratio(1)=r1peeg(11)/Speeg(11); %get ratio of noise power to signal power at
frequency of 1/3000 (point 11)
    ratio(2)=25*r1peeg(11)/Speeg(11);
    ratio(3)=100*r1peeg(11)/Speeg(11);
    ratio(4)=225*r1peeg(11)/Speeg(11);
    ratio(5)=400*r1peeg(11)/Speeg(11);
    ratio(6)=625*r1peeg(11)/Speeg(11);
    ratio(7)=2500*r1peeg(11)/Speeg(11);

    for i = 1:1:7 %predicted coherence based on actual observed Sensor and
simulated EEG power at f=1/3000
        precoh(i)=1/(1+ratio(i));
    end
    pred(j,:)=precoh;

```

```

    ratio(1)=0.005; %get ratio of average noise power to signal power at frequency
of 1/3000 (point 11)
    ratio(2)=0.125;
    ratio(3)=0.5;
    ratio(4)=1.125;
    ratio(5)=2;
    ratio(6)=3.125;
    ratio(7)=12.5;

Sensor = sin(6.28*time/3000); % create sinewave simulated Glucose with period of 10
points

% create simulated EEG power using r1 random noise to degrade signal to noise ratio
in simulated EEG realizations
    for i = 1:1:1
        avpower((i-1)*7 + 1,:) = sin(6.28*time/3000)+1*(r1-.5);
        avpower((i-1)*7 + 2,:) = sin(6.28*time/3000)+5*(r1-.5);
        avpower((i-1)*7 + 3,:) = sin(6.28*time/3000)+10*(r1-.5);
        avpower((i-1)*7 + 4,:) = sin(6.28*time/3000)+15*(r1-.5);
        avpower((i-1)*7 + 5,:) = sin(6.28*time/3000)+20*(r1-.5);
        avpower((i-1)*7 + 6,:) = sin(6.28*time/3000)+25*(r1-.5);
        avpower((i-1)*7 + 7,:) = sin(6.28*time/3000)+50*(r1-.5);
    end

    for v = 1:1:7

[rsq,period,scale,coi,sig95,phase]=wtcncnp(Sensor,avpower(v,:), 'MakeFigure',1,'Black
andWhite',bw);
        mrsq28(v)=mean(rsq(28,[15:83]));
    end
    obs(j,:)=mrsq28;
end

```

The relationship between predicted and observed coherence at a period of 10 samples (mid-range of the periods computed) displays considerable variability across 500 realizations of uniform white noise.

Averaging across all 500 trials, the wct algorithm closely approximated predicted coherence for predicted values greater than 0.5, but consistently overestimated predicted values below 0.5.

Upper and lower dashed lines depict $\pm 1SD$ among the 500 trials. Predicted coherence values do not deviate from observed values by more than 1SD when predicted coherence exceeds 0.3. Therefore we believe we can rely on observed coherence values in the range of 0.3 to 1.0.

5. Identify Effect of Windowing Choice for Periodogram

```

time=0:300:28800; %create 1/300s time base with 97 values
r1 = rand(1,97); %generates random variable between 0 and 1 with length of time base

for j = 1:1:500 % generate 500 realizations of random noise to get mean and SD
stats
    r1=rand(1,97)-.5;

```

```

**    [rlpeeg,f]=periodogram(r1,hamming(97),97,1/300); %get power density spectrum
for random noise realization
**    [Speeg,f]=periodogram(Sensor, hamming(97),,97,1/300); %get power density
spectrum for sinewave glucose

    ratio(1)=rlpeeg(11)/Speeg(11); %get ratio of noise power to signal power at
frequency of 1/3000 (point 11)
    ratio(2)=25*rlpeeg(11)/Speeg(11);
    ratio(3)=100*rlpeeg(11)/Speeg(11);
    ratio(4)=225*rlpeeg(11)/Speeg(11);
    ratio(5)=400*rlpeeg(11)/Speeg(11);
    ratio(6)=625*rlpeeg(11)/Speeg(11);
    ratio(7)=2500*rlpeeg(11)/Speeg(11);

    for i = 1:1:7 %predicted coherence based on actual observed Sensor and
simulated EEG power at f=1/3000
        precoh(i)=1/(1+ratio(i));
    end
    pred(j,:)=precoh;

    ratio(1)=0.005; %get ratio of average noise power to signal power at frequency
of 1/3000 (point 11)
    ratio(2)=0.125;
    ratio(3)=0.5;
    ratio(4)=1.125;
    ratio(5)=2;
    ratio(6)=3.125;
    ratio(7)=12.5;

Sensor = sin(6.28*time/3000); % create sinewave simulated Glucose with period of 10
points

% create simulated EEG power using r1 random noise to degrade signal to noise ratio
in simulated EEG realizations
    for i = 1:1:1
        avpower((i-1)*7 + 1,:) = sin(6.28*time/3000)+1*(r1-.5);
        avpower((i-1)*7 + 2,:) = sin(6.28*time/3000)+5*(r1-.5);
        avpower((i-1)*7 + 3,:) = sin(6.28*time/3000)+10*(r1-.5);
        avpower((i-1)*7 + 4,:) = sin(6.28*time/3000)+15*(r1-.5);
        avpower((i-1)*7 + 5,:) = sin(6.28*time/3000)+20*(r1-.5);
        avpower((i-1)*7 + 6,:) = sin(6.28*time/3000)+25*(r1-.5);
        avpower((i-1)*7 + 7,:) = sin(6.28*time/3000)+50*(r1-.5);
    end

for v = 1:1:7

[rsq,period,scale,coi,sig95,phase]=wtcncnp(Sensor,avpower(v,:), 'MakeFigure',1, 'Black
andWhite',bw);
    mrsq28(v)=mean(rsq(28,[15:83]));
    end
    obs(j,:)=mrsq28;
end

```

The relationship of computed to observed coherence was not significantly affected by windowing choice (rectangular versus Hamming).

6. Determine the Impact of Period on Relationship Between Observed and Predicted Coherence

As demonstrated above, the relationship between predicted and observed coherence is influenced by the period of the sine wave within the target range (2 to 35 samples; or 10 to 175 minutes):

- For a period of 5 samples (25 minutes) the wct algorithm consistently underestimates predicted coherence for predicted coherences greater than ~ 0.5 and overestimating predicted coherence at lower values
- For a period of 10 samples (50 minutes) the wct algorithm accurately estimates predicted coherence in the range of ~ 0.5 to 1.0; but again overestimates predicted coherence in the lower range
- For a period of 20 samples (100 minutes) the wct algorithm consistently overestimates predicted coherence throughout the range, but this overestimation increases as predicted coherence decreases
- At all periods, the wct coherence estimates appear to approach a plateau in the range of 0.4 for very low predicted coherence values

7. Identify the Coherence Computed Between Independent Random Samples: noisersq.m

```
groupmeanrsq = zeros(50,97);
for v = 1:1:100
    r1=rand(1,97)-.5;
    r2=rand(1,97)-.5;

    [rsq,period,scale,coi,sig95,phase]=wtcncnp(r1,r2,'MakeFigure',1,'BlackandWhite',bw);

    sumrsq = 0;
    numrsq = 0;
    for i = 1:1:50
        for j = 1:1:97
            groupmeanrsq(i,j) = groupmeanrsq(i,j)+(rsq(i,j)/97);
            if period (i) <= coi(j)
                sumrsq = sumrsq + rsq(i,j);
                numrsq = numrsq + 1;
            end
        end
    end
    avnoisersq(v) = sumrsq/numrsq;
end
```

The lower plateau observed for predicted coherences below ~ 0.5 may relate either to a limitation of the wavelet coherence calculation itself or of a lack of independence in the random process generator of matlab.

Testing 100 realizations of random noise: $r1 = \text{rand}(1, 97)$ vs $r2 = \text{rand}(1, 97)$ yielded an average calculated coherence value of 0.3325 ± 0.05 (SD) (range 0.27 to 0.69) across the samples for all periods and all time points within outside the COI.

Although the average computed coherence outside the COI is visibly lower than the values computed within the COI, the mean coherence not influenced by “end effects” remains in the range of 0.3 to 0.35, rather than approaching zero.

This does not appear to be primarily a function of “data length” because increasing the length of the random noise realizations to 500 points yielded an overall average computed coherence of 0.3368 ± 0.04 (SD) with a range of 0.25 to 0.44.

D. Validation of Coherence and Correlation for Multiple Channels and Statistics with Actual Data

1. Import a PSG EDF into Matlab

- a. EDF is imported into Matlab using EEGLab
 - i. Import the Channels Desired
 1. 1,2,4,5,6,7 are the two frontal (F3/A2 and F4/A1), two central (C3/A2 and C4/A1) and two occipital (O1/A2 and O2/A1) leads
 - a. They become channels 1-6 after importing
 - ii. Data Range should start at the second corresponding with lights out from the start of the PSG recording
- b. Define Epochs-Creates 300 second epochs (5 minutes)
 - i. Create a text file with latency, type and duration as header
 - ii. Latency begins at 0 and increases at each row by 300, type is “deltaepoch” for every row, duration is 300 at every row
 - iii. Import the text file using the “Import Event Information” under the “File” menu in EEGLab
- c. Extract epochs using “extract epochs” under the “Tools” menu
 - i. Tabs are latency type duration
 - ii. One line of header
 - iii. Do not remove baseline

2. Import glucose values from excel spreadsheet into Matlab

- a. Ensure there are no NaN in the column for glucose

3. Run SWAGbands300FFT to determine power in each band

- a. Example:


```
>> SWAGFFT300bands
Please enter the channel numbers or ranges for
analysis >1:6
Name of file to save graph for first specified
analysis channel >1
Please enter the first epoch for analysis >1
Please enter number of epochs for analysis >93
```
- b. Inspect graph to ensure no obvious abnormalities in power graphs

4. Run SWAGEEGcorr.m file

- a. Example Input:


```
>> SWAGEEGcorr
Please enter the subject ID> 1
Please enter the name of the ".cor" and ".corstat"
files for output> test
Do you want to append (enter "a") or overwrite (enter
"w") data in these files? w
Please enter maximum number of lags for analysis >20
```
- b. Inspect graph outputs

- i. Expected that graphs will be similar for each EEG band but slightly different by each channel

5. Run SWAGEEGhere.m

a. Example Input:

```
>> SWAGEEGhere
Please enter the subject ID> 1
Output file name: test
Do you want to append (enter "a") or overwrite (enter
"w") data in these files? w
Color (enter 0) or Black and White (enter 1) plot?>0
```

- b. Expect to get coherence graphs for 7 bands for 4 statistics for 6 channels (168) per subject

6. Run SWAGEEGgcfinal.m file for subject

a. Expected input:

```
>> SWAGEEGgcfinal
Please enter the name of the stats output file ".gc"
> test
Do you want to append (enter "a") or overwrite (enter
"w") data in these files? w
Please input the starting channel number >1
Please input the ending channel number >3
```

- b. Expected output (for one channel and one statistic and one band):

```
*** tsdata_to_infocrit
model order = 1
model order = 2
model order = 3
model order = 4
model order = 5
model order = 6
model order = 7
model order = 8
model order = 9
model order = 10
model order = 11
model order = 12
model order = 13
model order = 14
model order = 15
model order = 16
model order = 17
model order = 18
model order = 19
model order = 20
*** tsdata_to_infocrit took 0.466499 secs
```

```
best model order (AIC) = 9
best model order (BIC) = 20
```

```
using AIC best model order = 9
```

```
*** tsdata_to_var... 0.121453 secs
*** var_to_autocov... 0.198131 secs
```

```
VAR info:
  no errors
  no warnings
  spectral radius      : 0.974752
  ac relative error    : 7.89205e-13
  minimum ac lags     : 721
  actual ac lags      : 721

*** autocov_to_pwcgc... 0.297270 secs

causal density = 0.088246

*** autocov_to_spwcgc... 0.624719 secs

checking that frequency-domain GC integrates to time-domain GC...
maximum absolute difference OK: = 2.74e-12 (< 1.00e-05)

*** tsdata_to_infocrit
model order = 1
model order = 2
model order = 3
model order = 4
model order = 5
model order = 6
model order = 7
model order = 8
model order = 9
model order = 10
model order = 11
model order = 12
model order = 13
model order = 14
model order = 15
model order = 16
model order = 17
model order = 18
model order = 19
model order = 20
*** tsdata_to_infocrit took 0.025103 secs

best model order (AIC) = 8
best model order (BIC) = 20

using AIC best model order = 8

*** tsdata_to_var... 0.003158 secs
*** var_to_autocov... 0.030785 secs

VAR info:
  no errors
  no warnings
  spectral radius      : 0.977766
  ac relative error    : 2.21642e-13
  minimum ac lags     : 820
```

```
actual ac lags : 820

*** autocov_to_pwcgc... 0.265406 secs

causal density = 0.110133

*** autocov_to_spwcgc... 0.440382 secs

checking that frequency-domain GC integrates to time-domain GC...
maximum absolute difference OK: = 5.03e-14 (< 1.00e-05)

*** tsdata_to_infocrit
model order = 1
model order = 2
model order = 3
model order = 4
model order = 5
model order = 6
model order = 7
model order = 8
model order = 9
model order = 10
model order = 11
model order = 12
model order = 13
model order = 14
model order = 15
model order = 16
model order = 17
model order = 18
model order = 19
model order = 20
*** tsdata_to_infocrit took 0.006487 secs

best model order (AIC) = 7
best model order (BIC) = 7

using AIC best model order = 7

*** tsdata_to_var... 0.000285 secs
*** var_to_autocov... 0.003442 secs

VAR info:
no errors
no warnings
spectral radius : 0.967330
ac relative error : 9.36279e-14
minimum ac lags : 555
actual ac lags : 555

*** autocov_to_pwcgc... 0.117003 secs

causal density = 0.142482

*** autocov_to_spwcgc... 0.229166 secs
```

Appendix C

Detailed Methods for Measurement of Interleukin-6 (IL-6) and Tumor Necrosis Factor-alpha (TNF- α), and Cortisol Using Enzyme-Linked Immunosorbent Assay (ELISA)

A. Protocol of sample Collection and Storage

Blood was collected from each subject immediately prior (within 10 minutes) to lights out, immediately after lights on (within 10 minutes) and an hour (within five minutes) after the second blood draw occurred. Each sample was drawn with a 21-gauge needle from an antecubital vein while subjects were either lying in bed or sitting comfortably in a chair. The samples were drawn into an Ethylenediaminetetraacetic acid (EDTA) coated 10-ml tube. The sample was labeled with subject ID, date and time of collection and placed in a 2-4° Celsius refrigerator. After collection of all the samples, they were delivered to the UI Biorepository laboratory in the Research Resources Center at UIC. Trained lab technicians spun each sample down using an Eppendorf 5810 R™ centrifuge at 1800 revolutions per minute for 12 minutes at 4° Celsius. The plasma was equally aliquoted using a pipette into four tubes (400-800 μ L total volume per aliquot). Aliquots were labeled with subject ID number, sample number (time point of collection) and stored in a -80° Celsius freezer until the completion of the study. Upon completion of the study, enzyme-linked immunosorbent assay (ELISA) was used to measure levels of IL-6, TNF-alpha and cortisol.

The ELISA procedures were carried out at the University of Illinois at Chicago in the lab of Giamilla Fantuzzi, PhD, in the Applied Health Sciences Building. Rand Akaesh, PhD candidate, carried out the protocols with the assistance of Sarah Farabi.

B. Enzyme-Linked Immunosorbent Assay (ELISA) Method

1. Background on ELISA Method-Rationale for Selection

ELISA, a heterogeneous enzyme immunoassay, was invented in 1971 by Peter Perlmann and Eva Engvall as an alternative way to measurement of antibodies in a sample by radioimmunoassay (RIA) which required radioactive labeling (201). ELISA is widely used for measurement of inflammatory cytokines and there are many commercially available kits for measurement. The ELISA method quantifies presence of a specific antibody. Four types of heterogeneous ELISAs, direct, indirect, sandwich and competitive have been since developed (202). Sandwich ELISA was the mechanism used to quantify plasma IL-6 and TNF- α and competitive ELISA was used to quantify cortisol levels in the plasma.

Competitive binding ELISA was developed in 1976 by Yorde and colleagues for determination of human chorionic gonadotropin (203). There are several types of competitive binding assays (204), however, in the type used for this study, the sample antigen competes with a fixed amount of labeled antigen for sites on an antibody which binds to another antibody which is bound to the wells of the plate. After washing the plate, a substrate specific to the enzyme affixed to the competing antigen is added to measure the amount of binding. The color absorbance (optical density) of the enzyme (reaction is a color change) is determined. An inverse relationship for optical and level of substrate for sample is expected: higher levels of color (optical density) are seen for lower levels of the antigen of interest present in the sample (202,204,205). Competitive binding ELISAs are highly sensitive and good for use for soluble hormone detection (202,203).

The Sandwich ELISA is highly efficient and recommended for use when levels of the protein of interest are low as they are highly sensitive (202). The Sandwich ELISA technique was reported by Kato and colleagues in 1977 (206) and there are many commercially available ELISA kits based on the sandwich ELISA technique (207). In the Sandwich ELISA, the wells are coated with an antibody specific to antigen of interest. The sample is added to the wells and incubated. After washing, an antibody linked with an enzyme is added which bind to the antigen of interest. Another round of washing occurs to remove any unbound antibody. A substrate is added to detect the level of enzyme present and color absorbance (optical density) is detected to measure the amount of antigen present. The optical density of the color is directly proportional to the level of antigen present in the sample (202,204,205).

2. Steps for the Competitive Binding ELISA for Cortisol

Two Parameter™ Cortisol 96-well plate kits (KGE008) were purchased from R&D systems (Minneapolis, MN). As per manufacturer instruction, the kits were kept in a refrigerator, between 2-4° Celsius, until used. Microplates with 96 polystyrene wells coated with a goat-anti-mouse polyclonal antibody were provided in the kits and used for this analysis.

Masks and gloves were worn during the entire procedure. The protocol provided by the company with the kits was followed (167). A standard solution was created for reference when running the cortisol assay; lyophilized (free-dried) buffered cortisol was reconstituted with distilled water. 7 concentrations were created: 10 ng/mL, 5 ng/mL, 2.5 ng/mL, 1.25 ng/mL, 0.625 ng/mL, 0.313 ng/mL, 0.156 ng/mL.

The plasma samples were thawed to room temperature and diluted using a 20-fold dilution. 20 µL of the plasma was combined with 280 µL of Diluent (buffered protein base). 100 µL of the diluted sample was added to the microplate wells (each sample run in duplicate). 100 µL of each concentration of standard were added to 2 wells, making 14 standard wells. Each sample and standard was run in duplicate. One well served to measure non-specific binding (NSB- no primary antibody is added), one well and one well was used as zero standard (diluent with no sample or standard is added). After addition of the diluted sample or standards to the plate, 50 µL of a mixture of Cortisol conjugated to horseradish peroxidase with red dye was added to all wells. Next, 50 µL of mouse monoclonal antibody (to Cortisol) with blue dye was added to the wells, except to the well measuring NSB. The well-plates were then incubated at room temperature for 2 hours on a horizontal orbital microplate shaker (set at 500 rpm).

After 2 hours, the plates were aspirated and washed with 440 µL of wash buffer four times. The buffer was a 500 mL volume mixture of 20 mL of a 25-fold concentrated solution of buffered surfactant and 480 mL of distilled water.

After washing, 200 µL of substrate solution (50/50 mixture of hydrogen peroxide and chromogen) was added to each well. The plate was covered and incubated at room temperature for 30 minutes. Next, 50 µL of sulfuric acid was added to the wells to stop the conversion of enzyme and color development. A microplate reader measured the spectral density of each well at a wavelength of 450, a wavelength of 550 nm was used for correction. The average absorbencies of the duplicates of each standard and sample were calculated and the absorbency of the NSB was subtracted from the average. A standard curve was created using the microplate reader software from the standard concentrations (x-axis) and the optical density of the standards (y-axis). A log-log transformation was used to plot the

OD versus absorbencies. The concentration of each sample of cortisol was determined using the curve. High concentrations corresponded to low optical density.

The mean lower limit of detection for the cortisol assay was reported by the manufacturer as 0.071 ng/mL. Average intra-assay precision CV was 6.97% and the average inter-assay CV was 13.6% for the cortisol assay.

The mean concentrations for Cortisol were determined using a 4 Parameter Logistic Regression with the following equations for the standard curves:

Plate 1:

$$\text{Abs (Optical Density)} = (0.493 - 0.0566) / (1 + (\text{Conc (ng/mL)} / 0.797)^{1.19}) + 0.0566$$

Plate 2:

$$\text{Abs (Optical Density)} = (0.486 - 0.0405) / (1 + (\text{Conc (ng/mL)} / 1.38)^{1.27}) + 0.0405$$

Mean concentrations derived from the equation were multiplied by 20 since a 20-fold dilution was used for the samples. Data are reported in ng/mL for cortisol concentrations. Concentrations that were reported as below the detection level, above the range of the standard curve or below the range of the standard curve were excluded from the data set.

3. Sandwich ELISA for TNF- α

Two Quantikine[®] High Sensitivity ELISA kits for Human TNF- α Immunoassay were purchased from R&D systems (Minneapolis, MN). As per manufacturer instruction, the kits were kept in a refrigerator, between 2-4[°] Celsius, until used. Microplates with 96 polystyrene wells coated with a monoclonal antibody specific for human TNF- α were provided in the kits and used for this analysis.

Masks and gloves were worn during the entire procedure. The protocol provided by the manufacturer was followed (165). Plasma samples were thawed to room temperature. A standard solution of 32 pg/mL of TNF- α was prepared for reference (high standard) using lyophilized recombinant human TNF- α substrate reconstituted with 6.0 mL of a diluent (buffered solution with stabilizers). Next a series of 7 concentrations (using 500 μ L of calibrator Diluent RD6-13 (a buffered protein base)) of standards were created using polypropylene tubes: 16pg/mL, 8pg/mL, 4 pg/mL, 2 pg/mL, 1 pg/mL and 0.5 pg/mL; 0 pg/ml (zero standard, Calibrator diluent only).

50 μ L of Assay Diluent RD15 (buffered protein base with preservative) was added to each of the 96 wells on the microplate. 200 μ L of the plasma samples (each sample run in duplicate) were added to the wells of the plates. On each plate, there were 16 wells that served as the standard wells (2 wells per standard dilution concentration). After addition of the plasma and standards to the wells, the plate was incubated for 3 hours at room temperature.

The liquid was removed from the wells by inverting the plate and rapping the plate on a clean paper towel. Next, 400 μ L of Wash Buffer (100 mL of concentrated buffered surfactant combined with 900 mL of distilled water) was added to each well. The liquid was removed from the wells and the steps were repeated 5times for a total of 6 washes. Next, 200 μ L of Human TNF- α HS Conjugate (polyclonal antibody specific for human TNF- α and conjugated to alkaline phosphatase) were added to each well on the plate. The plate was covered and incubated at room temperature for 2 hours. The washing steps (stated previously) were repeated.

Next 50 μL of Substrate solution (dehydrated NADPH reconstituted with Substrate Diluent) was added to each well and incubated for 1 hour at room temperature. After one hour, 50 μL of Amplifier solution (lyophilized amplifier enzymes) was added to each well and incubated for 30 more minutes. Finally, 50 μL of Stop Solution (2 N sulfuric acid) was added to each of the wells. The optical density (color absorbance) was measured by a microplate reader at 490 nm and a correction wavelength of 650 was used. The average absorbencies of the duplicate plasma samples and standards were obtained and subtracted from the optical density for the zero standard. A standard curve was created using the microplate reader software from the standard concentrations (x-axis) and the optical density of the standards (y-axis). A log-log transformation was used to plot the OD versus absorbencies. The concentration of each sample of TNF- α was determined using the curve. High concentrations corresponded to high optical density.

The mean lower limit of detection was reported by the manufacturer to be 0.106 pg/ml. The average intra-assay coefficient of variation (CV) was 5.4% for TNF- α and average inter-assay CV was 8.3%.

The mean concentrations for TNF- α were determined using a 4 Parameter Logistic Regression with the following equations for the standard curves:

Plate 1:

$$\text{Abs (Optical Density)} = (0.0172 - 2.1) / (1 + (\text{Conc (pg/mL)} / 12.3)^{1.27}) + 2.1$$

Plate 2:

$$\text{Abs (Optical Density)} = (-0.00238 - 2.1) / (1 + (\text{Conc (pg/mL)} / 12.7)^{1.3}) + 2.1$$

Data are reported in picograms/milliliter (pg/mL) for TNF- α concentrations. Concentrations that were reported as below the detection level, above the range of the standard curve or below the range of the standard curve were excluded from the data set.

4. Sandwich ELISA for IL-6

Two Quantikine[®] High Sensitivity ELISA kits for Human IL-6 Immunoassay were purchased from R&D systems (Minneapolis, MN). As per manufacturer instruction, the kits were kept in a refrigerator, between 2-4[°] Celsius, until used. Microplates with 96 polystyrene wells coated with a monoclonal antibody specific for human IL-6 were provided in the kits and used for this analysis.

Masks and gloves were worn during the entire procedure and the protocol provided by the manufacturer was followed (166). Plasma samples were thawed to room temperature. A standard solution of 10 pg/mL of IL-6 was prepared for reference (high standard) using lyophilized recombinant human IL-6 reconstituted with Calibrator Diluent RD6-11 concentrate (buffered protein base with preservatives). A series of 7 concentrations (using using 500 μL of calibrator Diluent RD6-11) were created: 5pg/mL, 2.5 pg/mL, 1.25 pg/mL, 0.625 pg/mL, 0.313 pg/mL, 0.156 pg/mL and 0 pg/mL 0 pg/ml (zero standard, Calibrater diluent only).

100 μL of Assay Diluent RD1-75 (buffered animal serum with preservative) were added to each well on the 96 well-plate. Next 100 μL of plasma samples (each sample run in duplicate) were added to each of the wells. On each plate, there were 16 wells that served as the standard wells (2 wells per standard dilution concentration). After addition of the plasma and standards to the wells, the plate was incubated for 2 hours at room temperature on a horizontal orbital microplate shaker (set at 500 rpm).

The liquid was removed from the wells by inverting the plate and rapping the plate on a clean paper towel. Next, 400 μ L of Wash Buffer (100 mL of concentrated buffered surfactant combined with 900 mL of distilled water) was added to each well and allowed to sit for 30 seconds. The liquid was removed from the wells and the steps were repeated 5times for a total of 6 washes. Next, 200 μ L of Human IL-6 HS Conjugate (polyclonal antibody specific for human IL-6 and conjugated to alkaline phosphatase) were added to each well on the plate. The plate was covered and incubated at room temperature for 2 hours on a horizontal orbital microplate shaker (set at 500 rpm). The washing steps (stated previously) were repeated.

Next 50 μ L of Substrate solution (dehydrated NADPH reconstituted with Substrate Diluent) was added to each well and incubated for 1 hour at room temperature. After one hour, 50 μ L of Amplifier solution (lyophilized amplifier enzymes) was added to each well and incubated for 30 more minutes. Finally, 50 μ L of Stop Solution (2 N sulfuric acid) was added to each of the wells. The optical density (color absorbance) was measured by a microplate reader at 490 nm and a correction wavelength of 650 was used. The average absorbencies of the duplicate plasma samples and standards were obtained and subtracted from the optical density for the zero standard. A standard curve was created using the microplate reader software from the standard concentrations (x-axis) and the optical density of the standards (y-axis). A log-log transformation was used to plot the OD versus absorbencies. The concentration of each sample of TNF- α was determined using the curve. High concentrations corresponded to high optical density.

The mean lower limit of detection for the assay was reported to be 0.106 0.039 pg/ml. The manufacturer reported average intra-assay coefficient of variation (CV) was 7.4% and average inter-assay CV was 7.8% for the assay.

The mean concentrations for IL-6 were determined using a 4 Parameter Logistic Regression with the following equations for the standard curves:

Plate 1:

$$\text{Abs (Optical Density)} = (0.0146 - 1.97) / (1 + (\text{Conc (pg/mL)} / 4.3)^{1.32}) + 1.97$$

Plate 2:

$$\text{Abs (Optical Density)} = (0.00521 - 2.08) / (1 + (\text{Conc (pg/mL)} / 4.32)^{1.31}) + 2.08$$

Data are reported in picograms/milliliter (pg/mL) for IL-6 concentrations. Concentrations that were reported as below the detection level, above the range of the standard curve or below the range of the standard curve were excluded from the data set.

APPENDIX D

**UNIVERSITY OF ILLINOIS
AT CHICAGO**

Office for the Protection of Research Subjects (OPRS)
Office of the Vice Chancellor for Research (MC 672)
203 Administrative Office Building
1737 West Polk Street
Chicago, Illinois 60612-7227

**Approval Notice
Continuing Review**

February 6, 2015

Sarah Farabi, BSN

Department of Biobehavioral Health Science

845 S. Damen

M/C 802

Chicago, IL 60612

Phone: (314) 556-4574 / Fax: (312) 996-7008

RE: Protocol # 2013-0030

“Sleep, Glucose Variability, CVD Risk and CV Stress in Young Adults with T1DM”

Dear Dr. Farabi:

Your Continuing Review was reviewed and approved by the Convened review process on February 4, 2015. You may now continue your research.

Please note the following information about your approved research protocol:

Protocol Approval Period: February 20, 2015 - February 20, 2016

Approved Subject Enrollment #: 60 (21 Enrolled to date)

Additional Determinations for Research Involving Minors: These determinations have not been made for this study since it has not been approved for enrollment of minors.

Performance Sites: UIC
Sponsor: Department of Biobehavioral Health, American Association of Diabetes Educators Research Foundation

PAF#: 2015-01898, Not available

Grant/Contract No: Not available, Not available

Grant/Contract Title: Sleep, Glucose, Variability, CVD Risk & CV Stress in Young Adults with T1DM, Not available **Research Protocol(s):**

- a) Sleep, glucose variability, CVD risk and CV stress in young adults with T1DM, Version 0011, 2/4/15

Recruitment Material(s):

- a) Patient Letter, Version 004, 05/08/2014
- b) Protocol 2013-0030 Public Flyer, Version 003, 05/19/2014
- c) Flyer: Research at UIC, Research Study for Young Adults with Type 1 Diabetes, Version 003, 02/02/15
- d) Internet Recruitment Text, Version 001, 6/30/2014
- e) Phone Screen Form - Sleep, Glucose Variability, CVD Risk & CV Stress in Young Adults with T1DM; Protocol 2013-0030; Version 001, 05/21/14 **Informed Consent(s):**

- a) Waiver of Informed Consent for recruitment purposes granted under [45 CFR 46.116(d)]
- b) Sleep, Glucose Variability, CVD Risk and CV Stress in Young Adults with T1DM- Pharmacogenomic Analysis Consent, Version 004, 05/09/2014
- c) Combined Consent/Authorization: Sleep, Glucose Variability, CVD Risk and CV Stress in Young Adults with T1DM, Version 010, [09/10/2014]
- d) Alteration of Informed Consent for Telephone Screening granted under 45 CFR 46.116(d)
- e) Waiver of Documentation of Consent for Telephone Screening granted under 45 CFR 46.117(c)

HIPAA Authorization(s):

- a) Waiver of HIPAA Authorization granted for recruitment purposes under [45 CFR 164.512(i)(1)(i)]

Please note the Review History of this submission:

Receipt Date	Submission Type	Review Process	Review Date	Review Action
--------------	-----------------	----------------	-------------	---------------

01/13/2015	Continuing Review	Convened	02/04/2015	Approved
------------	-------------------	----------	------------	----------

Please remember to:

→ Use your **research protocol number** (2013-0030) on any documents or correspondence with the IRB concerning your research protocol.

→ Review and comply with all requirements on the enclosure,
"UIC Investigator Responsibilities, Protection of Human Research Subjects"
(<http://tigger.uic.edu/depts/ovcr/research/protocolreview/irb/policies/0924.pdf>)

Please note that the UIC IRB has the prerogative and authority to ask further questions, seek additional information, require further modifications, or monitor the conduct of your research and the consent process.

Please be aware that if the scope of work in the grant/project changes, the protocol must be amended and approved by the UIC IRB before the initiation of the change.

Page 3 of 3

We wish you the best as you conduct your research. If you have any questions or need further help, please contact OPRS at (312) 996-1711 or me at (312) 413-1835. Please send any correspondence about this protocol to OPRS at 203 AOB, M/C 672.

Sincerely,

Jonathan W. Leigh, MPH

IRB Coordinator, IRB # 1

Office for the Protection of Research Subjects

Enclosure(s):

1. Informed Consent Document(s):

- a) Combined Consent/Authorization: Sleep, Glucose Variability, CVD Risk and CV Stress in Young Adults with T1DM, Version 010, [09/10/2014]
- b) Sleep, Glucose Variability, CVD Risk and CV Stress in Young Adults with T1DM- Pharmacogenomic Analysis Consent, Version 004, 05/09/2014

2. Recruiting Material(s):

- a) Patient Letter, Version 004, 05/08/2014
- b) Protocol 2013-0030 Public Flyer, Version 003, 05/19/2014
- c) Flyer: Research at UIC, Research Study for Young Adults with Type 1 Diabetes, Version 003, 02/02/15
- d) Internet Recruitment Text, Version 001, 6/30/2014
- e) Phone Screen Form - Sleep, Glucose Variability, CVD Risk & CV Stress in Young Adults with T1DM; Protocol 2013-0030; Version 001, 05/21/14

cc: Mariann R. Piano, Department of Biobehavioral Health Science, M/C 802

Lauretta Quinn, Faculty Sponsor, M/C 802

OVCR Administration, M/C 672

Privacy Office, Health Information Management Department, M/C 77

VITA

Sarah S. Farabi

(Formerly Sarah Schwarz)

330 West Grand Ave, Chicago IL, 60654
(314) 556-4574; schwarzsar@gmail.com

EDUCATION

PhD 2016
University of Illinois at Chicago

Bachelor of Nursing Science, *summa cum laude* 2009
Saint Louis University

RESEARCH EXPERIENCE

2013-2014 Research Assistant
“Cannabimimetic treatment of obstructive sleep apnea: A proof of concept trial”
5UM1HL112856-02

2011-2014 Research Assistant
“Multivariable Closed-Loop Technologies for Physically Active Young Adults with
Type 1 Diabetes”
R01DK085611

TEACHING EXPERIENCE

2011-2015 Seminars for Nursing Excellence Summer Lecture Series
Lectures in Cellular, Endocrine and Gastrointestinal Physiology
University of Illinois at Chicago, College of Nursing

2011-2014 Endocrine and Diabetes Lecture for Undergraduate Pathophysiology
University of Illinois at Chicago, College of Nursing

2011-2013 Teaching Assistant, College of Nursing
University of Illinois at Chicago, Chicago, IL

2006-2009 Student Tutor, College of Nursing
Saint Louis University, St. Louis, MO

PROFESSIONAL EXPERIENCE

2013-present Registered Nurse, Private Practice
Piano Vein and Vascular, Chicago, IL

2010-2011 Registered Nurse, Outpatient Clinic
Rehabilitation Institute of Chicago, Chicago, IL

2009-2010 Registered Nurse, Labor & Delivery Unit
Northwestern Memorial Hospital, Chicago, IL

2008-2009 Nurse Technician, Labor & Delivery Unit
Northwestern Memorial Hospital, Chicago, IL

2006-2008 Nurse Technician, Float Pool
Barnes-Jewish Hospital, St. Louis, MO

HONORS AND AWARDS

2013	NIH Clinical and Translational Research Course Attendee
2013	MNRS Student Poster Competition Representative for UIC
2009	Sister Mary Teresa Noth Excellence in Nursing Award, St. Louis University,
2007-2009	President's List, St. Louis University
2007-2009	Dean's List, St. Louis University
2007-2009	Jesuit Transfer Scholarship, St. Louis University

FUNDED RESEARCH GRANTS**Ongoing Research Support**

AADE Foundation/Sigma Theta Tau International Grant 01/01/15- 01/01/16
 This grant award is awarded for studies designed to provide information essential to advance the practice of Diabetes Self-Management Education/Training.
 Direct Expenses: \$6,000

Completed Research Support

5TL1TR000049-05 (NIH) 03/15/14 – 03/31/15

“Center for Clinical and Translational Science”

This is an institutional training award to foster multidisciplinary clinical translational research by providing graduate fellowship support to outstanding doctoral candidates engaged in appropriate dissertation research.

Role: Fellow

Direct Expenses: \$5,000 and tuition coverage

College of Nursing PhD Student Research Award 03/31/13 – 03/31/14

“Sleep, Glucose Variability, CVD Risk & CV Stress in young adults with T1DM”

Direct Expenses: \$500

Sigma Theta Tau International Alpha Lambda Chapter Award 04/15/13-04/15/14

“Sleep, Glucose Variability, CVD Risk & CV Stress in young adults with T1DM”

Direct expenses \$1,000

PUBLICATIONS**Journal Articles: * indicates data based publication**

* Martyn-Nemeth, P., Phillips, S., Mihailescu, D. **Farabi, S.S.**, Park, C., Lipton, R., Quinn, L. (under review).

Poor Sleep Quality among Young Adults with Type 1 Diabetes is Associated with Glycemic Variability, Diabetes Distress, and Fear of Hypoglycemia. Endocrine Practice

***Farabi, S.S.**, Carley, D.W., Quinn, L. (under review). Glucose Variations and Activity are Strongly Coupled during Sleep and Wake over a 60-Hour Period in Young Adults with Type 1 Diabetes. Journal of Sleep Research.

Farabi, S.S. (in press). Type 1 Diabetes and Sleep. Diabetes Spectrum.

Carley, D.W., **Farabi, S.S.** (in press). Physiology of Sleep. Diabetes Spectrum.

- *Farabi, S.S.,** Carley, D.W., Cinar, A., Quinn, L. (under review). Routine Daily Physical Activity and Glucose Variations are Strongly Coupled in Adults with T1DM. *Physiological Reports*.
- Martyn-Nemeth, P., **Farabi, S.S.,** Quinn, L. (2015). Fear of Hypoglycemia in Type 1 Diabetes: Impact of Therapeutic Advances and Strategies for Prevention. *Journal of Diabetes and its Complications*. Epub ahead of print. 7 September 2015. doi: 10.1016/j.jdiacomp.2015.09.003
- *Farabi, S.S.,** Carley, D.W., Smith, D., Quinn, L. (2015). Impact of Exercise on Diurnal and Nocturnal Markers of Glycemic Variability and Oxidative Stress in Obese Individuals with Type 2 Diabetes or Impaired Glucose Tolerance. *Diabetes and Vascular Disease Research*, 12(5): 381-5. doi: 10.1177/1479164115579003.
- Weaver, T.E., Calik, M.W., **Farabi, S.S.,** Fink, A.M., Galang-Boquiren, M.T., Kapella, M.K., Prasad, B., Carley, D.W. (2014). Innovative treatments for obstructive sleep apnea. *Nature and Science of Sleep*, 6: 137-147. doi: <http://dx.doi.org/10.2147/NSS.S46818>
- *Farabi, S.S.,** Prasad, B., Quinn, L., Carley, D.W. (2014). Impact of dronabinol on quantitative electroencephalogram (qEEG) measures of sleep in obstructive sleep apnea syndrome. *Journal of Clinical Sleep Medicine*, 10 (1): 49-56. doi: 10.5664/jcsm.3358

Abstracts:

- Farabi, S.S.,** Quinn, L., Carley, D.W. (2015). The Relationship Between Glucose Variations and Sleep EEG in Young Adults with Type 1 Diabetes. *Sleep*, 38 (Abstract Supplement): A299.
- Farabi, S.S.,** Carley, D.W., Quinn, L. (2015). Glucose Variations Are Strongly Coupled to Sleep Disruption in Young Adults with Type 1 Diabetes (T1DM). *Late Breaking Abstracts*. 65LB. http://professional.diabetes.org/Meeting_ListByType.aspx?ctyp=1
- Farabi, S.S.,** Quinn, L. (2014). Effects of moderate intensity exercise on glucose variability in obese T2DM adults. *Diabetes*, 63 (Suppl 1): A587. doi:10.2337/db14-2293-2343
- Park, H., Quinn, L., Cinar, A., Park, C., Turksoy, T., Bayrak, E.S., Littlejohn, E., **Schwarz, S.,** Fisher, D. (2013). Glucose variability and physical activity among people with type 1 diabetes. *Late Breaking Abstracts*. LB11. www.diabetes.org/diabetes
- Schwarz, S.,** Prasad, B., Quinn, L., Carley, D.W. (2013). The effect of dronabinol on sleep architecture in patients with obstructive sleep apnea. Abstract for poster presentation, Annual Meeting of the Associated Professional Sleep Societies, Baltimore, MD.

PROFESSIONAL ORGANIZATION MEMBERSHIP

2012-present	Midwest Nursing Research Society
2012-present	Sleep Research Society
2012-present	American Association of Diabetes Educators
2012-present	American Diabetes Association
2009-present	Sigma Theta Tau International Honor Society of Nurses
2008-present	Alpha Sigma Nu Honor Society

SERVICE

2014	Reviewer, <i>Applied Journal of Physiology-Endocrine and Metabolism</i>
------	---

2012-2014	Chicago Children's Diabetes Center-La Rabida Children's Hospital Clinic Volunteer
2011-2014	American Diabetes Association Triangle D Camp for Children with Diabetes Volunteer Nurse

CERTIFICATIONS AND LICENSURE

2009-present	Registered Nurse, State of Illinois
--------------	-------------------------------------